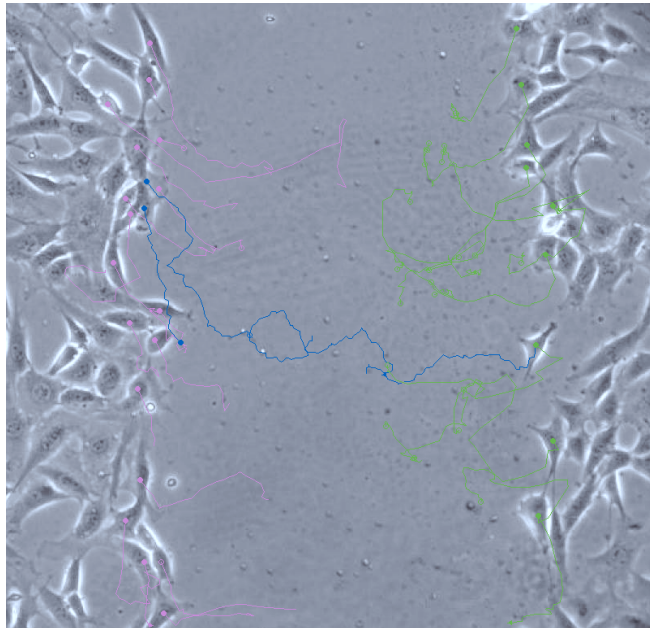




**UNIVERSITA' DEGLI STUDI DI NAPOLI
"FEDERICO II"**

**DOTTORATO DI RICERCA IN BIOCHIMICA
E BIOLOGIA CELLULARE E MOLECOLARE
XXIII CICLO**

***RAS AND ITS EFFECTORS: A DOUBLE ROLE IN
REGULATING CELL MIGRATION***



**Candidate: Maria Carla Ferrari
Tutor: Prof. Giovanni Paoletta**



**UNIVERSITA' DEGLI STUDI DI NAPOLI
"FEDERICO II"**

**DOTTORATO DI RICERCA IN
BIOCHIMICA E BIOLOGIA CELLULARE E MOLECOLARE
XXIII CICLO**

**RAS AND ITS EFFECTORS: A DOUBLE ROLE IN
REGULATING CELL MIGRATION**

**Candidate
Maria Carla Ferrari**

Tutor
Prof. Giovanni Paoella

Coordinator
Prof. Paolo Arcari

Academic Year 2010/2011

RINGRAZIAMENTI E DEDICHE

Ringrazio il prof. Giovanni Paoletta, per avermi seguita in questi anni istillandomi il senso critico e stimolando incessantemente il mio intelletto. Leandra Sepe, Francesca Fioretti e Maria Manzo, con le quali la proficua collaborazione professionale non è stata mai scissa da un leale, sincero e rassicurante rapporto di amicizia. I miei colleghi dell'edificio 18 del DBBM, ed in particolare Davide Esposito e Michele Olivieri per il sorriso che hanno fatto sorgere sul mio volto anche nelle giornate più buie.

Ringrazio le persone che hanno sempre creduto in me spronandomi ad essere, giorno dopo giorno, degna della loro stima.

Ringrazio la mia isola felice, Cristian, per avermi accompagnata in questi mesi tendendomi la mano e non privandomi mai della sua rassicurante ed amorevole presenza.

Ringrazio i miei familiari ed in particolare i miei genitori per aver costruito intorno a me un universo parallelo di serenità, valori, amore e comprensione che mi ha avvolta permettendomi di seguire le ambizioni con maturità e scevra di preoccupazioni materiali.

Ringrazio quel fuoco sacro della passione che non smette di ardere dentro di me, e quell'arcana forza della caparbia ed ostinata determinazione che mi ha spinto ad andare avanti, rialzandomi dopo ogni caduta.

SUMMARY

Within this work, time-lapse microscopy and quantitative analysis of motion parameters were used to characterize Ras regulation of the phenomena determining directional cell migration. The behaviour of NIH3T3 and NIHRasV12 fibroblasts, expressing RasV12, a constitutively activated variant, was characterized in terms of kinetic, morphological and biochemical features.

Constitutive RasV12 activation results in both morphological changes and increased proliferation and speed, and confers to NIH3T3 cells the ability to close the wound faster in wound healing assays. Since neither increased cell proliferation nor higher speed explain, alone, the accelerated wound closure, other parameters, descriptive of specific aspects of cell motion, such as linearity, persistence and directionality, were quantitatively evaluated. For both NIH3T3 and NIHRasV12 fibroblasts, the wound acts as a directional stimulus, but the presence of constitutively activated RasV12 amplifies the directional response: NIHRasV12 migration is characterized by paths more directional and directed towards the wound. The role of the effectors through which Ras drives directional cell migration, was evaluated by separately blocking two main signaling pathways downstream from Ras, PI3K and MAPK pathway. The inhibition of PI3K pathway reduced speed but not the directional component of cell migration; instead, the selective block of ERK activation showed that directionality, more than speed, is associated with MAPK pathway and strictly depend on ERK phosphorylation.

Immunofluorescence stainings showed that ERK activates at the wound edge immediately after wound. The biochemical analysis, by western blot, of cell extracts enriched with cells located in the proximity of a wound, showed that ERK phosphorylation occurs in a prolonged and biphasic way. Moreover, both peaks of ERK activation resulted dependent on neo-phosphorylation by MEK.

Actin modifications, induced by the wound, are impaired by the inhibitor of ERK activation, in both NIH3T3 and NIHRasV12 fibroblasts, suggesting that the cellular response, responsible for starting and driving directional movement, depend on early ERK activation by Ras, after the wound stimulus.

RIASSUNTO

Nell'ambito di questo lavoro, tecniche di microscopia *time-lapse* ed analisi quantitative dei parametri descrittivi il movimento, sono state utilizzate allo scopo di caratterizzare la regolazione Ras mediata dei fenomeni determinanti la migrazione cellulare direzionale. Il comportamento dei fibroblasti NIH3T3 e NIH-RasV12, esponenti RasV12, una variante costitutivamente attiva, è stato definito in termini di caratteristiche cinetiche, morfologiche e biochimiche.

L'attivazione costitutiva di Ras determina cambi morfologici, incrementata proliferazione e velocità, e conferisce alle cellule NIH3T3 l'abilità di chiudere la ferita più rapidamente in saggi di *wound healing*. Poiché l'incrementata proliferazione e la più alta velocità, da sole, non sono in grado di spiegare l'accelerata chiusura del *wound*, sono stati valutati quantitativamente altri parametri descrittivi specifici aspetti del movimento cellulare, quali la linearità, la persistenza e la direzionalità. Il *wound* agisce come stimolo direzionale per i fibroblasti NIH3T3 e NIH-RasV12, ma la presenza della forma costitutivamente attiva, RasV12, amplifica la risposta direzionale: la migrazione delle NIH-RasV12 è caratterizzata da percorsi più direzionali e diretti verso il *wound*. Il ruolo degli effettori attraverso cui Ras guida la migrazione direzionale, è stato valutato bloccando separatamente i due principali *pathway* a valle di Ras, PI3K e MAPK. L'inibizione del *pathway* di PI3K ha ridotto la velocità ma non la componente direzionale della migrazione cellulare; il blocco selettivo dell'attivazione di ERK, invece, ha mostrato che la direzionalità, più della velocità, è associata al *pathway* delle MAPK e strettamente dipendente dalla fosforilazione di ERK.

Analisi d'immunofluorescenza hanno mostrato che ERK si attiva al bordo immediatamente dopo l'introduzione del taglio nel *monolayer*. L'analisi biochimica, mediante *western blot*, di estratti cellulari arricchiti di cellule localizzate in prossimità della ferita, ha mostrato che la fosforilazione di ERK avviene in modo prolungato e bifasico. Inoltre, entrambi i picchi d'attivazione di ERK sono risultati dipendenti da neo-fosforilazione mediata da MEK.

Le modifiche del citoscheletro di actina, indotte dal *wound* in fibroblasti NIH3T3 e NIH-RasV12, sono ridotte per effetto dell'inibitore dell'attivazione di ERK, suggerendo che la risposta cellulare, responsabile dell'avvio e della guida del movimento direzionale, dipende dall'attivazione precoce di ERK mediata da Ras, in seguito allo stimolo del *wound*.

INDEX

| | |
|--|-----------|
| 1. INTRODUCTION..... | 1 |
| 1.1 <i>RAS PROTEINS</i> | 1 |
| 1.1.1 <i>Ras superfamily</i> | 1 |
| 1.1.2 <i>Ras subcellular localization</i> | 2 |
| 1.1.3 <i>Ras in human tumors</i> | 3 |
| 1.2 <i>RAS EFFECTORS: PI3K AND MAPK PATHWAYS</i> | 3 |
| 1.2.1 <i>PI3K pathway</i> | 4 |
| 1.2.2 <i>MAPK pathway</i> | 4 |
| 1.2.3 <i>ERK proteins</i> | 5 |
| 1.2.4 <i>ERK regulation: positive and negative feedback loops</i> | 6 |
| 1.2.5 <i>Subcellular localization of ERK signaling: scaffold proteins</i> | 7 |
| 1.3 <i>RAS EFFECTS ON CELLULAR TRANSFORMATION</i> | 7 |
| 1.4 <i>CELL MIGRATION: FIND THE WAY BY SENSING THE DIRECTION</i> | 9 |
| 1.4.1 <i>Motility and cell polarity: membrane and cytoskeletal structure</i> | 9 |
| 1.4.2 <i>Actin in protrusive structures</i> | 10 |
| 1.4.3 <i>Focal adhesions</i> | 11 |
| 1.4.4 <i>Contractile forces, traction and rear release</i> | 13 |
| 1.5 <i>RAS AND ITS EFFECTORS IN REGULATING CELL MIGRATION</i> | 13 |
| 1.5.1 <i>Rho GTPases</i> | 14 |
| 1.5.2 <i>PI3K pathway</i> | 16 |
| 1.5.3 <i>MAPK pathway</i> | 17 |
| 1.6 <i>METHODS FOR STUDYING CELL MIGRATION</i> | 19 |
| 1.6.1 <i>Time-lapse microscopy</i> | 20 |
| 1.6.2 <i>Wound healing assay</i> | 21 |
| 1.6.3 <i>Computational method: MotoCell</i> | 21 |
| 1.7 <i>SCIENTIFIC HYPOTHESIS AND AIM OF THE WORK</i> | 22 |
| 2. MATERIALS AND METHODS..... | 24 |
| 2.1 <i>CELL CULTURE AND PROPAGATION</i> | 24 |
| 2.2 <i>MATERIALS</i> | 24 |
| 2.3 <i>RANDOM MOTILITY ASSAY</i> | 24 |
| 2.4 <i>WOUND HEALING ASSAY</i> | 24 |
| 2.5 <i>TIME LAPSE MICROSCOPY AND IMAGE ACQUISITION</i> | 25 |
| 2.6 <i>CELL TRACKING AND QUANTITATIVE ANALYSIS OF CELL MIGRATION</i> | 25 |
| 2.7 <i>IMMUNOFLUORESCENCE</i> | 26 |
| 2.7.1 <i>BrdU assay</i> | 27 |
| 2.8 <i>LYSATES AND IMMUNOBLOTTING</i> | 27 |
| 2.8.1 <i>Gel electrophoresis</i> | 27 |
| 2.8.2 <i>Transfer method</i> | 28 |
| 2.8.3 <i>Immunodetection</i> | 28 |

| | |
|--|-----------|
| 3. RESULTS..... | 29 |
| 3.1 <i>CONSTITUTIVE RASV12 ACTIVATION CONFERS TO NIH3T3 CELLS THE ABILITY TO CLOSE THE WOUND FASTER</i> | 29 |
| 3.1.1 <i>RasV12 transformed fibroblasts show morphological changes, increased proliferation rate and speed</i> | 29 |
| 3.1.2 <i>Increased cell proliferation is not the main factor for wound closure</i> | 30 |
| 3.1.3 <i>Increased speed alone does not explain enhanced wound healing</i> | 30 |
| 3.1.4 <i>Under wound stimulus NIH3T3 cells show better directional movement</i> | 31 |
| 3.1.5 <i>Directional movement is a function of the distance from the wound edge</i> .. | 33 |
| 3.2 <i>MAPK AND PI3K DIFFERENTLY AFFECT DIRECTIONAL MIGRATION</i> | 33 |
| 3.2.1 <i>Speed is affected by both PI3K and MAPK pathway inhibition</i> | 34 |
| 3.2.2 <i>MAPK pathway is the main regulator of the directional component of cell migration</i> | 34 |
| 3.3 <i>ERK ACTIVATION PLAYS AN IMPORTANT ROLE IN RESPONDING TO THE WOUND</i> | 36 |
| 3.3.1 <i>Localization of phosphorylated ERK at the border with the wound</i> | 36 |
| 3.3.2 <i>ERK phosphorylation occurs in a prolonged and biphasic way</i> | 36 |
| 3.3.3 <i>The two peaks of ERK activation are independent and both depend on neophosphorylation</i> | 37 |
| 3.4 <i>THE ACTIN ORGANIZATION AT THE LEADING EDGE IS IMPAIRED BY MAPK INHIBITOR PD 98059</i> | 38 |
| 4. DISCUSSION/CONCLUSIONS..... | 39 |
| 5. REFERENCES | 44 |

LIST OF TABLES AND FIGURES

| | | | |
|------------------|--|------------|----|
| Figure 1 | Quantitative analysis of migration. | After page | 26 |
| Figure 2 | Wound healing of NIH3T3 fibroblasts. | After page | 29 |
| Figure 3 | Constitutive RasV12 activation confers to NIH3T3 cells the ability to close the wound faster. | After page | 29 |
| Figure 4 | Constitutive RasV12 activation induces morphological changes. | After page | 29 |
| Figure 5 | RasV12 transformation induces increased proliferation rate and speed. | After page | 30 |
| Figure 6 | Increased proliferation is not the main factor for wound closure. | After page | 30 |
| Figure 7 | Wound healing assay in limiting growth conditions (0.5% serum). | After page | 30 |
| Figure 8 | Linearity, persistence and directionality of random migration are not modified by RasV12. | After page | 31 |
| Figure 9 | Quantitative analysis of NIH3T3 and NIHRasV12 movement during wound healing. | After page | 32 |
| Figure 10 | Quantitative analysis of NIH3T3 and NIHRasV12 movement during wound healing in 0,5% serum. | After page | 33 |
| Figure 11 | Identification and analysis of subpopulations. | After page | 33 |
| Figure 12 | All NIHRasV12 subpopulations move with high directionality while only NIH3T3 cells surrounding the wounds move in a directional way. | After page | 33 |
| Figure 13 | Kinetic analysis of NIH3T3 and NIHRasV12 migration in presence of PD 98059 and LY 294002. | After page | 34 |
| Figure 14 | Analysis of NIH3T3 and NIHRasV12 directional migration in presence of PD98059. | After page | 35 |

| | | | |
|------------------|--|------------|----|
| Figure 15 | Analysis of NIH3T3 and NIHRasV12 directional migration, in presence of LY 294002. | After page | 35 |
| Figure 16 | Fit to Von Mises distribution. | After page | 36 |
| Figure 17 | Phosphorylated ERK quickly appears at the leading edge of migrating cells. | After page | 36 |
| Figure 18 | ERK activation occurs in a prolonged and biphasic way in front cells. | After page | 37 |
| Figure 19 | Spatial and temporal localization of ERK activation following the wound. | After page | 37 |
| Figure 20 | The biphasic pattern of ERK activation is affected by PD 98059. | After page | 37 |
| Figure 21 | The two peaks of ERK activation are independent. | After page | 37 |
| Figure 22 | The two peaks of ERK activation both depend on neophosphorylation. | After page | 38 |
| Figure 23 | Actin and paxillin organization at leading edge of migrating cells. | After page | 38 |
| Figure 24 | Actin organization at the leading edge of migrating cells in presence of PD 98059. | After page | 38 |

INTRODUCTION

1.1 *Ras proteins*

The Ras superfamily includes over one hundred small GTPases (20-25 kDa) that are involved in cellular signaling pathways responsible for growth, migration, adhesion, cytoskeletal integrity, survival, differentiation and more. The proteins of this superfamily are all related in structure because they share substantial primary sequence homology in their N-terminal, particularly in the phosphate-binding loop and in the nucleotide-sensitive switch I and II regions (Krister W., 2005).

1.1.1 Ras superfamily

Ras is the prototypical member of the superfamily. Like other small GTPases, Ras acts as binary switch alternating between GTP and GDP-bound conformations, where the GTP-bound conformation represents the “On” and GDP-bound the “Off” state. Only the GTP-bound conformation possesses high affinity for effector targets. Although Ras has a measurable intrinsic GTPase activity, it is too low to be relevant at the physiological level, therefore the transitions between the “On” and “Off” states require additional help from specialized proteins accelerating GTP hydrolysis. These accelerators are named GTPase activating protein (GAP) and increase the GTP hydrolysis of Ras by approximately 100 000 fold. In order to recharge the GTPase, the binding of GDP must be weakened by the action of guanine nucleotide exchange factors (GEFs), which catalyze its replacement (Krishnaraj R., 2007).

Three highly related Ras genes, H-, N-, and K-ras (K-RasA and K-RasB) are found in the mammalian genome and they perform distinct cell type and tissue specific functions. The isoforms display very high degree of sequence homology and the major differences are confined to hypervariable region (HVR). It encompasses approximately 25 aa, which are required for posttranslational modifications that direct plasma membrane anchoring as well as trafficking of newly synthesized Ras proteins to the inner surface of the plasma membrane from the cytosolic surface of the endoplasmic reticulum (ER) (Weiquan L., 2004). Ras proteins are not intrinsic membrane proteins and they lack signal sequences and hydrophobic membrane-spanning domains. They are synthesized as hydrophilic proteins terminating in a CAAX motif, the cysteine in this box is recognized by farnesyltransferases that catalyze the addition of a farnesyl isoprenoid, which permits a transient association to the ER. For stable membrane association Ras requires a second signal: H-

Introduction

Ras, N-Ras, and K-Ras4A are further modified by one or two palmitates at the Golgi complex (GC). K-Ras4B second signal consists of a polybasic region rich in lysine residues, which exerts a strong electrostatic interaction with membrane phospholipids; this isoform bypasses the GC to reach the plasma membrane.

1.1.2 Ras subcellular localization

Ras proteins do not act exclusively at the plasma membrane but they translocate between cellular compartments: while farnesylation is fairly stable, palmitoylation is rapidly reversible, so N- and H-Ras undergo a palmitoylation/depalmitoylation cycle, whereby palmitoylated forms at the plasma membrane are released following depalmitoylation, and traffic, via retrograde transport, to the Golgi. Once there, Ras proteins are repalmitoylated and sent back to the plasma membrane by vesicular transport (Calvo F., 2010). The three Ras isoforms were also detected in endosomes and mitochondria. Interestingly, Ras association to endosomes exhibits isoform specificity: whereas N- and H-Ras establish stable interactions with endosomal compartment, K-Ras does not. There is a further complexity at the plasma membrane where Ras segregates at distinct microdomains: H and N-Ras are present in lipid raft (cholesterol rich domains) and in disordered membrane domains, whereas K-Ras is only detected in the latter. Importantly, Ras sublocalization appears to depend on its activation status: inactive, GDP-bound, H-Ras is associated predominantly to lipid rafts, translocating to disordered membrane when GTP-loaded (Fehrenbacher N., 2009).

The presence of Ras at multiple sites markedly influences which effector pathways are activated and how intensively. Probably, this depends on the abundance and availability of effector molecules at different sites. For example, ubiquitination of H- and N-Ras promotes their association to endosomes, where reduced availability of Raf results in diminished ERK activation (Jura N., 2006). Furthermore, in murine fibroblasts Ras effectively supports proliferation and cellular transformation from the ER, disordered membrane and lipid rafts, but not from Golgi (Matallanas D., 2006). Besides, K-Ras may be phosphorylated by PKC that promotes its rapid dissociation from the plasma membrane and its translocation to mitochondria, where it induces apoptosis, while K-Ras signaling at plasma membrane can induce transformation. This observation demonstrates that the same actor, K-Ras, at two different sites, PM versus mitochondria, can yield two diametrically opposed biological outcomes, proliferation or death (Bivona T.G., 2006).

1.1.3 *Ras in human tumors*

The cellular homologues of the viral Harvey and Kirsten transforming ras gene sequences were first identified in rat genome in 1981 and were subsequently found in mouse and human genome. Protooncogenes, such as ras, residing in the genome of normal cells can be activated into potent oncogenes by retroviruses, which acquire these sequences and convert them into active oncogenes. The Harvey sarcoma virus associated oncogene was named Ha-ras (H-ras in mammals), whereas that of Kirsten sarcoma virus was defined Ki-ras (K-ras in mammals). Mutant alleles of these ras sequences were soon discovered in many human cancer cell lines, including those of bladder, colon and lung (Parada L.F., 1982; Der C.J., 1982). By 1983, the third member of the mammalian family of ras-related genes, N-ras, had been cloned from neuroblastoma and leukaemia cell lines (Taparowsky E., 1983).

After these observations a rich Ras research was started, and now it is known that Ras family members are involved in almost all steps of multi-step tumorigenesis. It has been calculated that one ras gene is oncogenically activated in over 30% of human cancers (Ahmedin J., 2010). The frequency of somatic mutations in the three ras genes in the “Catalogue of Somatic Mutations in Cancer” are different: H-Ras is mutated with the highest frequency in salivary gland, urinary tract (bladder cancer), cervix and skin; for K-Ras the highest frequency is in pancreas, lung, biliar tract, large and small intestine; N-Ras in skin, nervous system, hematopoietic and lymphoid tissues (Forbes S.A., 2010). In most cases, the somatic missense ras mutations, found in cancer cells, introduce aminoacid substitutions at positions 12, 13 and 61. These changes impair the intrinsic GTPase activity and confer resistance to GAPs, thereby causing cancer associated mutant Ras proteins to accumulate in the active, GTP-bound conformation. Particularly, glutamine 61 is essential for GTP hydrolysis, and substituting any amino acid at this position, except glutamic acid, blocks hydrolysis. Instead, replacing glycine 12 of Ras with any other amino acid except for proline also biochemically activates Ras: these substitutions are thought to be unfavourable in the GTP-GDP transition state because of a steric clash of side chains with catalytic arginine of GAP proteins (Schubbert S., 2007).

1.2 *Ras effectors: PI3K and MAPK pathways*

Ras effectors are defined as proteins with a strong affinity to GTP-Ras, which they bind with a putative Ras binding domain or RBD. The interaction of Ras proteins with their effectors occurs through a stretch of

Introduction

amino acids (32-40), generally known as the effector region, which assumes a different conformation in GTP-bound Ras compared to GDP-bound Ras. Binding of Ras effector proteins to GTP-Ras triggers distinct signaling cascades that modulate cell behaviour. Indeed, an effector of Ras would be expected to possess, or control, some sort of enzymatic activity, regulated by its interaction with Ras-GTP and responsible for at least some of the cellular effects of Ras (Krishnaraj R., 2007). PI3K and Raf-MEK-ERK cascades are the best-characterized Ras effector pathways.

1.2.1 PI3K pathway

PI3K is a heterodimeric enzyme composed of two subunits, the regulatory p85 subunit harbouring two SH2 domains, and the catalytic p110 subunit. PI3K activation is achieved by binding of the p85 subunit to an activated receptor. Alternatively active Ras can directly interact with the catalytic subunit of PI3K, recruit PI3K to the plasma membrane and induce a stimulatory conformational change in this lipid kinase (Rodriguez-Viciana P., 1994). Among the Ras isoforms, H-Ras was identified to be a more potent activator of the PI3K in comparison to K-Ras (Yan J., 1998). Upon activation, PI3K catalyses the conversion of phosphatidylinositol-4,5-bisphosphate (PIP₂) to produce phosphatidylinositol-3,4,5-trisphosphate (PIP₃) at the inner leaflet of the plasma membrane, which serves as a docking site for various proteins containing phospholipids binding domains, such as the PH domain, including the kinase PDK1 and Akt/PKB. Recruitment of Akt to the plasma membrane, along with Akt phosphorylation by PDK1, enables its activation and subsequent phosphorylation of various substrate proteins. Akt is a kinase that promotes survival in many cell types by phosphorylating and therefore inactivating several pro-apoptotic proteins including Bad. It also activates mammalian target of rapamycin (mTOR) to increase ribosomal biogenesis and mRNA translation. Additionally, as described below, active PI3K stimulates the GTP-binding Rac protein, a regulator of the actin cytoskeleton (DeNicola G.M., 2009).

The PI3K pathway also includes the phosphatase PTEN that acts as a negative regulator of growth-promoting effects of PI3K activity removing the phosphates from PIP₃.

1.2.2 MAPK pathway

The MAP kinase (MAPK) cascade is activated in response to many different signals, including those originating at growth factor receptors,

integrins and G-protein coupled receptors, and conveys signals in the form of phosphorylation events. The canonical pathway is activated when any of several growth factors engage their cognate protein tyrosine kinase receptors (PTKRs). Ligation of PTKRs promotes their dimerization, which in turn allows cross-phosphorylation of tyrosine residues in their cytosolic domains, catalyzed by the kinase intrinsic to that domain. These phosphotyrosine residues serve as docking sites for signaling molecules and adapter proteins that contain SH2 domains (Src homology region 2). Among these is the adapter protein Grb2 that uses the SH3 domain to interact with the guanine nucleotide exchange factor for Ras, Sos. Thus, Sos is recruited to the plasma membrane where it can encounter Ras and promote the exchange of GDP for GTP. The active Ras-GTP can then bind and activate the serine/threonine kinase Raf. Upon activation, Raf phosphorylates the serine residue in the activation loop of MEK, a dual specificity tyrosine/threonine kinase. Thereafter, activated MEK1/2 phosphorylates the MAPK proteins, ERK1/2, on adjacent threonine and tyrosine residues, spaced by glutamic acid residue, at the activation loop (McCubrey J.A., 2007).

1.2.3 *ERK proteins*

ERK proteins are serine/threonine kinases that have numerous cytosolic and nuclear substrates. Under resting conditions, ERK is found in the cytoplasm, as a consequence of its interaction with several types of cytoplasmic anchors, such as the same MEK1/2. Cytoplasmic localization of MEK is achieved by means of a nuclear export signal (NES) located in its amino-terminal domain. In addition to MEK, PEA-15, which also contains a NES, binds ERK and retains it in the cytoplasm (Formstecher E., 2001). Once phosphorylated, ERK loses its affinity for these partners and undergoes a rapid relocalization to the nucleus, where it phosphorylates multiple targets. In the nucleus, ERK performs essential functions that regulate transcription, DNA replication, chromatin remodeling, and miRNA synthesis. ERK can phosphorylate and activate various transcription factors, including Sp1, E2F, Elk-1 and AP1, this last composed of two short-lived proteins, Jun and Fos. Activation of these transcriptional regulators can lead to the expression of proteins that control cell-cycle progression, such as cyclin D, that in turn promotes DNA synthesis through CDK4 and CDK6 regulation. After producing its effects in the nucleus, ERK must relocalize to the cytoplasm to react to a new stimulation. This relocalization is achieved by a NES-dependent nuclear export: MEK, which mostly localizes to the cytoplasm due its

NES, can shuttle between the cytoplasm and the nucleus. It has been suggested that the relocalization of inactive ERK involves MEK-dependent active transport: MEK transiently enters the nucleus and binds inactive ERK to export it from the nucleus (Torii S., 2004). ERK extranuclear component is just as important: nearly half of the ~80 proteins thus far identified as ERK substrates, are non-nuclear proteins. It has been estimated that, after stimulation and ERK phosphorylation, about half of it remains in the cytoplasm and becomes involved in processes such as formation of cell-matrix contacts, adhesion, endosomal traffic, Golgi fragmentation and antiapoptotic signaling (Yoon S., 2006).

1.2.4 ERK regulation: positive and negative feedback loops

One of the most potent mechanisms for shutting off MAP kinase signaling is by dephosphorylation of the threonine and tyrosine residues in the activation loop. A family of dual specificity threonine/tyrosine MAP kinase phosphatases (MKPs), also known as dual specificity phosphatases (DUSPs), are responsible for this process. MKPs can be restricted to the cytoplasm, the nucleus, or travel between both. Regulation of these phosphatases appears to be central in controlling ERK activity. Some of these MKPs, in fact, are encoded by genes that are transcriptionally activated by ERK (MKP1) and provide a negative feedback loop to downregulate ERK activity (Ramos J.W., 2008). On the other hand, a positive feedback loop involves phosphorylation of cytosolic dual specificity phosphatase DUSP6 (MKP3) that inactivates ERK by dephosphorylating it. ERK phosphorylates DUSP6 at two serine residues (S159 and S197) and thus targets DUSP6 for degradation in the proteasome (Marchetti S., 2005). Another example of positive feedback is Raf phosphorylation by ERK that results in increased Raf activity (Balan V., 2006).

There are also points of negative feedback in the ERK pathway that limit signal duration and return the pathway to the basal state. MEK is one target and it can be inhibited by ERK phosphorylation at Thr292 and Thr212. Phosphorylation prevents further enhancement of MEK activity by PAK1 and thereby reduces activation of ERK (Slack-Davis J.K., 2003). Moreover, the ERK-dependent phosphorylation of Sos, in proximity of its proline rich sequences, inhibits Sos interaction with the Grb-2 SH3 domains. This prevents recruitment of Sos to the plasma membrane, thereby reducing Ras activation (Corbalan-Garcia S., 1996). The significance of both positive and negative feedback loop is to regulate signal duration, which is of primary importance in determining

the outcome of ERK activation.

1.2.5 Subcellular localization of ERK signaling: scaffold proteins

Subcellular localization of MAPK is considered a major mechanism that controls signaling. In fact, in addition to the kinase cascade, ERK activation is also controlled by scaffold proteins, that regulate amplitude, intensity and spatial specificity of ERK signal. Their main function is to bring together members of the signaling cascade, forming a complex that helps in signal optimization. At the same time, they prevent interactions with molecules operating in parallel cascades, thus insulating the MAPK pathway from undesired interference (Dhanasekaran D.N., 2007). In addition, scaffold proteins play an important role in spatial selectivity of ERK signalling: KSR1 (kinase suppressor of Ras) is a multidomain protein that binds Raf1, MEK and ERK but preferentially acts upon ERK signal emanating from plasma membrane cholesterol rich domain; MP-1 (MEK partner 1) regulates ERK in endosomes. It binds MEK1 and ERK1 but not MEK2 and ERK2 and this binding facilitates the phosphorylation of ERK1 by MEK1. Sef is a MEK/ERK scaffold protein that resides in the Golgi complex. At the last, paxillin acts as a scaffold at focal adhesions, while beta-arrestins are abundant in clathrin-coated pits (Mor A., 2006). In addition, the microenvironment from which Ras signals emanate determine which substrates will be preferentially phosphorylated by active ERK, and this substrate specificity is governed by the participation of distinct scaffold proteins. Specifically, ERK activated by Ras at the ER utilize Sef1 to activate cPLA2. cPLA2 is also activated by ERK in response to Ras signals coming from lipid rafts, but in this case the mediating scaffold is KRS1. KRS1 is not the only scaffold protein utilized by lipid raft-generated signals, since phosphorylation in this site of another ERK substrate, EGFR, is mediated by IQGAP (Casar B., 2009).

1.3 Ras effects on cellular transformation

Normal cellular behavior in multicellular organisms is tightly controlled by a complex network of signaling pathways that ensures that cells proliferate only when it is required, for example, during development or wound healing. Cancer occurs when normal growth regulation breaks down, usually because of defects in these signaling mechanisms. Ras proteins were among the first identified proteins that possess the ability to regulate cell growth. Indeed, oncogenic Ras proteins deregulate downstream effector pathways to confer abnormal functional properties

Introduction

of cancer cells: uncontrolled cell growth, deregulated survival and differentiation. Earlier studies, using anti-Ras antibodies and Ras dominant negative mutants, suggested that Ras proteins are essential for cell proliferation (Mulchany L.S., 1985; Feig L.A., 1988). Due to ras genes redundancy (at least three isoforms exist in eukaryotic cells) formal evidence of the need for ras genes requires the generation of a triple MEF mutant where ablation of the N-, H- and K-ras genes at the same time, leads to blocked proliferation. In these cells activation of components of the MAPK pathway was sufficient to sustain normal proliferation. Activation of PI3K pathway failed to induce proliferation in the same cells, although PI3K and MAPK signalling cooperation is necessary for attaining a full proliferative response (Drosten M., 2010).

The effects of constitutively activated Ras variants have been studied in different cellular systems. H-RasV12 expression in fibroblasts produces high transforming ability in vitro, suppression of apoptotic cell death and anchorage-independent proliferation. Alterations of cytoskeleton structure with nearly complete loss of stress fibers and reduced focal adhesions at the edges of the cell have also been observed (Shima Y., 2007). In purified primary erythroid progenitors from mouse fetal liver, H-RasV12 blocks terminal erythroid differentiation and supports erythropoietin-independent proliferation. These effects may be reproduced by activation of the sole MEK/ERK pathway, such as when expressing a constitutively active MEK variant (Zhang J., 2004).

Expression of another Ras mutant, H-RasL61, alters the differentiation/proliferation balance with the acquisition of several transformation-associated properties. Anchorage-independent growth and proliferation required the highest levels of H-RasL61, whereas morphological transformation and loss of differentiative capacity were apparent even at lower Ras levels (Raptis L., 1997).

In addition, ras mutations have been described in a large number of human metastatic tumors, such as colon and breast cancer, where aberrant activation of Ras proteins is implicated not only in uncontrolled proliferation of cancer cells, but also in invasion and metastasis formation. A variety of experimental approaches have been undertaken to define the role of Ras GTPases in metastasis and invasion, in both in vitro and in vivo experimental models (Campbell P.M., 2004). Transfection of mutated, constitutively active form of Ras into noncancerous cells leads to invasive and metastatic phenotypes. NIH3T3 fibroblasts are one of the most commonly studied models of Ras activation. In these cells the ectopic expression of oncogenic, constitutively active Ras results in

transformation, increased invasion in vitro and in vivo, acquisition of tumorigenic properties after subcutaneous and metastatic after intravenous injection (Mushel R.J., 1985; Bondy G.P., 1985; Greig R.G., 1985). Expression of exogenous Ras has also been shown to promote invasive and metastatic properties of other cell types. Epithelial and other cell types from a variety of human and murine tissue have been made invasive and/or metastatic by introduction of mutated Ras genes (Fujimoto K., 2001).

Tumor progression and metastatic dissemination heavily depend on cell migration since a crucial requirement for tumor cell metastasis is the ability to transit from primary tumor to distant sites.

1.4 Cell migration: find the way by sensing the direction

Many types of cells respond with changes in morphology and motility to stimuli controlling cell migration and transduce them into intracellular biochemical signals. Interactions of transmembrane integrins that bind extracellular matrix (ECM) proteins, cell-surface receptors that bind growth factors, or mechanical stimuli such as shear stress that promote deformation of actin cytoskeleton have all been involved. In chemotaxis a chemical gradient serves as a directional signal that organizes cell movement. This process plays a central role in wound healing, immunity, development and tissue homeostasis, but also in some pathological states, such as metastasis (Devreotes P., 2003).

The terms directional sensing and polarity are often used interchangeably, but they are distinct and separable processes. Directional sensing refers to the ability of a cell to detect an asymmetric extracellular cue and generate an internal response. Directional sensing response does not require the cell to be polarized since unpolarized, immobilized cells can also detect gradients with a similar degree of signal amplification. Polarization is defined as the assumption of an asymmetric shape with a defined anterior and posterior region (Arkowitz R.A., 2008).

1.4.1 Motility and cell polarity: membrane and cytoskeletal structure

Migration is a highly coordinated process. Polarization of a cell subjected to a chemical gradient or other directional stimulus, is an early event and generates a “leading” and a “trailing” edge. In polarized cells the anterior (leading) surface is more sensitive to chemoattractants than other regions. When the gradient is changed, a polarized cell generally turns rapidly towards the new direction. Unlike directional sensing, polarization critically depends on actin cytoskeleton, and inhibitors of actin

polymerization are able to turn a polarized cell into an unpolarized one (Kortholt A., 2008).

Crawling involves a cycle where four steps may be distinguished: extension of a leading edge protrusion, establishment of new adhesion sites to the substratum at the front, cell body contraction, and detachment of adhesions at the cell rear. To migrate, cells must be able to turn intracellular signals into net cell body translocation. All these steps involve assembly, disassembly or reorganization of actin cytoskeleton, and each must be coordinated both in space and time to generate productive, net, forward directed movement (Pollard T.D., 2003). Specialized molecules associated with the leading edge include actin and actin-binding proteins such as Scar, WASP, filopodin, cofilin, and coronin, whereas molecules associated with the trailing edge include myosin II and cortexillin.

1.4.2 Actin in protrusive structures

Establishment of polarization involves a dynamic, coordinated interaction of directional sensing events with the activities of the cytoskeleton: an essential role of the actin cytoskeleton is to stabilize the asymmetric distribution of key components of the directional response apparatus. In polarization, an early event, is a change in distribution of F-actin from homogeneous around the cell rim to concentrated at a particular region where protrusive structures are being formed.

Protrusive structures at the leading edge of motile cells are highly dynamic and contain dense arrays of actin filaments. These filaments are organized with their barbed ends (fast growing, or plus ends) preferentially oriented in the direction of protrusion. The simplest protrusive structures are filopodia, thin cylinders that can extend tens of microns. Filopodia contain a tight bundle of long actin oriented in the direction of protrusion. Filaments are held together in the bundle by cross-linking proteins, such as fimbrin.

Lamellipodia are thin protrusive sheets that dominate the leading edges of cultured fibroblasts and other motile cells. The characteristic ruffling appearance of fibroblast leading edges is due to lamellipodia that lift up off the substrate and move backwards. The web of actin filaments that shapes lamellipodia is organized as an orthogonal cross-weave between two sets of filaments oriented at approximately 45° to the direction of the protrusion (Mitchison T.J., 1996). In all these structures, the protrusion of the membrane is tightly coupled to polymerization of actin filaments at the leading edge. New actin polymers may be generated in one of two

ways: by elongation of existing filaments, or by nucleation of new filaments followed by elongation.

The actin polymerization at the leading edge relies upon the synergistic interaction of Arp2/3 complex (Actin-Related Proteins) with actin-severing protein cofilin, which generates new actin barbed ends at the leading edge. Arp2/3 is activated by Wiskott-Aldrich syndrome protein (WASP) family. These proteins are multimodular and all possess a conserved C-terminal domain, preceded by several regulatory domains, which associate with a variety of signaling molecules like Rho GTP-ase (Yip S., 2007).

1.4.3 *Focal adhesions*

The molecular machinery that responds to the environmental cues is based on a crosstalk between the actin cytoskeleton and the mechano-responsive sensing machinery, whose elements are named focal adhesions. Focal adhesions are dot-like adhesion structures that are formed underneath the lamellipodium. They are dynamic actin-integrin links, the formation and maturation of which are driven by feedback from spatial and temporal interactions between the actin cytoskeleton and integrin. Actin filaments can be linked to the cytoplasmic domains of integrin subunits through numerous anchoring proteins, such as talin that connects two integrin dimers with actin filaments. Moreover, binding of vinculin to talin triggers the clustering of activated integrins and, through the vinculin tail, their association with actin, thereby strengthening the actin-integrin link (Geiger B., 2009).

Dynamic assembly and disassembly of focal adhesions plays a central role in cell migration. During cell migration, both composition and morphology of focal adhesions change. Initially, small ($0.25\mu\text{m}^2$) focal adhesions called "focal complexes" are formed at the leading edge of the cell in lamellipodia: they consist of integrin, and some of the adapter proteins, such as talin and paxillin. Many of these focal complexes fail to mature and are disassembled as the lamellipodia withdraw. However, some focal complexes mature into larger and stable focal adhesions, and recruit many more proteins, such as zyxin. Once in place, a focal adhesion remains stationary with respect to the extracellular matrix, and the cell uses this as an anchor on which it can push or pull itself over the ECM. As the cell progresses along its chosen path, a given focal adhesion moves closer and closer to the trailing edge of the cell. At the trailing edge of the cell focal adhesions must be dissolved. To this aim the phosphatase calpain could participate by cleaving components of focal adhesions

(Huttenlocher A., 1997).

Focal adhesions not only serve for cell anchorage, but can function as sensors, which inform the cells about the condition of the ECM and thus affect their behaviour (Riveline D., 2001). Indeed, at these sites there is a big molecular complexity: focal adhesions can contain over 100 proteins, not only structural but also regulatory, which suggest a considerable functional diversity. Sorting this group of proteins according to their expected functions reveals cytoskeleton proteins (besides vinculin and talin, e.g. paxillin); tyrosine kinases (e.g. Src, FAK, PYK2, Csk and Abl), serine/threonine kinases (e.g. ILK, PKC and PAK), modulators of small GTPases (e.g. ASAP1, Graf and PSGAP), tyrosine phosphatases (SHP-2 and LAR PTP) and other enzymes (PI 3-kinase and the protease calpain II) (Zamir E., 2001). The best-studied regulatory protein is the focal adhesion kinase (FAK). This is a non-receptorial Tyr kinase, which is localized to focal adhesions and acts as a key intermediary in numerous integrin-originated signaling pathways. In fact, it is activated by numerous stimuli and functions as a biosensor or integrator, which through multifaceted and diverse molecular connections, can influence cytoskeleton, structures of cell adhesion sites and membrane protrusion to regulate cell movement (Mitra S.K., 2005). Another focal adhesion associated protein is paxillin, a 68-70 kDa phosphotyrosine-containing protein. Since paxillin does not exhibit enzyme activity, but contains an array of docking sites for other proteins, it is believed to function as an adaptor protein to recruit to the focal adhesions diverse cytoskeleton and signaling proteins, or specific combinations of signaling molecules, into a complex to coordinate the transmission of downstream signals (Schaller M.D., 2001). Among the paxillin partners there are actin-binding proteins, such as vinculin, or enzymes and kinases, e.g. FAK and ERK. Several of the paxillin-binding proteins have oncogenic equivalents, such as v-Src and Bcr-Abl. These proteins probably use paxillin both as substrate and as a docking site to perturb, and even bypass, the normal adhesion and growth factor cascades necessary for controlled cell proliferation (Turner C., 2000). Paxillin is involved in a mechanism for regulation of cell motility that involves its nuclear-cytoplasmic shuttling. Paxillin interacts with PolyA-binding protein 1 (PABP1), promoting the export of PABP1-bound mRNAs into cytoplasm and the subsequent targeting of the ribonucleoprotein at the leading edge of a migrating cell. It is postulated that paxillin serves as a chaperone that directs the targeting of specific mRNAs to nascent focal adhesions, where localized protein translation has an impact on the focal adhesion turnover necessary for efficient cell

locomotion (Hervy M., 2006).

1.4.4 Contractile forces, traction and rear release

At least two distinct types of force must be generated independently by a moving cell. The first is the protrusive force needed to extend membrane processes, lamellipodia or filopodia. As discussed earlier, actin polymerization and structural organization provide this force independent of myosin motor activity. The second force is a contractile force, needed to move cell body forward. This force appears to depend on active myosin-based motors. In fact, translocation of the cell body forward, once the membrane protrusion has become adherent to the substratum, occurs by myosin interactions with actin filaments.

Detachment of the cell rear, instead, involves disruption of cell-substratum attachments, accelerated by myosin-mediated actin filament contraction pulling on adhesion complexes (Mitchison T.J., 1996; Bretscher M.S., 2008).

1.5 Ras and its effectors in regulating cell migration

Most models of cell motility involve Ras-GTPase. For example, expression of dominant negative H-Ras (S17N) has been shown to inhibit motility in many carcinoma cells, including serum-stimulated chemotaxis of T24 bladder carcinoma cells (Gildea J.J., 2000), hepatocyte growth factor (HGF) stimulated chemotaxis of various ovarian carcinoma cells (Ueoka Y., 2000) and chemotaxis of MCF-7 breast cancer cells toward uPA (Nguyen D.H., 1999). In these cases, the effects of H-Ras on cell motility appeared to be through activation of MAP kinase cascade. In EGF-stimulated MTLn3 carcinoma cells, it was demonstrated that Ras is required for PI3K activation, PIP3 production and lamellipodial extension thus suggesting a role for Ras in forming protrusions required for cell motility (Yip S.C., 2007). Moreover, studies in *Dictyostelium discoideum* and mammalian neutrophils, showed that Ras is rapidly and transiently activated in response to chemoattractant stimulation at the leading edge of chemotaxing cells (Wilkins A., 2001; Sasaki A.T., 2004; Sasaki A.T., 2007). Although Ras is uniformly distributed along the plasma membrane, in chemotactic cells, Ras activation primarily takes place at the leading edge. This localized activation mediates leading edge formation through activation of basal PI3K present at the plasma membrane and other Ras effectors required for chemotaxis. These experimental results implicate Ras as an essential part of the system that controls the ability of cells to sense a chemoattractant gradient.

Introduction

Further understanding of the role of effectors, downstream from Ras, in regulating cell motility, is desirable. Given the growing number of Ras effectors, it is not surprising that the regulation of cell motility by Ras may involve many downstream pathways. Three effector pathways have been intensively studied for their involvement in Ras mediated cell migration: Rho GTPases, PI3K and ERK pathways.

1.5.1 Rho GTPases

The oncogenic properties of Ras were shown to be critically dependent on the functions of Rho family of GTPase, including Rac, Cdc42 and Rho. Ras can cause Rac activation via PI3K or Tiam1 (a GEF for Rac). How Ras regulates RhoA and Cdc42 function is not clearly understood. Possible mechanism includes Ral regulation of its effector, RalBP1, which acts as a GAP for Rac and Cdc42 (Campbell P.M., 2004).

Many observations point to the involvement of Rho GTPases in cell motility and invasive phenotypes. In fact, the best characterized function of Rho family members Rac, Cdc42, and RhoA is the regulation of the actin cytoskeleton (Raftopoulou M., 2004). Rho regulates the assembly of contractile actin-myosin filaments, while Rac and Cdc42 regulate the polymerization of actin to form peripheral lamellipodial and filopodial protrusions, respectively. In addition, all three GTPases promote the assembly of integrin-based matrix adhesion complexes and they can, in distinct ways, affect the microtubule cytoskeleton (Nobes C.D., 1999). Indeed, Rho GTPases can capture and stabilise microtubules through their effectors (e.g. IQGAP1, mDia and Par6) near the cell cortex, leading to polarised cell morphology and directional cell migration (Fukata M., 2003).

In cell migration, Rac is required at the front of the cell to regulate actin polymerization and for the formation of lamellipodia at the leading edge of the migrating cells and is thought to be the driving force for cell movement. Cdc42 also induces actin polymerization at the front of migrating cells, but for the formation of filopodia, not lamellipodia. The role of filopodia appears to be probing the extracellular milieu rather than being directly required for cell movement. Cdc42 has been suggested to be involved in the regulation of cell polarity, controlling the direction of cell movement. Between the cellular targets of Rac and Cdc42 that promote changes to the actin cytoskeleton, there is the Ser/Thr kinase p65PAK. It is commonly activated after either Rac or Cdc42 activation and is believed to play an important role in regulating actin dynamics and cell adhesion during migration. p65PAK regulates focal adhesions

Introduction

turnover, with the help of PIX and GIT1 (GRK interactor 1), but how it does so is not known. In addition, p65PAK phosphorylates and activates LIM kinase (LIMK), which in turn phosphorylates and inactivates cofilin. Cofilin facilitates subunit dissociation from the pointed end of actin filaments and induces filament severing and is essential for promoting filament treadmilling at the front of migrating cells. Members of the WASP/SCAR/WAVE family of scaffold proteins are key regulators of actin polymerization. In their activated state, each of these proteins is able to stimulate the Arp2/3 complex, which can initiate actin polymerization either de novo or at the barbed end or sides of preexisting filaments. WASP/WAVE can also bind to profilin, which acts synergistically with Arp2/3 to speed up actin polymerization. Cdc42 activates WASP and N-WASP directly, but Rac activates the Scar/WAVE family indirectly and this involves an Nck-adaptor complex (Machacek M., 2009).

Rho is involved in regulation of the contraction/retraction forces required in the cell body and at the rear, and it follows an inverse distribution of Rac. Rho regulates assembly of actin stress fibers and associated focal adhesions through activation of its down-effectors mDia and the p160ROCK kinase (Begum R., 2004). In its active state, p160ROCK, like p65PAK, can phosphorylate and activate LIMK, which in turn phosphorylates and inactivates cofilin leading to stabilization of actin filaments within actin:myosin filament bundles. p160ROCK interacts with and phosphorylates the myosin binding subunit (MBS) of myosin light chain phosphatase and thereby inactivates it. This leads to increased levels of myosin phosphorylation, which then can cross-link actin filaments and generate contractile force. At the rear of a migrating cell, this promotes movement of the cell body and facilitates detachment of the cell rear. The other downstream target of Rho is mDia. The binding of Rho to mDia opens up and activates this scaffold protein. It cooperates with p160ROCK in the assembly of actin-myosin filaments, but its biochemical mechanism of action is still unclear. Since Rho negatively influences cell migration by increasing stress fiber-dependent adhesions to the substrate, a tight control of Rho activity is required to balance the opposing effects of cell body contraction and adhesion. Rho activity at the front of a migrating cell is incompatible with membrane protrusion and mechanisms must be in place to inhibit its activity at the leading edge. One way this might occur is through Rac. Studies conducted in fibroblasts demonstrated that the expression of activated Rac inhibits Rho function and that the reciprocal balance between Rac and Rho activity determines cellular morphology and migratory behavior (Sander E.E., 1999).

1.5.2 *PI3K pathway*

As described above, upon activation, PI3K induces local PIP3 formation at the inner leaflet of the plasma membrane, resulting in a net accumulation at the leading edge of PIP3, which serves as a docking site for various proteins containing phospholipid binding domains, such as the PH domain. The production of PIP3 leads to an increase in GTP-bound Rac (Raftopoulou M., 2004). The mechanism by which this lipid promotes GTP loading on Rac is thought to be through a direct interaction with Rac GEFs. All members of the Dbl family of Rac GEFs contain a PH domain and at least some of these can bind phospholipids. In this case, a major role of PIP3 is thought to be in inducing membrane translocation. Tiam-1, a Rac specific GEF, provides an example where the PH domain regulates targeting to the plasma membrane. When localized at the front of a migrating cell, Tiam1 activates Rac and promotes actin polymerization. However, the relationship between Rac and PI3K during cell migration may be more interesting, since the two are able to directly interact with each other. Rac activation stimulates PI3-kinase, since Rac can activate this kinase by binding the breakpoint cluster region (BCR) of the regulatory p85 subunit, leading to the production of PIP3. Moreover, Rac effectors such as SCAR (WAVE) and WASP proteins bind to and are regulated by PIP3, leading to localized polymerization of F-actin. This would provide an opportunity for a positive feedback loop that amplifies the signal and leads to massive F-actin polymerization at the leading edge of chemotaxing cells. The disruption of this feedback loop results in a jerky, non-polarized cell response to chemoattractants (Yip S.C., 2007). On the other hand, ArhGAP15, a PH-domain containing Rac-GTPase-activating protein (GAP), binds to and is activated by PIP3 in migrating cells, suggesting that PIP3 also regulates the GAP-promoted inactivation of Rac during chemotaxis (Costa C., 2007). Another mechanism, which could be parallel to or intertwined with Rac-PI3K, is Ras-PI3K feedback loop. The possibility of a local positive feedback loop between Ras and PI3K is supported by studies showing that Ras-GTP activates PI3K by direct interaction with the p110 catalytic subunit, and that PI3K contributes to Ras activation through the PIP3 mediated enhancement of Gab1 phosphorylation and recruitment of Grb2/Sos (Yip S.C., 2007).

A well-known downstream effector of PI3K signaling is Akt, which directly binds to and is positively regulated by PIP3. Although Akt is mostly known for its role in cell growth and survival, increasing evidence suggests that it is also involved in cell migration (Kolsch V., 2008). Akt

regulates myosin II assembly by activating PAKa (p21-activated kinase-a) and it has also been proposed to regulate actin dynamics via direct binding to and phosphorylation of actin or via phosphorylation of the actin-binding protein Girdin (Akt phosphorylation enhancer, APE). APE localizes to the leading edge and is essential for the integrity of the actin cytoskeleton in migrating cells.

Initial experiments in *Dictyostelium* suggested that PI3K activity and the subsequent formation of localized intracellular PIP3 gradients, are required for chemotaxis, especially for external-gradient sensing during chemotaxis. However, studies over the past years indicate that PI3K and localized PIP3 gradients, although important, are dispensable for chemotaxis under many conditions. For example, a multiple-knockout strain lacking all five *Dictyostelium* class I *pi3k* genes is still able to undergo chemotaxis in strong chemoattractant gradients, but shows reduced speed (Hoeller O., 2007). Polarization of membrane PIP3 is therefore not required for directed chemotaxis, but rather helps by ensuring rapid movement in response to chemoattractants. In *Dictyostelium*, the link of PI3K and polarized PIP3 to control of cell speed and pseudopod formation is highly important in basic cell motility and shallow gradients but becomes less so in the presence of a strong chemotactic signal (Wessels D., 2007; Sasaki A.T., 2007).

In mammalian cells, localized PIP3 production and PI3K activity control polarization and migration during chemotactic movement. In neutrophils, PIP3 accumulates at the leading edge in a PI3K γ -dependent manner. Neutrophils lacking PI3K γ move more slowly than wild-type cells, but do not show defects in directional sensing, similar to the *Dictyostelium* multiple *pi3k* knockout. In addition, *pi3k γ ⁻* neutrophils exhibit strong defects in adhesion. The decrease in speed observed in these cells might reflect the involvement of PI3K in regulating integrin-based adhesion (Ferguson G.J., 2007).

1.5.3 MAPK pathway

Ras oncogenic transformation leads to disruption of actin cytoskeleton and activation of the MAPK pathway. Emerging data implicate the MAPK pathway in the control of F-actin polymerization and focal adhesions turnover, required for cell morphogenesis and migration.

In Ras-transformed cells, the ERK pathway is involved in Rho kinase downregulation; how this regulation is produced is still unclear, although likely targets would include GEFs and GAPs that control Rho GTP loading. In addition, other proteins, such as Fra1, also play a role: in colon

Introduction

carcinoma cells loss of Fra1 results in an up-regulation of RhoGTP levels and ROCK activity. As Fra1 expression is controlled by ERK, these studies demonstrate that ERK activity can promote migration of colon carcinoma cells by Fra1-dependent suppression of Rho/ROCK activation (Vial E., 2003).

ERK signaling can also contribute to membrane ruffling formation, downstream from oncogenic Ras, through mechanisms, such as transcriptional upregulation of urokinase plasminogen receptor (uPAR), an activator of Rac (Barros J.C., 2005).

Regarding focal adhesions, ERK activation is temporally and spatially associated with integrin clustering during cell spreading and may play a role in regulating the focal adhesion assembly process. Active ERK may be targeted to newly forming focal adhesions after integrin engagement. In this case, both active ERK targeting and cell spreading may be blocked by UO126, an inhibitor of MEK1 (Fincham V.J., 2000). Components of the integrin to focal adhesions pathway include several ERK substrates that might be responsible for ERK-induced peripheral effects on cell migration. One of this is myosin light chain kinase (MLCK). Active ERK induces the phosphorylation of MLCK that in turn induces phosphorylation of the myosin light chain, which promote myosin ATPase activity. Thus, MLCK activation might be involved in turnover of focal adhesions and extension of membrane protrusions at the front of polarized cells, which are important for cell migration. Inhibition of the ERK pathway impairs MLCK, MLC phosphorylation and limits cell migration. On the other hand, expression of active MEK1 promotes phosphorylation of MLCK and MLC and enhances cell migration in COS-7, MCF-7 human breast cancer and HT1080 fibrosarcoma cells (Klemke R.L., 1997).

Another target of active ERK is calpain. Calpains are a family of Ca²⁺-activated proteolytic enzymes that are involved in cell migration. ERK phosphorylates calpain at Ser50 both in vitro and in vivo. Phosphorylation of this residue is required for adhesion turnover and cell migration, as Ser50 to Ala mutation in calpain inhibits migration of murine fibroblast cell line (Glading A., 2004). Calpain may associate with the N-terminus of FAK, thus targeting it to focal adhesions, where it can act on a number of substrates including regulatory and cytoskeletal proteins, eventually causing disassembly of focal adhesions and detachment of the cell membrane from the substrate (Huang C., 2004). Calpain affects Rho signaling by removing its membrane targeting sequence and releasing its association with the membrane. Calpain-mediated proteolytic inactivation

of actin binding proteins, such as WASP, cortactin and spectrin, may result in F-actin turnover. FAK itself is also a target for calpain proteolysis. Thus, the relationship between FAK and calpain is complex: FAK is required to recruit calpain to focal adhesions and for calpain activation, but it is also a target for calpain mediated proteolysis during focal adhesion turnover. Indeed, FAK serves as an adapter to bring calpain close to its activator ERK; once activated calpain exerts its effect on FAK by proteolysis (Pullikuth A.K., 2007).

Recently, a novel ERK substrate was characterized: epithelial protein lost in neoplasm (EPLIN). It was originally identified as the product of a gene transcriptionally down-regulated or lost in a number of human epithelial tumor cells, including oral, prostate, and breast cancer cell lines. When present, EPLIN cross-links and bundles actin filaments, thereby stabilizing actin stress fibers. In addition, EPLIN inhibits nucleation of new actin filaments by Arp2/3 complex. These effects result in overall reduction of cell motility. ERK is able to control EPLIN activity by phosphorylation of Ser360, Ser602, and Ser692 in the C-terminal region. These phosphorylation events reduce EPLIN affinity for actin filaments, and cause destabilization of stress fibers and reorganization of the actin cytoskeleton in protrusive structures, eventually enhancing cell migration. A similar effect may be observed by RNAi-mediated silencing of EPLIN, which also results in enhanced cell motility. In contrast, expression of an EPLIN mutant, not phosphorylatable by ERK, prevents stress fiber disassembly and membrane ruffling and inhibits cell migration (Han M.Y., 2007).

Finally, ERK may regulate cellular motility by promoting transcription of specific genes, including early responsive genes AP-1, and the already mentioned Fra-1. Some late responsive genes are also induced via ERK, such as the receptor for urokinase-type plasminogen activator (uPA), and matrix metalloproteinases (MMP), matrix degradation enzymes associated with formation of lamellipodia extensions and tumor invasion (Gialeli C., 2010). Early and late genes activation are probably related, as genes coding for some proteolytic enzymes (e.g., MMP-1, MMP-3, MMP-7 and MMP-9) have an AP-1 consensus sequence in their promoters, and are known to undergo up-regulation upon activation of ERK1/2 (Wu W.S., 2008; Katz M., 2007).

1.6 Methods for studying cell migration

Cell cultures are often studied as model systems for movement, as cells growing *in vitro* typically move on the culture surface using the same

Introduction

complex membrane machinery used by cells *in vivo*. Cultures of eukaryotic cells are a complex system where most cells move according to apparently ‘random’ patterns, but may be induced to a more coordinate migration by means of specific stimuli, such as the presence of chemical attractants or the introduction of a mechanical stimulus. Random movement is characterized by minimal or no directionality and occurs in the absence of any external guidance cue. If a motogenic stimulus, such as a chemical gradient or another external guidance cue, influences movement, the cell steering mechanism reacts to the asymmetric environment and the cell undergoes directed migration.

The nature of the asymmetric cue will often define the type of directed migration and it is important to distinguish between different modes of cell movement and how they are measured. Chemokinesis and chemotaxis are processes where cell motility is generated in response to soluble molecules, such as growth factors or cytokines. Chemokinesis consists of a non-directional movement triggered by uniformly distributed signal molecules, while chemotaxis indicates a directional movement driven by a concentration gradient of signal molecules. Similarly, haptokinesis and haptotaxis are forms of non-directional and directional movement, respectively, occurring in response to extracellular matrix (ECM) molecules, such as fibronectin or hyaluronan (Petrie R.J., 2009).

1.6.1 Time-lapse microscopy

Video time-lapse microscopy of cultured cells is a technically challenging method, and allows to dynamically study movement, by keeping track of multiple cells in a single experiment. By acquiring multiple images of the same field over time, a collection of images is produced which together describe migration in two dimensions. This approach has been modified to detect cell movement in artificial 3-dimensional matrices, which in some cases may, better than with the 2-dimensional approach, reflect the motility of carcinoma cells *in vivo* (Horino K., 2001). By altering the concentration of stimulating molecules, all four forms of cell motility described above may be studied. The involvement of specific proteins in motility may be assayed both genetically and pharmacologically. Moreover, by expressing fluorescently tagged proteins, such as fusion to green fluorescent protein (GFP), the cellular locations of specific proteins during locomotion may be determined.

With this approach cell motion is evaluated by tracking subsequent cell positions, with the assistance of a computer, either manually, by marking the positions assumed by individual cells in stacks of recorded images, or

automatically. Automatic cell tracking algorithms are not generally as accurate as manual recording, but require less time and may be used for the analysis of a larger number of cells. They use simple methods that calculate the position assumed by a labelled cell or the nucleus, after segmenting the image on the basis of intensity (Dmytriiev A., 2006), or more sophisticated methods, where subsequent deformations of an initial contour model are used to identify cell boundaries in the next frames (Chenglu W., 2007). Paths are typically described by lists of coordinates corresponding to the trail followed by moving cells, and are subsequently analyzed in order to extract descriptive parameters.

1.6.2 Wound healing assay

The in vitro scratch assay is an easy, low-cost and well-developed method to measure cell migration in vitro. Confluent or subconfluent cell monolayers are scraped to create a “wound”, i.e. an acellular area, which is then monitored to see how the remaining cells move into it and fill the empty space. This method is based on the observation that, upon creation of an artificial gap on a confluent cell monolayer, the cells on the edge of the newly created gap move toward the opening space to close the “wound” (Liang C.C., 2007). Capturing images before and after migration and comparing them to evaluate the ability of cells to close the gap is the typical end point wound healing assay (Fenteany G., 2000). The wound-healing assay can be coupled to time-lapse microscopy by acquiring images at regular intervals during the process, comparing and analyzing the images to quantify the migration rate of the cells. It provides the advantage of easily determine the actual speed of wound closure at any phase and allows to follow the movement of each individual cell.

Wound healing assays coupled to live cell imaging, allow the analysis of intracellular signaling events during cell migration by means of constructs such as GFP-fusion proteins which may be used to detect changes in localization within moving cells (Danninger C., 2000). The assay is also used to study the regulation of cell migration by cell-matrix and cell-cell interactions (Schultz G.S., 2009). This method has been used, combined with other techniques, such as microinjection or gene transfection, to assess the effects of expression of exogenous genes on the migration of individual cells (Simpson K.J., 2008).

1.6.3 Computational methods: MotoCell

A web application, MotoCell, developed in our laboratory, was used to evaluate the motility of cell populations within this work. The application

uses an online approach to create an environment where cell tracking, parameter evaluation and statistical analysis are tightly integrated (Cantarella C., Sepe L., 2010, <http://motocell.ceinge.unina.it>).

Cell tracking is performed by clicking at the various positions occupied by a moving cell in subsequent frames; x-y coordinates are recorded and written to a table. The destiny of each cell following its path is also recorded: paths may last for the whole observation time, but may also prematurely end with the death of a moving cell, with a cell split in two as a consequence of a mitotic event, or with the loss of a cell, which moves beyond the limits of the observation field. Cell coordinates for each time steps are stored in text files and used to perform calculations through the web interface. Tables and plots reporting the results of statistical analysis may be downloaded as text or PDF files. The system permits the association of cells to one or more subsets, which may be separately evaluated. Statistical analysis of cell behaviour consists of the evaluation of descriptive parameters such as average speed and angle, directional persistence, path vector length, calculated for the whole population as well as for each cell and for each step of the migration; in this way the behaviour of a whole cell population may be assessed as a whole or as a sum of individual entities. The directional movement of objects may be studied by eliminating the modulo effect in circular statistics analysis, to evaluate linear dispersion coefficient (R) and angular dispersion (S) values together with average angles.

1.7 Scientific hypothesis and aim of the work

Directional cell migration is essential in physiological and pathological processes, such as wound healing and metastatization. The involvement of Ras, a small GTPase, in these processes has been extensively demonstrated. In wound healing, many extracellular signals act by converging towards the Ras pathway. On the other hand, Ras is oncogenically activated in more than 30% of human cancers and it has been shown that its activation plays a role in inducing metastatization.

In this thesis an attempt is done to clarify the role of Ras and its principal effector pathways, MAPK and PI3K, in regulating distinct features of cell movement. To this aim wound healing assays were used as an *in vitro* tool to study cell migration, by coupling time-lapse microscopy to quantitative analysis of motion parameters, such as linearity, persistence and directionality. Another target of this thesis is understanding the biochemical phenomena activated downstream from Ras and involved in determining directional cell migration. By using quantitative western blot

Introduction

analysis of ERK phosphorylation, coupled to immunofluorescence staining, spatial and temporal ERK activation has been related with cytoskeletal changes, following the wound stimulus.

MATERIALS AND METHODS

2.1 Cell culture and propagation

Murine fibroblasts with normal and transformed phenotype, respectively NIH3T3, NIHRasV12 and NIHSrc527, were grown in 100mm diameter Petri plates, containing DMEM (Dulbecco's Modified Eagle's Medium) culture medium and 10% FBS (fetal bovine serum). Penicillin (10U/ml) and streptomycin (10 ng/ml) antibiotics and L-Glutamine 2mM were added to culture medium. Each operation was conducted in conditions of sterility under a laminar flow hood vertical. Cells were maintained in incubator at 37°C and with atmosphere made up to 95% by air and 5% CO₂. The culture conditions and cell growth were followed by optical microscope observations.

Cell propagation was performed by detaching cells with a solution of trypsin / EDTA (trypsin 0.05% and 0.53 mM EDTA) and collecting them with complete culture medium.

After centrifugation at 1200-rpm for 10 min, pellets were suspended in fresh medium, properly diluted, and plated again. In order to plate cells with a specific density, the chamber Burker counting was used.

2.2 Materials

PD 98059 (2'-amino-3'-methoxyflavone) was purchased from Calbiochem. A stock solution (20mM) was prepared in DMSO and stored at -20°C. LY 294002 (2-4-morpholinyl-8-phenyl-4H-1-benzopyran-4-one) was purchased from Calbiochem. A stock solution (10mM) was prepared in DMSO and stored at -20°C.

2.3 Random motility assay

To investigate the random movement ability, cells were seeded (25000/well) in 12 well plates and maintained in complete medium at 37°C in an incubator with 5% CO₂. After 16-18 hours, the multiwell was placed in the incubator chamber of the microscope. The motility of cells was determined by recording phase contrast images (with an objective 10x), once every 10 min with a video camera (Axiocam HR) for 10 hours. To determine the scale of the acquired images, a Burker chamber with known measures was recorded.

2.4 Wound healing assay

In order to study the dynamics of wound closure, cells were seeded in monolayers by plating 100000 cells/ml for NIH3T3 and NIHSrc527, and

200000 cell/ml for smaller NIH-RasV12 in complete medium. 24 hours after plating the cell layer was scratched with sterile pipette tip and the closure process was followed for further 24 hours by acquiring one digital frame every 10 min. In order to perform the experiments in low serum, after 16-18 hours in complete medium, the cells were starved by using DMEM 0.5% FBS for further 24 hours, treated (or not, for the control sample) with MEK inhibitor, PD 98059 2 μ M, or PI3K inhibitor, LY 294002 10 μ M, during 1 hour and 30 minutes respectively, then scratched and acquired.

2.5 Time lapse microscopy and image acquisition

Images from different samples have been acquired by using the Zeiss Cell Observer system. The system is composed by a motorized inverted microscope (Axiovert 200M), an incubator chamber for observation of living cells, and a digital camera (AxioCam H/R). The microscope is controlled by an Intel personal computer running Windows XP through the Zeiss acquisition software (Axiovision 6.0) that manages the microscope and captures images both in bright field and fluorescence. The microscope is equipped with a halogen light for bright field observation and a LED illumination system for fluorescence acquisitions. The instrument is equipped with phase contrast optics and provides an incubator chamber to control the temperature (maintained at 37°C), the CO₂ percent and the humidity for the long observation of living cells. Within this work, digital frames were acquired as 14 bit images of 650x514 pixels.

2.6 Cell tracking and quantitative analysis of cell migration

The acquired images were exported as TIFF files and fed to an external application, MotoCell, described in the section “Introduction” (Cantarella C., Sepe L., 2009). Briefly, it is a semi-automatic tool, since the tracking phase was performed manually, specifically developed to track the cell paths by inputting and storing x and y cell coordinates.

Quantitative analysis of migration was performed by using the statistical analysis tool available in MotoCell. The path length is defined as the sum of all subsequent smaller steps made by a cell; the *speed* (fig. 1a) as the average length of all the steps performed by a cell within the time interval; *linearity* (fig. 1b) as the ratio of net displacement (i.e. the distance between the starting and end point) to path length. The average *direction* of a population is the direction of the resulting vector obtained by composing the displacement vectors for each cell path (fig. 1c).

Finally, directional persistence is defined as the angular variations between consecutive steps within small angle, such as an interval of -60;+60 degrees (fig. 1d). Circular statistics analysis (fig. 1e) is used by MotoCell to evaluate descriptive parameters by treating the displacements of each step as circularly varying quantities, corresponding to the angle of each displacement vector, and without taking into account its module (Batschelet E., 1981). For each angle (i.e. α in fig. 1e) cosine and sine values are calculated. The average angle (ϕ) is obtained from the arithmetic mean of cosine and sine values for each angle:

$$\phi = \arctan\left(\frac{\bar{y}}{\bar{x}}\right)$$

The module of the average vector, having its origin in the centre of a circle with unit radius and as direction the ϕ angle, is named linear dispersion coefficient (R) and may be easily calculated as:

$$R = \sqrt{\bar{x}^2 + \bar{y}^2}$$

R is not dependent on the length of each step, and it is descriptive of the distribution of the angles of the step vectors. Its value ranges from 0 to 1, being close to 0 when the angles have a uniform distribution with no directional trend, but gets larger for an asymmetric distribution of angles clustered around a specific direction, reaching 1 for the special case when all the angles are identical. Beyond circular statistics analysis, inferential statistics is used by MotoCell to test the reliability of the calculated parameters.

2.7 Immunofluorescence

Cells plated on coverslips were washed once with PBS 1x, fixed for 20 min at room temperature with paraformaldehyde (3%, w/v in PBS), permeabilized for 5 min with Triton X-100 (0.2%, v/v in PBS) and incubated for 1 h with PBS 1x containing FBS (1%, v/v) to bind to any remaining sticky places. For pERK1/2 detection, coverslips were stained by 1 hour incubation with mouse anti-phospho-p44/42 MAPK mAbs (Cell Signaling Technology), 1:200 in PBS 1x, and washed with PBS 1x. Coverslips were then incubated in texas red-conjugated goat anti-mouse antibody (Santa Cruz Biotechnology), 1:200 in PBS 1x. For paxillin detection, coverslips were stained by 1 hour incubation with mouse anti-paxillin mAbs (clone 349 from BD Biosciences), 1:25 in PBS 1x, and washed with PBS 1x. Coverslips were then incubated in texas red-

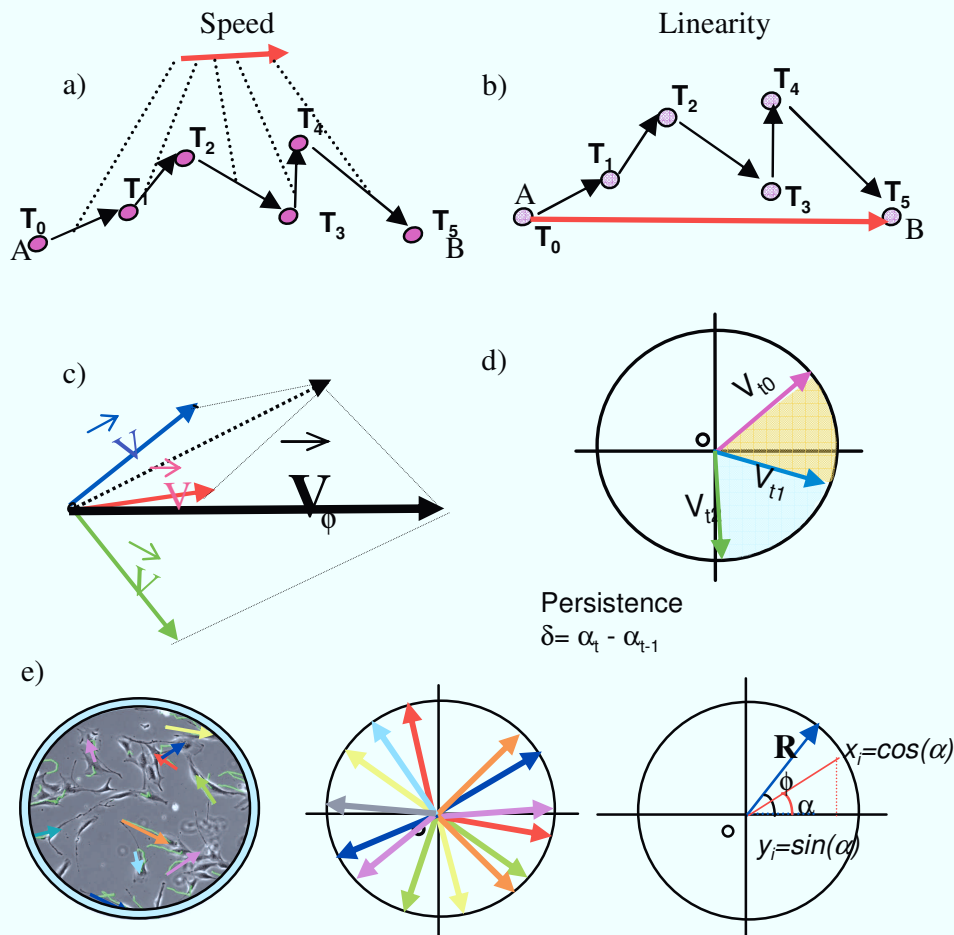


Fig. 1 Quantitative analysis of migration. **a)** Speed was calculated as the average of all step lengths; **b)** linearity as the ratio of net displacement, i.e. the distance between start and end point of a path, to path length. **c)** The average direction of a population is the direction of the resulting vector obtained by composing the displacement vectors for each cell path. **d)** Persistence was studied by calculating the angular variations between consecutive steps; variations within small angle, such as an interval of $-60; +60$ degrees, are considered compatible with persistent motion. **e)** In circular statistic, the directions of cell paths are inserted into a circle of unit radius to neglect the length and consider only the angle. By composing all the directions, a new vector was obtained. The linear dispersion coefficient R is defined as the module of this vector having its origin in the center of a circle with unit radius, and as direction the average angle ϕ . R may assume all values between 0 and 1.

Materials and Methods

conjugated goat anti-mouse antibody (Santa Cruz Biotechnology), 1:200 in PBS 1x. To visualize nuclei coverslips were incubated for 10 min with PBS 1x containing Hoechst 33258 (Fluka) at a final concentration of 1 µg/ml. To visualize actin cytoskeleton coverslips were incubated with 0,1microg/ml of phalloidin–tetramethylrhodamine-B-isothiocyanate (Sigma) for 45 min in a dark and wet place. The coverslips were mounted in Mowiol 4-88 (Calbiochem, CA) on glass slides. Slides were analyzed by using 40x oil objective.

2.7.1 BrdU assay

Proliferation rate was analyzed by BrdU assay. Cells were plated on coverslips and cultured up to 50% of confluence. Cells were then incubated with BrdU 100µM for 1 hour at 37°C and 5% CO₂. At the end of this incubation, coverslips were washed with PBS 1x, fixed for 20 min at room temperature with paraformaldehyde 3%, permeabilized for 5 min with Triton X-100 0.2% and incubated for 10 min with HCl (1.5M in PBS 1x). After coverslips were washed and incubated with diluted (1:10 in PBS 1x) primary antibody, mouse anti-BrdU mAbs (clone BU-33 from Sigma), then treated with diluted (1:200 in PBS 1x) secondary antibody, texas red-conjugated goat anti-mouse (Santa Cruz Biotechnology). To visualize nuclei coverslips were incubated for 10 min with PBS 1x containing Hoechst 33258 (Fluka) and finally washed three times with PBS 1x. The coverslips were mounted in Mowiol 4-88 (Calbiochem, CA) on glass slides. Slides were analyzed by using 40x oil objective.

2.8 Lysates and immunoblotting

NIH3T3 cells were washed twice with cold PBS 1x, directly solubilized in denaturing sample buffer (Tris/HCl 50mM pH 7.0, NP-40 0,5%, NaCl 250mM, NaOV 10mM, NaF 25mM, NaPP 20mM, protease inhibitor cocktail tablet) and the precipitates were collected by centrifugation for 15 min. Protein samples (20 microg) were supplemented with 5% Dye buffer 5x. Generally full denaturation of the proteins is achieved by boiling the cellular extracts at 90°C.

2.8.1 Gel electrophoresis

The polyacrylamide gels were used at 10% of acrylamide concentration. The electrophoresis was performed starting from 90V to 120V, using the 1X Tris-Glycine running buffer, until the bromophenol blue reached the bottom of the gel.

Materials and Methods

2.8.2 Transfer method

The proteins transfer from the gel to the nitrocellulose membrane was performed by using Tris-Glycine-1X transfer buffer with 20% (v/v) methanol. The transfer was conducted at constant intensity of 180 mA for 3 hours. To check the transfer efficiency, a reversible 0.2% Ponceau S red staining was done on the nitrocellulose membrane for 5 min, which was subsequently washed with distilled water before to be scanned.

2.8.3 Immunodetection

The nitrocellulose membrane was saturated with 5% non fat dry milk in TBS solution (TBST), at room temperature for 1 hour. The membrane was washed twice with TBST solution for 5 min at room temperature, and then incubated overnight at 4°C with the primary antibody. For pERK1/2 detection was used a mouse anti-phospho-p44/42 MAPK mAbs (from Cell Signaling Technology), 1:2000 in milk. For beta-tubulin detection, a rabbit anti-beta tubulin mAb (clone 9F3 from Cell Signaling Technology) was used 1:2000 in milk. The membrane was washed twice with TBST solution before to be incubated for 1 hour at room temperature with the secondary antibody. Anti-rabbit IgG coupled to the horseradish peroxidase (Amersham Biosciences) was used 1:3000 in milk; anti-mouse IgG coupled to the horseradish peroxidase (Amersham Biosciences) was used 1:2000 in milk. The membrane was then washed and the detection of proteins was done with Immobilion Western HRP chemiluminescent substrate (Millipore). Digital images were acquired with a Bio-Rad imaging system, ChemiDoc XRS-system, and quantitatively evaluated.

RESULTS

3.1 Constitutive RasV12 activation confers to NIH3T3 cells the ability to close the wound faster

In a typical wound-healing assay, NIH3T3 fibroblasts, grown as a monolayer at high density, are subjected to a scratch to create a gap in the culture layer (fig. 2). In these conditions they respond by extending finger-like protrusions and eventually migrating into the open gap. In fig. 2, timed frames, extracted from a time-lapse acquisition of a wounded NIH3T3 monolayer, show the progression in filling the space, which after 7 hours is in an advanced state of closure.

In a wound healing experiment many factors cooperate to stimulate the remaining cells to move and invade the space left empty by the injury. Since many of these identified signals converge to the Ras pathway, the role of Ras in regulating cell migration was tested by examining the ability of NIHRasV12 fibroblasts, obtained by transfection of parental NIH3T3 with the constitutively activated RasV12 mutant, to close a wound in time-lapse acquisitions (Fig. 3a). Within the 24h of observation, these cells completely repair the wound, unlike the parental NIH3T3 cells, which, as described above, move towards the other side of the wound, but are not able to completely close the gap. The observation of the movies demonstrated a different way used by NIHRasV12 fibroblasts to move towards the empty space. The migratory NIH3T3 cells move as a bit like sheet-like structure by extending filopodial and lamellipodial protrusions at the leading edge. In contrast, RasV12 transformed NIH3T3 cells move quickly towards the wound, as isolated individual cells (Fig. 3b).

3.1.1 RasV12 transformed fibroblasts show morphological changes, increased proliferation rate and speed

The behaviour of NIHRasV12 transformed fibroblasts in wound healing experiments raises some questions, such as what are the cellular effects of Ras overactivation and how does Ras regulate and determine wound closure. RasV12 cells are quite different from the parental NIH3T3 line and are characterized by long and narrow contours and devoid of specific cytoskeletal features such as stress fibers (fig. 4). This phenotype is associated to overexpression of constitutively activated Ras, as the same effect is seen in the epithelial T24, a bladder carcinoma cell line expressing the same constitutively activated RasV12 variant, and also, although at a lower extent, in fibroblasts transformed by the

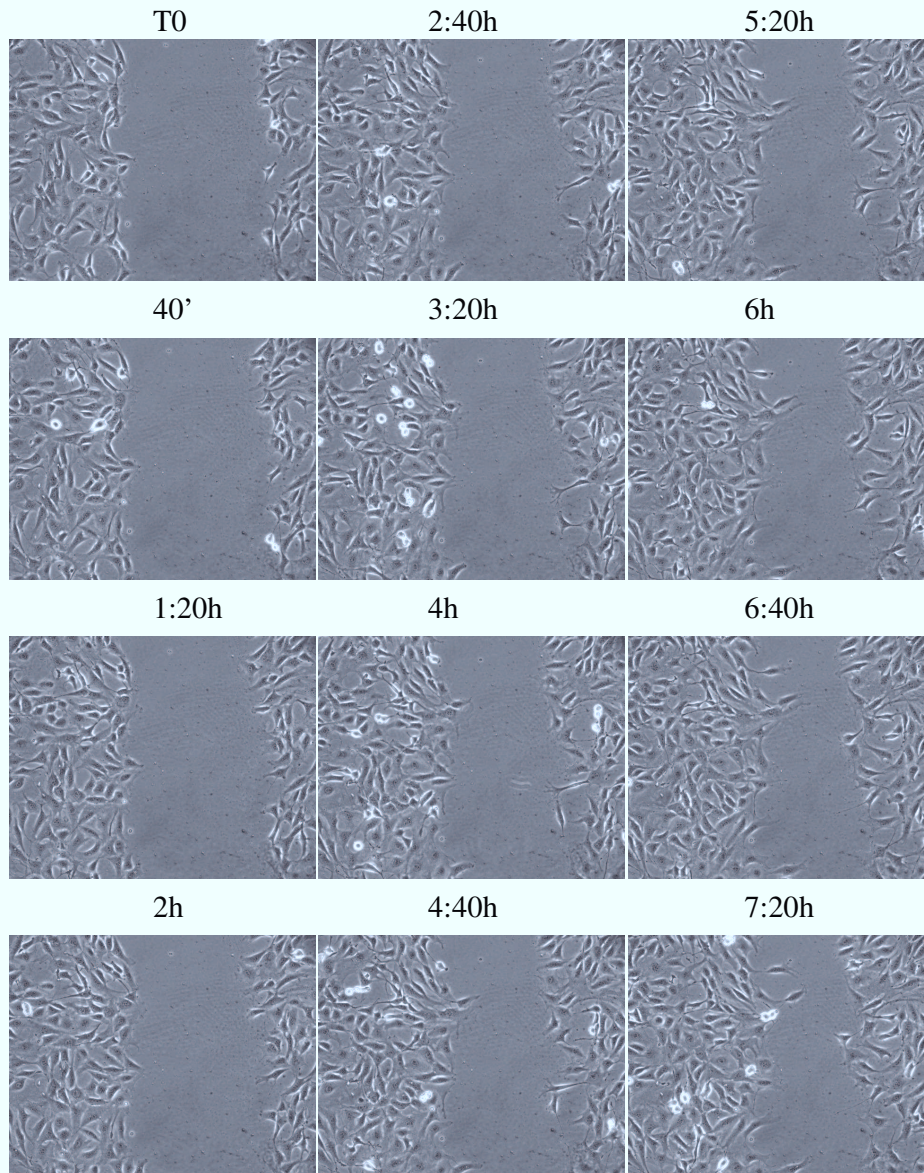


Fig. 2 Wound healing of NIH3T3 fibroblasts. Cells were cultured till 90% confluence and wounded. Subsequent frames of a time-lapse acquisition allow to observe the behaviour of the cells following the wound injury.

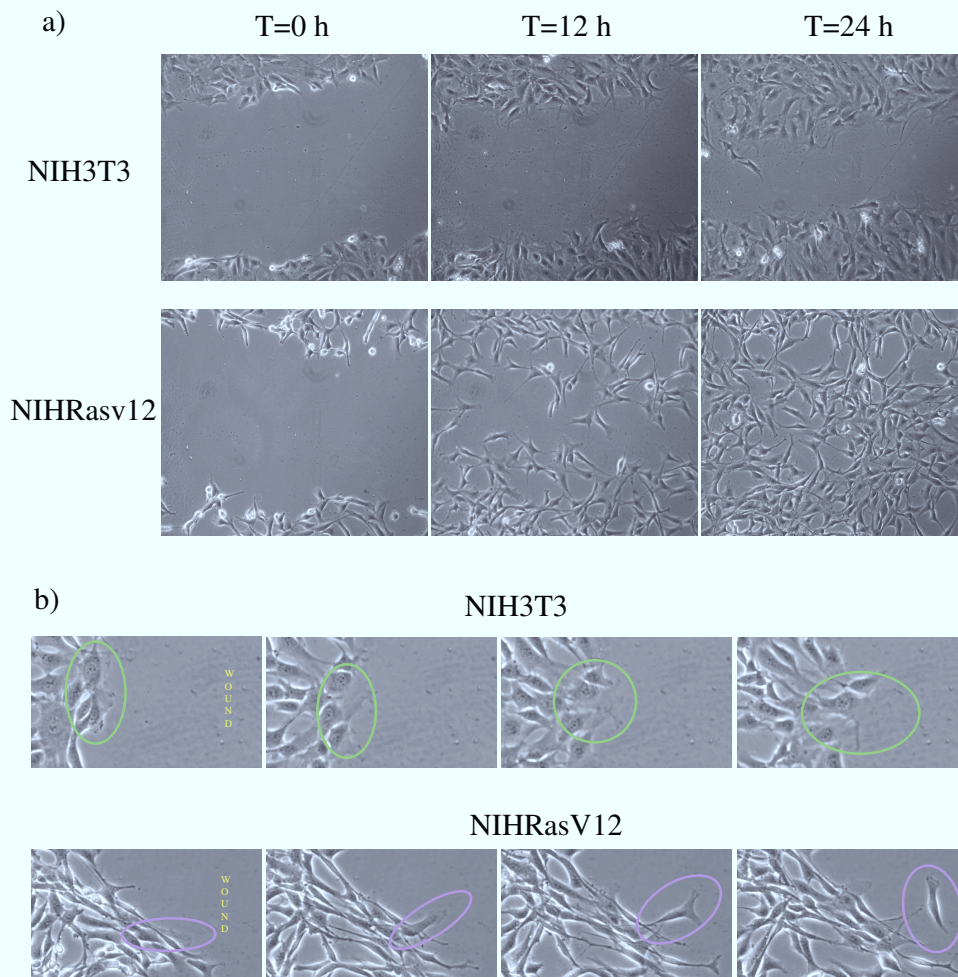


Fig. 3 Constitutive RasV12 activation confers to NIH3T3 cells the ability to close the wound faster. **a)** NIH3T3 and NIHRasV12 behavior in wound healing assay: frames at start (T0), middle (T12h) and end (24h) extracted from 24h time lapse acquisition. After 24 hours of observation NIH3T3 fibroblasts only cover a small portion of the gap and do not succeed in closing. NIHRasV12, on the contrary, perfectly repair the wound within the same period. **b)** Significant frames extracted from time-lapse acquisition showing a selection of NIH3T3 cells (green circle) moving as a sheet-like structure, and NIHRasV12 cells (purple circle) migrating towards the wound singly.

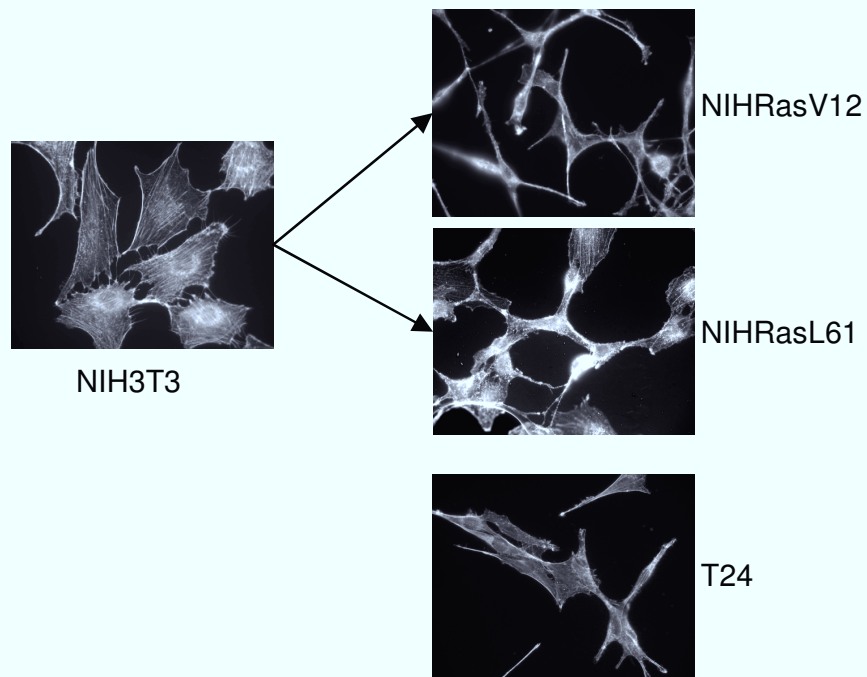


Fig. 4 Constitutive RasV12 activation induces morphological changes. Actin cytoskeleton of parental NIH3T3, RasV12 and RasL61-transformed NIH3T3 fibroblasts, and epithelial T24, bladder carcinoma cells, expressing the constitutively activated RasV12 variant. Control NIH3T3 fibroblasts present several stress fibres and rare membrane rufflings. Ras transformed fibroblasts and T24 cells are characterized by long and narrow contours and devoid of specific cytoskeletal features such as stress fibers.

Results

overexpression of another Ras mutant, RasL61.

NIHRasV12 cell proliferation rates, when assessed by BrdU incorporation assay, are, as expected, increased with values at least twice or more the parental NIH3T3 line (fig. 5a).

Motility was analyzed by studying random movement of cells cultured on plastic surfaces. The observation of the paths covered by parental and transformed cells, shows that fibroblasts with Ras iperactivation move covering longer paths than the parental cell line (fig. 5b). Quantitative analysis of these movements shows that NIHRasV12 average speed is increased when compared to NIH3T3. T24 bladder carcinoma cells move with speed comparable to Ras transformed fibroblasts (fig. 5c).

3.1.2 *Increased cell proliferation is not the main factor for wound closure*

Filling the empty space and closing the wound involve at least two factors: proliferation and migration. Since Ras activation, as described above, positively regulates both events, also without wound stimulus, how Ras intervenes during wound healing was evaluated. To assess if Ras induced high proliferation is directly responsible for wound closure, NIH3T3 fibroblasts transformed with another oncogene, Src527, were observed after subject them to wound (fig. 6a). NIHSrc527 were unable to close the wound within the 24h observation time, although NIHRasV12 and NIHSrc527 transformed cells both have higher proliferation rates, as showed by BrdU incorporation values (fig. 6b).

On the other hand, quantitative analysis of NIHSrc527 random motility shows that Src527 transformed fibroblasts move with average speed comparable to NIH3T3, but lower than NIHRasV12 (fig. 6c).

3.1.3 *Increased speed alone does not explain enhanced wound healing*

As Src527 transformed cells show higher proliferation rates, but speed values similar to NIH3T3, it was asked whether the kinetic advantage of cells migrating towards the gap may explain the accelerated closure. To explore this hypothesis the above wound healing experiments were repeated in 0.5% serum (fig. 7). This limiting condition leads to a strong speed reduction for both parental and transformed cells (fig. 7a), with NIHRasV12 cells moving at 5 $\mu\text{m}/40$ min, even below the 6 $\mu\text{m}/40$ min seen for NIH3T3 and NIHSrc527 in 10% serum. However, under these conditions, NIHRasV12 fibroblasts are still able to fully invade the space left open by the wound, within 24 hours. NIH3T3 cells, instead, are affected by this limiting condition and show only little progress within the same time (fig. 7b).

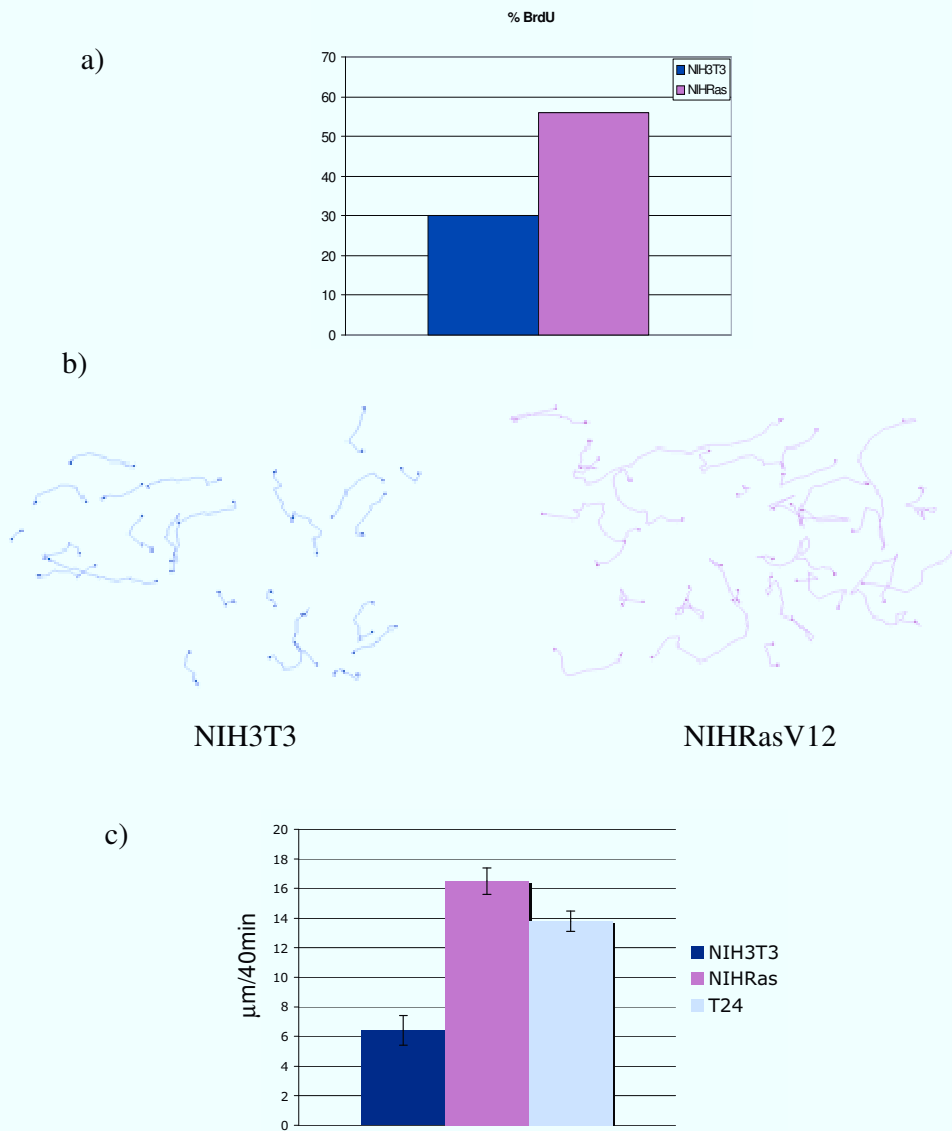


Fig. 5 RasV12 transformation induces increased proliferation rate and speed. **a)** BrdU incorporation of parental and transformed RasV12 fibroblasts. **b)** Paths covered by NIH3T3 and NIHRasV12 cells in random motility assays. **c)** Average speed of NIHRasV12 fibroblasts and T24 bladder carcinoma cells, both expressing activated RasV12 mutant, is compared with that of parental NIH3T3 cells.

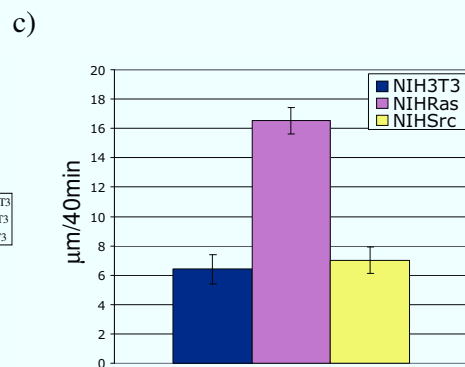
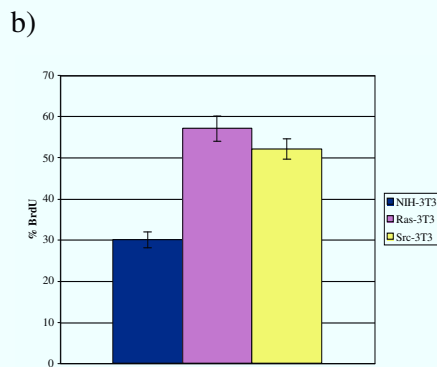
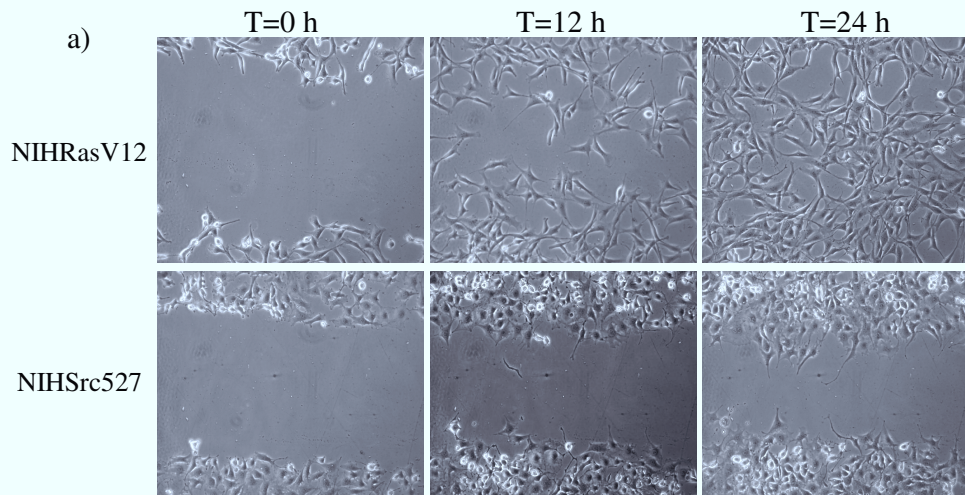


Fig 6 Increased proliferation is not the main factor for wound closure. **a)** Wound healing assay for NIHRasV12 and NIHSrc527 cells: frames at start (T0), middle (T12h) and end (24h) extracted from time lapse acquisition of 24h. **b)** BrdU incorporation rates, **c)** average speed of migration in random conditions, are reported for NIH3T3, NIHRasV12 and NIHSrc527.

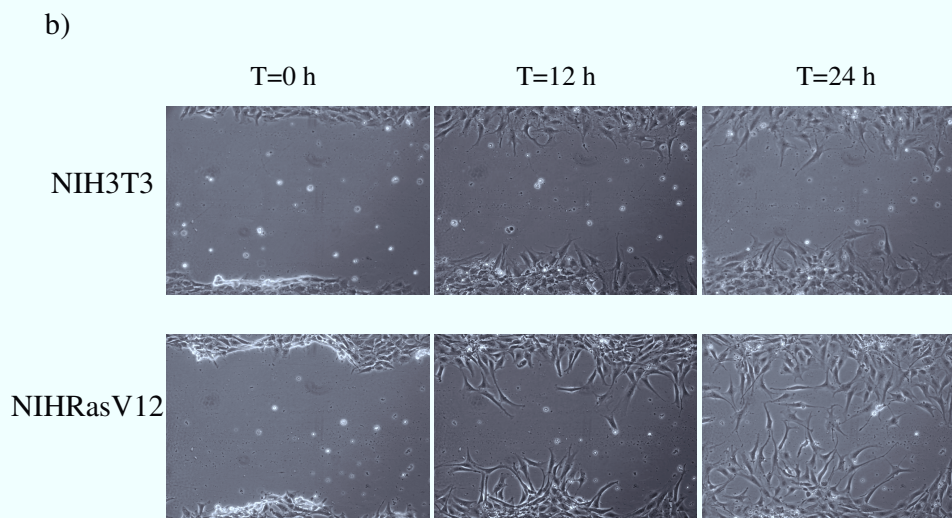
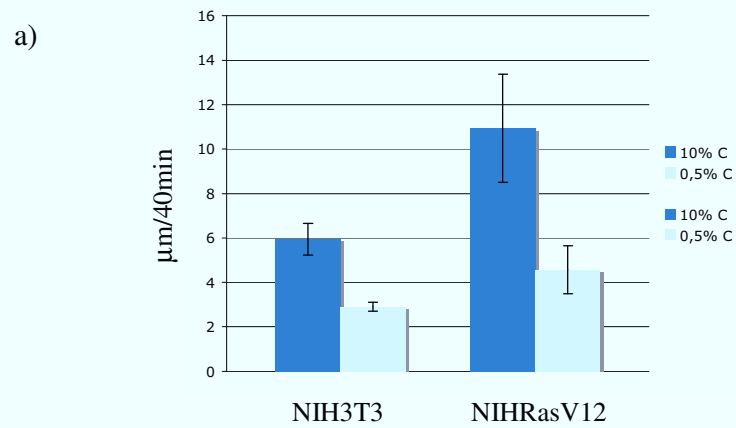


Fig. 7 Wound healing assay under limiting growth conditions (0.5% serum). **a)** Average speed values obtained in low serum culture conditions, for NIH3T3 and NIHRasV12 fibroblasts, are reported, compared with those observed under standard conditions (10% serum). **b)** In 0.5% serum, NIHRasV12 are still able to close the gap, while NIH3T3 continue to fail.

3.1.4 *Under wound stimulus NIHRasV12 cells show better directional movement*

Cell migration may be described by other measurable parameters beyond speed, such as linearity, persistence and directionality. To assess whether Ras constitutive activation changes these parameters, linearity was analyzed together with persistence and directionality. These analysis were performed initially in random conditions, i.e. in absence of stimulus, for both NIH3T3 and NIHRasV12 cells by using MotoCell application (see “introduction” and “materials and methods” sections).

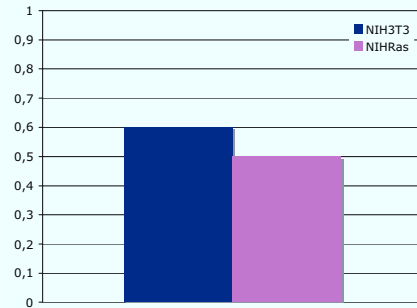
Within this work, linearity is defined as the ratio between the module of the vector describing the distance between the start and end point (the net cell displacement), and the length of the path really followed by the cell. Persistence is defined as the angular variations between consecutive steps within small angle, such as an interval of -60;+60 degrees (see “materials and methods” section, fig. 1).

In both cell lines linearity values are similar, as shown in fig 8a. It is also true for persistence, showed in fig 8b, because for both NIH3T3 (on the left) and NIHRasV12 cells (on the right) the major part of shift angles are concentrated in the persistence interval between -60 and +60 degree, whereas only few shifts are distributed in the not persistence interval of motion.

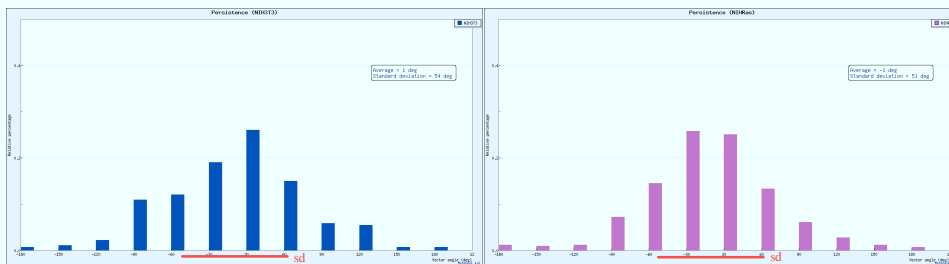
Circular statistics analysis (described in “materials and methods” section, fig. 1) was carried out to separately assess the directional component of cell movement. Evaluating directionality means testing the “null” hypothesis of uniform distribution of cell movements, against the alternative hypothesis of non-uniform distribution of directions, i.e. unimodal, or other patterns leading to an asymmetric distribution of the angles (Bentley J., 2006). The significance of the results was assessed by using the Rayleigh test, which compares the R parameter with a threshold level corresponding to the R value expected from a random distribution, for a given probability ($P < 0,01$) and number of samples (n). The results obtained for transformed and parental cell lines show linear dispersion values indicative of a uniform, non directional movement (fig. 8c). In fact, linear dispersion values for both cell lines are not very high and lower than the significance levels for $P < 0,01$, reported as transparent boxes overlaid onto the histogram in fig. 8c.

These results show that constitutive Ras activation does not alter the described migration features in random conditions. But, how does the wound affect them? To assess whether Ras regulates these motion parameters during wound healing, quantitative analysis of NIH3T3 and

a)



b)



c)

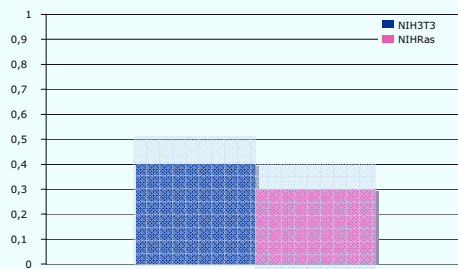


Fig. 8 Linearity, persistence and directionality of random migration are not modified by RasV12. Values of linearity **a)**, persistence (left NIH3T3, right NIHRasV12) **b)**, and linear dispersion (R) **c)**, are reported for NIH3T3 and NIHRasV12 fibroblasts moving in random conditions. In **c)** the significance levels, for $P < 0,01$, are reported as transparent boxes overlaid onto the histogram.

Results

NIHRasV12 cells movement during wound healing was done. Fig. 9a (left) shows that NIHRasV12 cells migrating towards the wound space have speed nearly twice higher than parental line. Although the wound stimulates cells to move faster, their speed is similar to that observed in random motility assays.

Directional analysis shows changes if compared to random motility assays. Linearity values are higher in fibroblasts with Ras iperactivation and are indicative of non tortuous paths (fig. 9a, right). To understand if the wound acts as a directional stimulus for these cells and if the presence of constitutively activated Ras amplifies the directional response, polar plots have been generated with MotoCell by plotting the area defined by connecting all net displacements. These plots graphically visualize at the same time distance covered in each step and distribution of directions. Fig. 9b (left) shows polar plots obtained for random moving cells. Random distribution of directions is easily recognized in both NIH3T3 and NIHRasV12 cell populations, by observing the circular shape of the areas in the charts. The size of each area depends on the length of the various steps: larger for NIHRasV12 cells and smaller for the slower NIH3T3. Both cell lines, when subjected to a wound, respond by turning to directional migration. In fact, in fig 9b (right) the asymmetric shape of each area clearly shows the directional movement, which is more evident for NIHRasV12 cells.

Circular statistics analysis shows, for transformed and parental cell lines, linear dispersion values indicative of directional movement, although at a different extent: 0.45, for NIH3T3 cells, 0.76, for NIHRasV12. These linear dispersion values are both higher than the threshold levels for $P < 0,01$ (fig. 9c).

Furthermore, while parental fibroblasts do not modify the persistence in wound healing assays compared with random migration (fig 9d, left), fibroblasts having constitutive Ras activation migrate in the wound area with angle shifts more concentrated in the persistence interval (fig. 9d, right).

The enhancement of directional migration mediated by Ras, is more evident in 0,5% serum. In fact, although the limiting condition induced by reduced serum causes cells from both lines to slow down, the directional component of RasV12 migration, unlike speed, is enhanced. The shape of polar plot (fig 10a) graphically displays the directionality of cell displacements although the reduced size of the area delimited by the plot highlights the drop of speed. The directional shifts are plotted in fig. 10b. For NIHRasV12 cells (magenta bars) they are clustered in the persistence

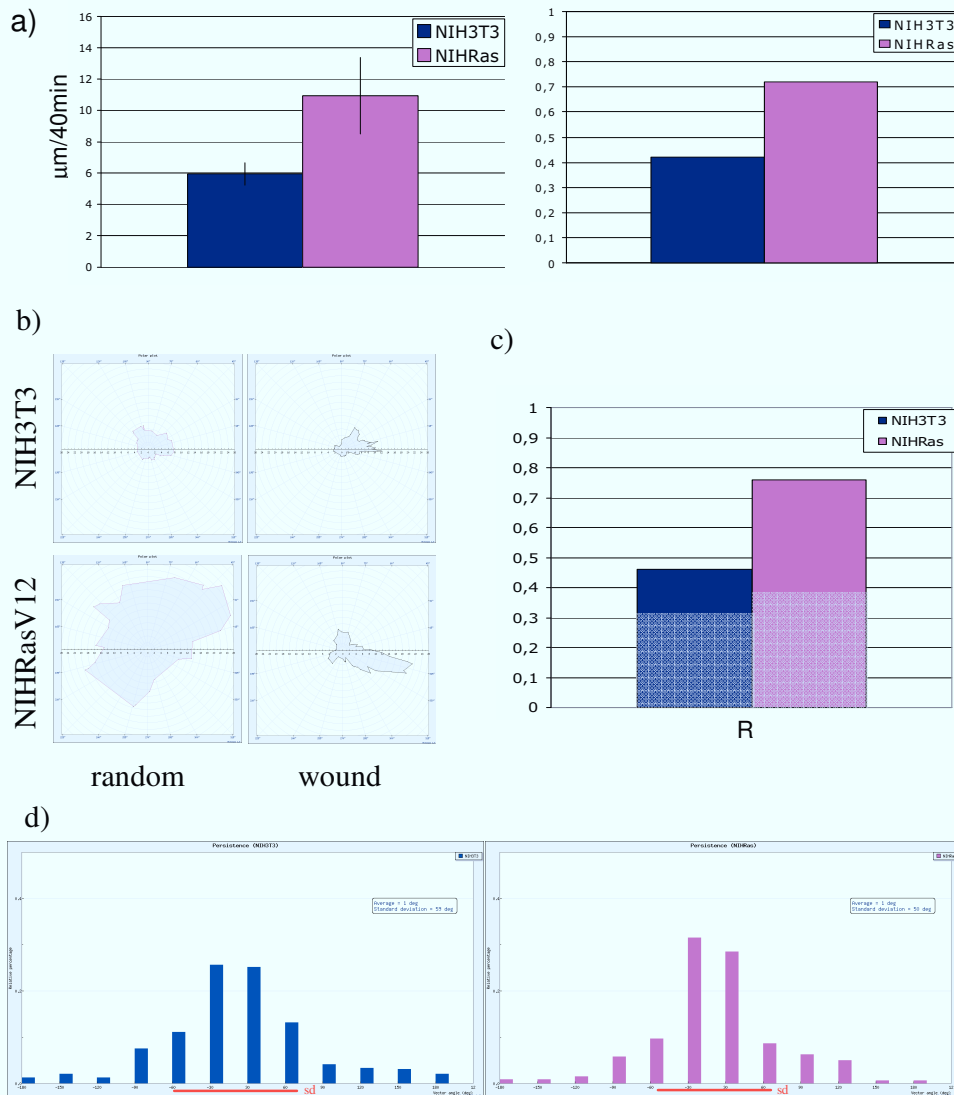


Fig. 9 Quantitative analysis of NIH3T3 and NIHRasV12 movement during wound healing. **a)** NIHRasV12 cells show consistently higher speed (left) and linearity (right) than the parental cell line. **b)** Polar plots representing the distribution of directions for NIH3T3 and NIHRasV12 populations moving random (left) are compared with those obtained for both populations wounded (right). **c)** Linear dispersion values, R, for both NIH3T3 and NIHRasV12 are reported together with the significance levels (transparent boxes). **d)** Directional persistence of NIH3T3 (left) and NIHRasV12 (right) fibroblasts.

interval between -60 and +60 degrees, more than for the parental cell line (blue bars), which show shifts more distributed, also in the not persistence interval of motion. In fig 10c shifts are plotted as the deviation angle from the expected direction, that is towards the centre of the wound, for each path. This deviation for fibroblasts overexpressing RasV12 (magenta) is low, indicating a directional movement compatible with wound closure.

3.1.5 Directional movement is a function of the distance from the wound edge.

By watching the movies, a different behaviour is visible in cells close to the wound edge; in order to quantitatively assess this observation, cells surrounding a wound were separately analyzed as three different sub-populations, selected according to their distance from the wound (front, middle, inner) (fig. 11a).

Circular statistic analysis shows the predominant effect of the wound edge on the front population of both parental NIH3T3 (fig. 11b, left) and NIHRasV12 cells (fig. 11c, left). In 10% serum these sub-populations have stronger directionality with R values high and, for NIHRasV12 fibroblasts well above the threshold for $P < 0,01$. For RasV12 transformed cells directionality remains high also in the other two subpopulations, unlike NIH3T3 cells, where directionality is reduced in a distance dependent way. The pattern remains the same in 0,5% serum, where directionality of RasV12 transformed cells (fig. 11c, right) is increased to even higher values, well above the Rayleigh coefficient for $P < 0,01$, in all subpopulations, while for NIH3T3 (fig. 11b, right) only cells surrounding the wounds move in a directional way.

These results are graphically reported by polar plots in fig. 12a and b (left). The deviation angle from the expected direction, plotted in fig. 12 (right), is very low for all RasV12 cellular populations and for the external subpopulation of NIH3T3 fibroblasts. While the deviation becomes more significant for the far populations of NIH3T3 (fig 12a, right), which also show low directionality.

3.2 MAPK and PI3K differently affect directional migration

To evaluate how and through which effectors Ras regulates speed and directionality of cell migration, wound healing assays were performed by incubating cells in the presence of two inhibitors, PD 98059 and LY 294002, known to block two important signaling pathways downstream from Ras, MAPK and PI3K respectively.

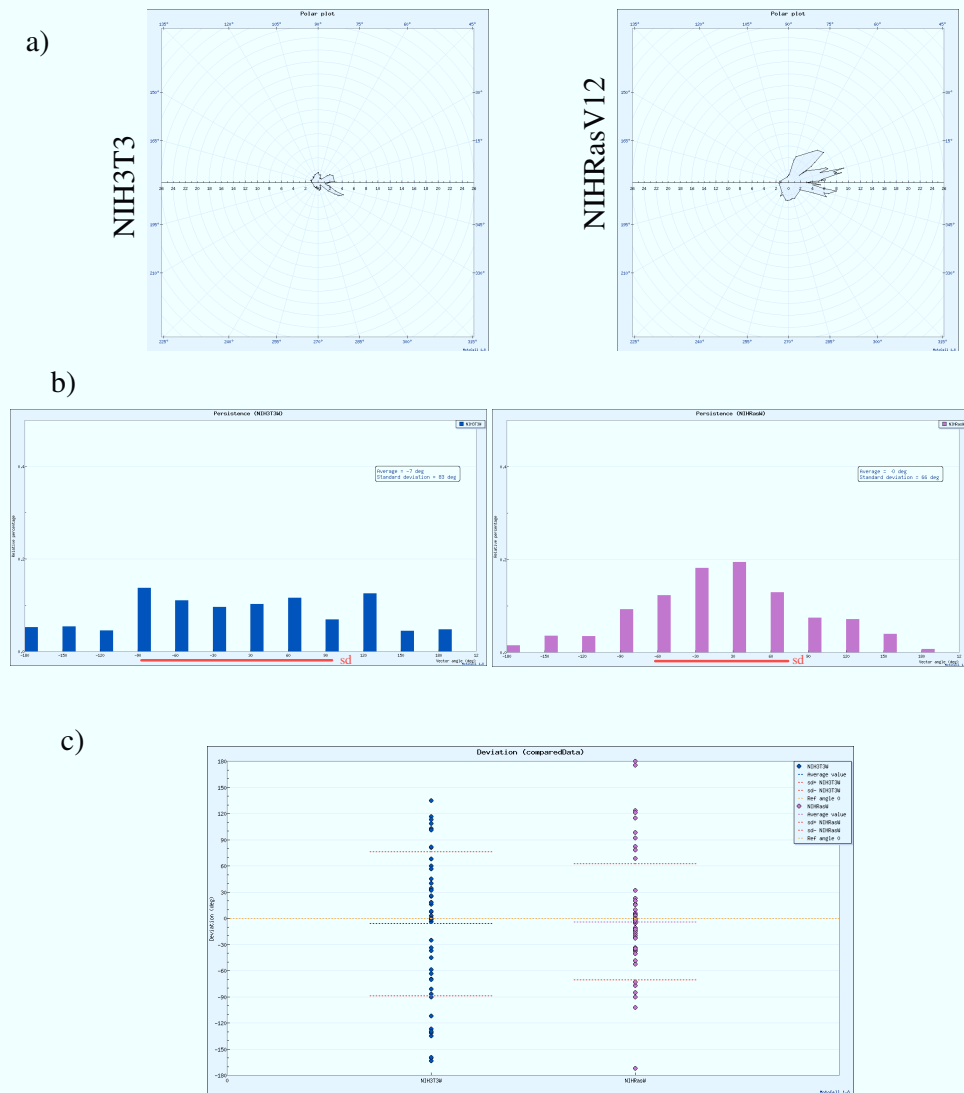


Fig. 10 Quantitative analysis of NIH3T3 and NIHRasV12 movement during wound healing in 0,5% serum. **a)** Polar plots visually represent the distribution of directions for NIH3T3 (left) and NIHRasV12 (right) populations. **b)** Directional persistence of NIH3T3 (blu) and NIHRasV12 (magenta) fibroblasts. **c)** Distribution of deviations angle from the wound direction for NIH3T3 (blu) and NIHRasV12 (magenta) cells. Dotted lines indicate the average direction for NIH3T3 (blu) and NIHRasV12 (magenta). Red dotted lines indicate the standard deviation intervals.

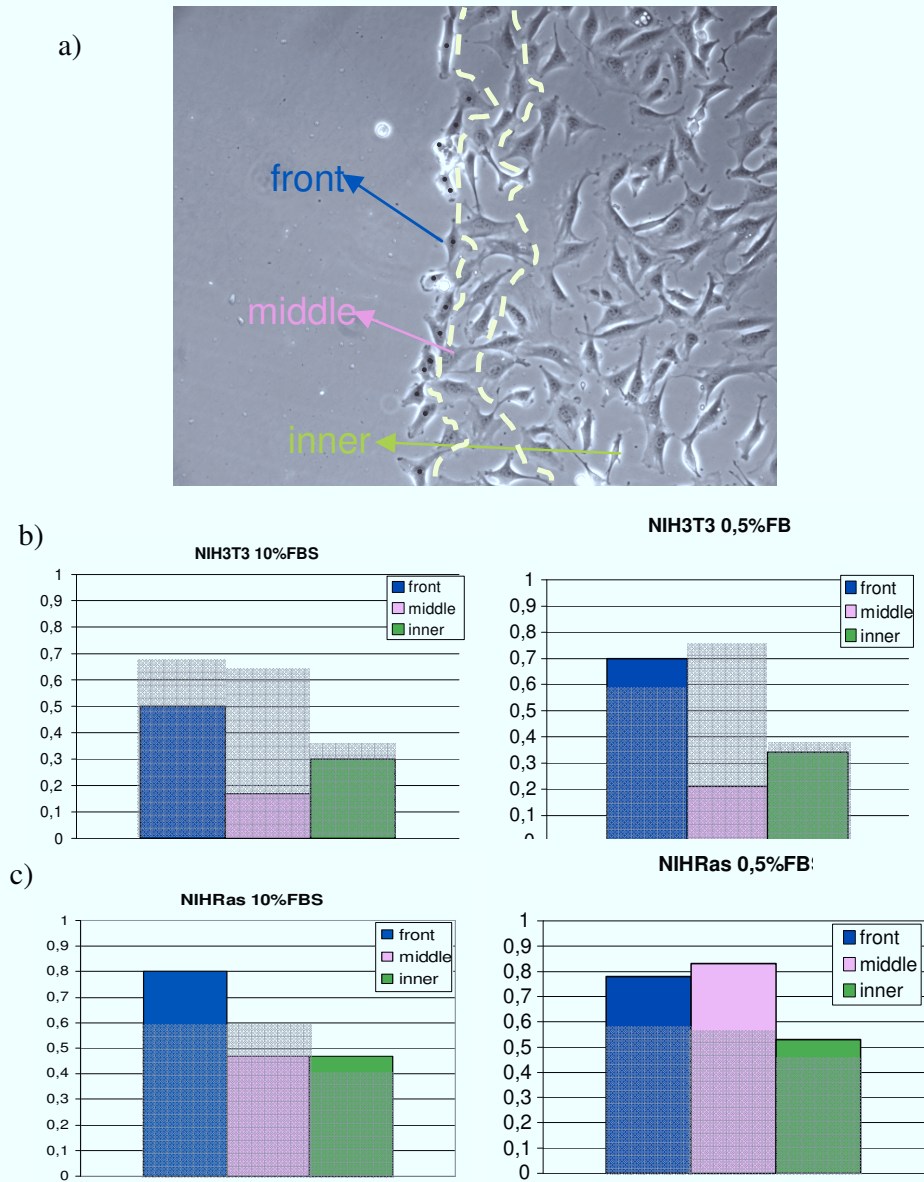
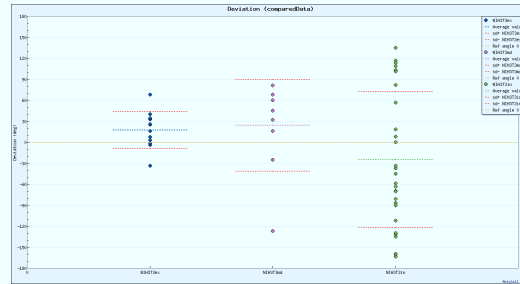
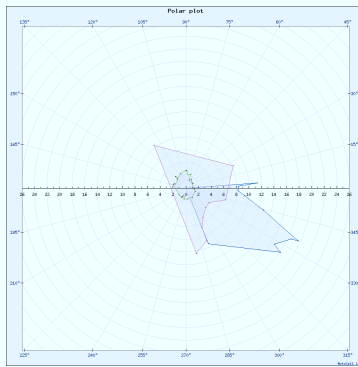


Fig. 11 Identification and analysis of subpopulations. Three subpopulations, front, middle and inner, separated according to their distance from the wound, are represented in a). The R coefficient values obtained for each sub-population are plotted in b) for NIH3T3 and in c) for NIHRasV12 fibroblasts. Plots on the left are indicative of wound healing assays in 10% serum, on the right in 0,5% serum.

a)

NIH3T3



b)

NIHRasV12

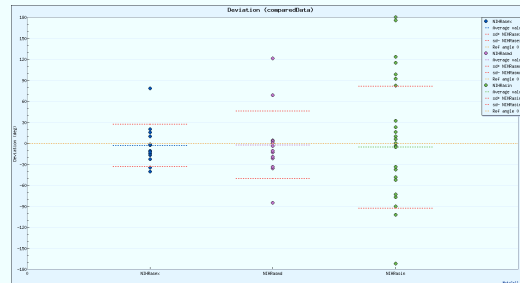
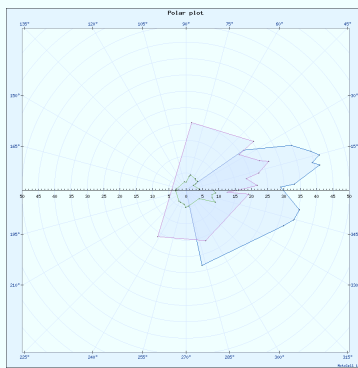


Fig. 12 All NIHRasV12 subpopulations move with high directionality while only NIH3T3 cells surrounding the wounds move in a directional way. In **a)** and **b)**, on the left side, are reported for NIH3T3 and NIHRasV12, respectively, a merge of polar plots of each subpopulation. The deviations from the expected direction have been calculated and reported for each subpopulation on the right side of **a)** for NIH3T3 and in **b)** for NIHRasV12. Dotted lines indicate the average direction for NIH3T3 (blu) and NIHRasV12 (magenta). Red dotted lines indicate the standard deviation intervals.

Results

3.2.1 *Speed is affected by both PI3K and MAPK pathway inhibition*

The role of the MAPK pathway was evaluated by adding PD 98059, an inhibitor known to affect this pathway by blocking MEK activity and consequently ERK phosphorylation and activation. Ras is also known to activate the PI3K pathway, which may be inhibited by using LY 294002, an inhibitor of the PI3Kinase activity. The effects of adding the two inhibitors to a standard wound healing assay are reported in fig. 13. Both NIH3T3 and NIHRasV12 cell populations (13a and b, left panels), when wounded (W) move at higher speed than cells in not wounded monolayers (NW). PD 98059 inhibition of MAPK pathway affects speed of both NIH3T3 and NIHRasV12 cells, as shown in fig. 13a and b (W+PD). In NIH3T3 fibroblasts speed is reduced to the same levels as the unstimulated culture, while NIHRasV12 suffer a stronger speed reduction producing values well below those of the unstimulated culture, probably reflecting the fact that, in this culture, Ras pathway is constitutively activated. Inhibition of the other branch of Ras signalling, mediated by LY 294002, also reduces the speed of fibroblasts (W+LY) and this drop is similar to that observed in presence of ERK activation inhibitor PD 98059.

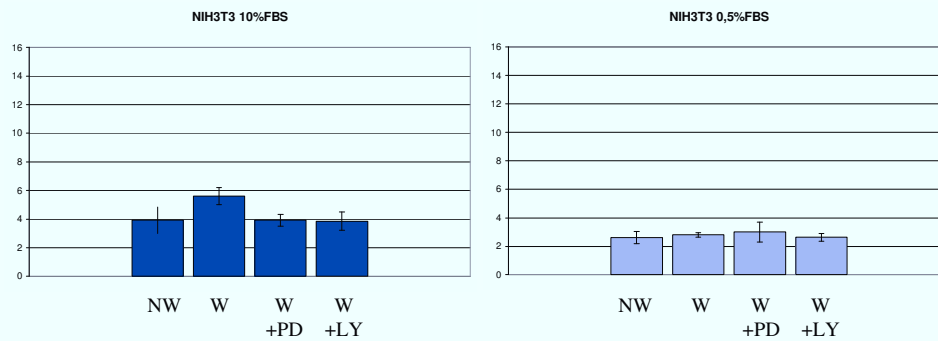
For both cell lines, under limiting conditions (0,5% serum, on the right panels of fig.13 a and b), the effect of the inhibitors on speed is very reduced or absent. Of course here the general speed reduction, due to limiting growth conditions (see fig. 7), should be taken into account.

3.2.2 *MAPK pathway is the main regulator of the directional component of cell migration*

The relevance towards directional movement of the two pathways described above was tested by evaluating directional movement in cells cultured in presence of the two inhibitors. The effect of PD98059 is reported in fig. 14, where it is shown to strongly affect the directional migration of both NIH3T3 and RasV12 cells. The R coefficient, determined for the three subpopulations, is low or very low in all of them, for both cell lines (fig. 14a and b, left panel), and is dramatically reduced in the population closest to the wound, which was, as described above, the only subpopulation having high values of R coefficient in absence of the inhibitor for NIH3T3 cells (fig 11b). This is also clearly visible in the polar plots, which show cell displacements randomly distributed around the polar plot area to form a circular shape (fig. 14a and b, right panel).

To evaluate the ability of NIH3T3 and NIHRasV12 cells to maintain the same direction during the observation time, linear dispersion R

a)



b)

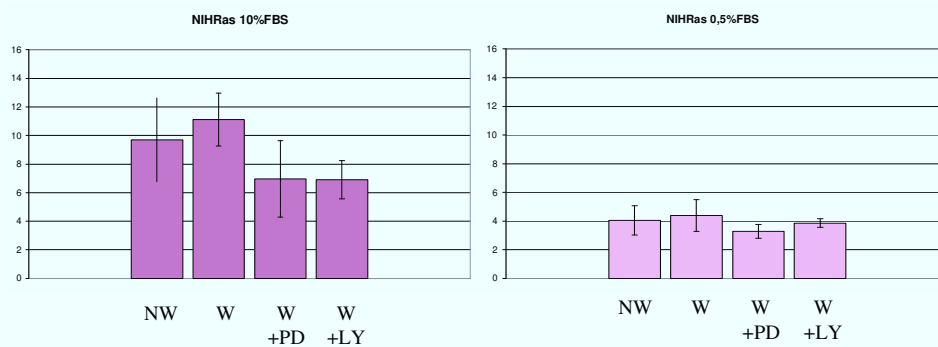


Fig. 13 Kinetic analysis of NIH3T3 and NIHRasV12 migration in presence of PD 98059 and LY 294002. The values of average speed for NIH3T3 **a)**, and NIHRasV12 **b)**, obtained in 10% (left) and in 0,5% serum (right), are tested under the following conditions: no wound (NW), wound (W), wound in presence of PD 98059 (W+PD), wound in presence of LY 294002 (W+LY).

Results

coefficients and average angles were calculated for the whole population for each migration step. In fig. 14c, linear dispersion coefficient and average angle are plotted against time for the sole external sub-populations of NIH3T3 and NIH3T3 fibroblasts. R values (bottom curve, scale on the left vertical axis) are consistently higher and often above the threshold level for $P < 0.01$ (lower dotted line) in the panels on the left (C). These numbers drop to much lower values in cells treated with PD, as reported in the right panels (+PD).

The directional behavior is also confirmed by the angular deviations from reference direction, that is towards the centre of the wound, reported in the same graphs in the top curve and using the right Y axis. The two panels on the left, where control cells are reported, show that the average angle changes only by a few degrees and remains centred on the reference angle, for most of the observation time. The panels on the right, for cells growing in presence of PD 98059, show angular deviations scattered along the whole range from -180° to $+180^\circ$, and very often far from the reference angle. These features indicate a population characterized by non-directional movement. In synthesis, control fibroblasts, both normal and Ras transformed, show a strong directional behavior, which, in presence of MEK inhibitor, is lost.

The role of PI3K pathway in determining directionality was tested by using LY 294002, as reported in fig. 15. Here, linear dispersion values and the distribution of directions, respectively shown on the left and right side of fig. 15a for NIH3T3 and 15b for NIH3T3 cells, are high and comparable to those measured in absence of the inhibitor (fig. 11). As for the previous figure, in fig. 15c linear dispersion R and average angle are reported for the front sub-populations during the whole 24h observation time. Despite the inhibition of PI3K pathway, the subpopulations surrounding the wound maintain their directional migration within most of the time, with R values high and angles often very close to the reference angle.

The von Mises distribution, often used to describe unimodal circular distributions, was used to model the behaviour of the previously described cell populations. It fits well to points tightly concentrated around a mean direction. In order to attempt to model the behaviour of a cell population according to a von Mises distribution, the net displacements of each cell following a path have been used to compute the maximum likelihood estimates for the parameters of a von Mises distribution. Furthermore to evaluate the fit of the calculated model to the experimental data, the Watson test was used to test for both a von Mises and a uniform

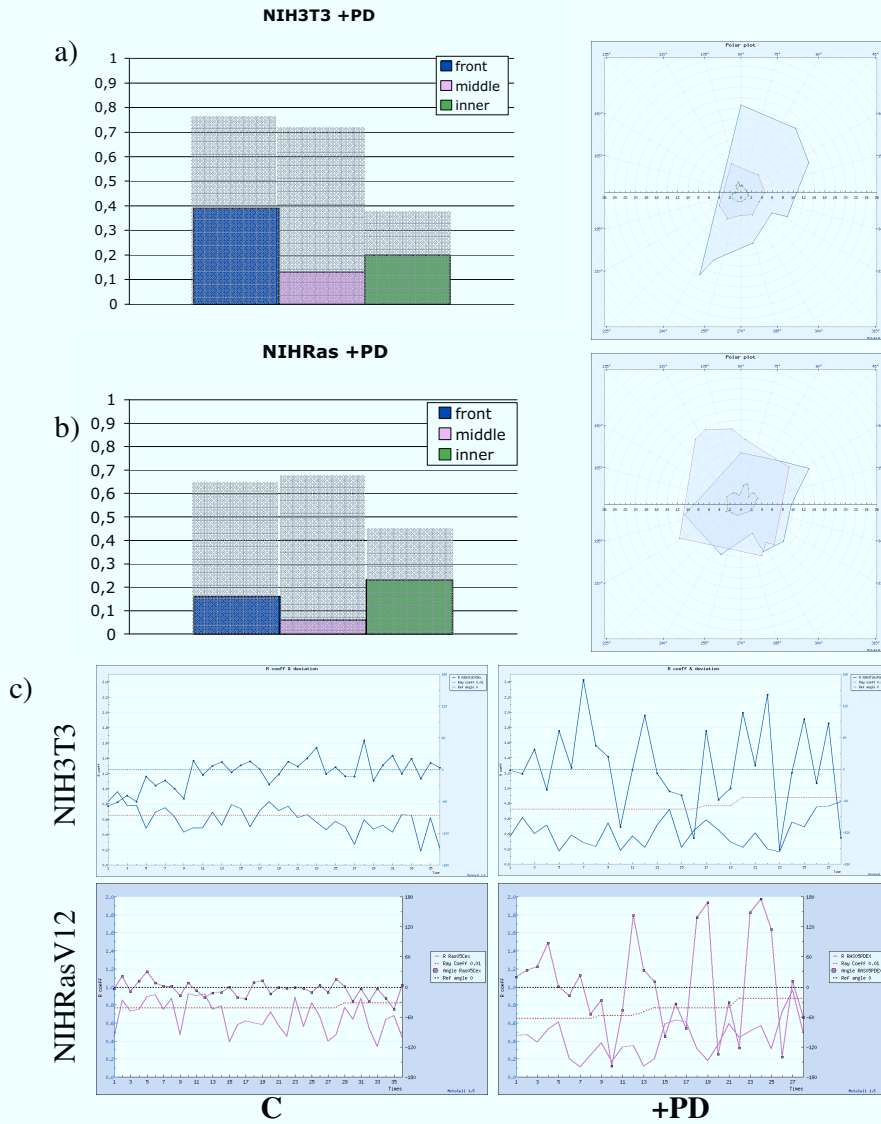


Fig. 14 Analysis of NIH3T3 and NIHRasV12 directional migration, in presence of PD 98059. On the left are plotted R coefficients, calculated for each sub-population of NIH3T3 (a) and NIHRasV12 (b) cells wounded in presence of PD 98059. On the right are reported a merge of polar plot of all subpopulations. In c) linear dispersion R and average angle values are plotted against time for the external sub-populations of NIH3T3 (upper) and NIHRasV12 (lower) cells cultured in absence (left) or in presence of PD 98059 (right).

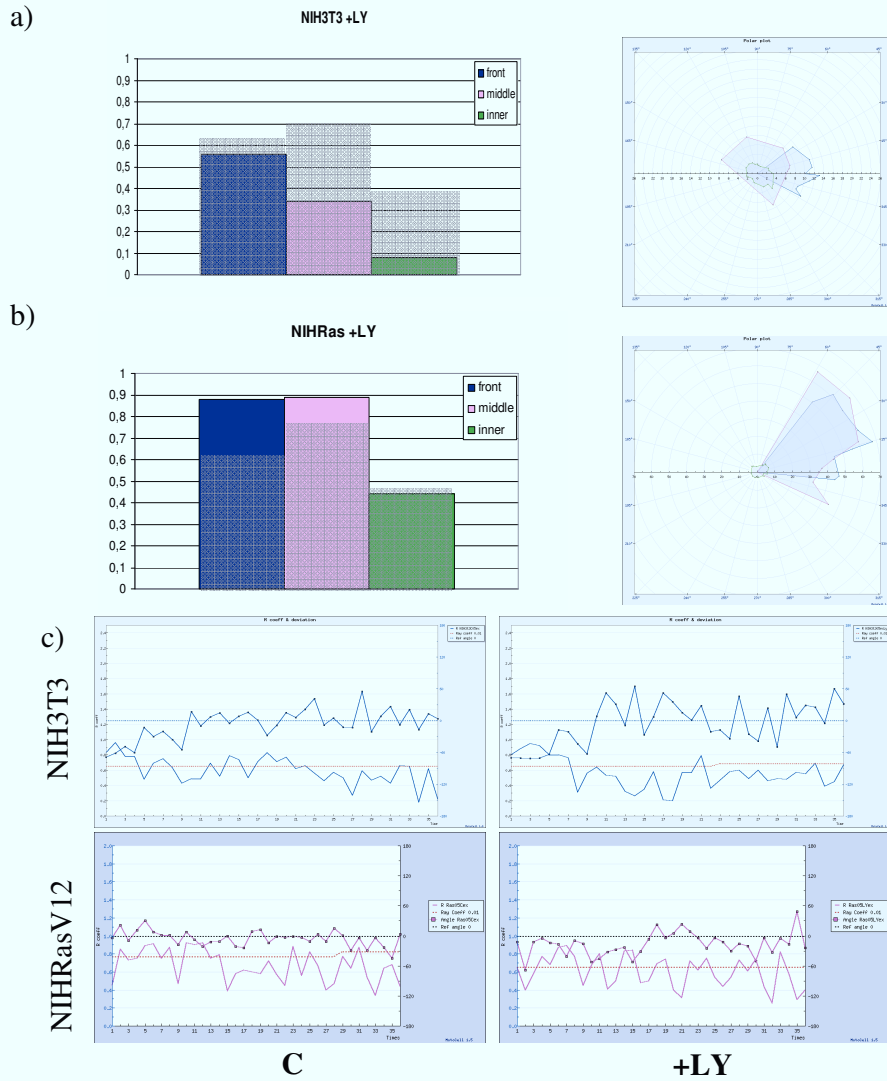


Fig. 15 Analysis of NIH3T3 and NIHRasV12 directional migration, in presence of LY 294002. On the left are plotted R coefficients, calculated for each sub-population of NIH3T3 (a) and NIHRasV12 (b) cells wounded in presence of LY 294002. On the right are reported a merge of polar plot of all subpopulations. In c) linear dispersion R and average angle values are plotted against time for the external sub-populations of NIH3T3 (upper) and NIHRasV12 (lower) cells cultered in absence (left) or in presence of LY 294002 (right).

distribution (Watson G.S., 1961). In all cases a significance level of 0.01 was chosen. Overlays of the theoretical curve with the experimental data obtained for the external sub-populations are reported in fig. 16. For both NIH3T3 and NIH3T3 fibroblasts, in control conditions, the hypothesis of von Mises distribution, that is a distribution of angles concentrated around a mean direction, may be accepted (fig 16a and b, left). Blocking of PI3K pathway downstream from Ras, does not modify the distribution of cell directions compared to that observed in untreated conditions, in fact, it still fits well to von Mises but not to a uniform distribution (fig 16a and b, centre). Inhibition of MAPK pathway, instead, produces a drastic change, with the distribution becoming very wide and flat. Therefore, although still accepted as a von Mises distribution, it also perfectly matches a uniform circular one (fig 16 a and b, right).

3.3 ERK activation plays an important role in responding to the wound

As the essential directional movement is strictly associated with MAPK but not with PI3K pathway, ERK activation was examined on wounded cell monolayers, in an effort to better understand the biochemical phenomena involved in regulating the observed migratory behavior.

3.3.1 Localization of phosphorylated ERK at the border with the wound

NIH3T3 cells were subjected to a wound and then stained with an anti-phospho-ERK1/2 antibody (fig.17). The basal level of ERK phosphorylation in a cell monolayer before wounding is shown on top of the panel (no wound). Immediately after wounding (T0), ERK phosphorylation is selectively increased at the wound edge and becomes very evident 3 minutes after the injury (T3') in the cell population of the front; it is then reduced at later time points.

3.3.2 ERK phosphorylation occurs in a prolonged and biphasic way

ERK activation was further and quantitatively analyzed by Western Blot. In these experiments, a protocol was developed for enriching the cellular populations closer to the wound, to test how they respond to the wound injury, while they migrate towards the neo-opened space with strong directionality. Briefly, confluent NIH3T3 monolayers were wounded repeatedly with a tool able to create parallel wounds separated by narrow (about 1mm) stripes of monolayer (fig. 18a). Cells were collected at various times up to 24h after wounding. The phosphorylation patterns of ERK in both standard (10% serum) and limiting (0,5% serum) culture conditions are reported in fig. 18b and c, respectively. The response is

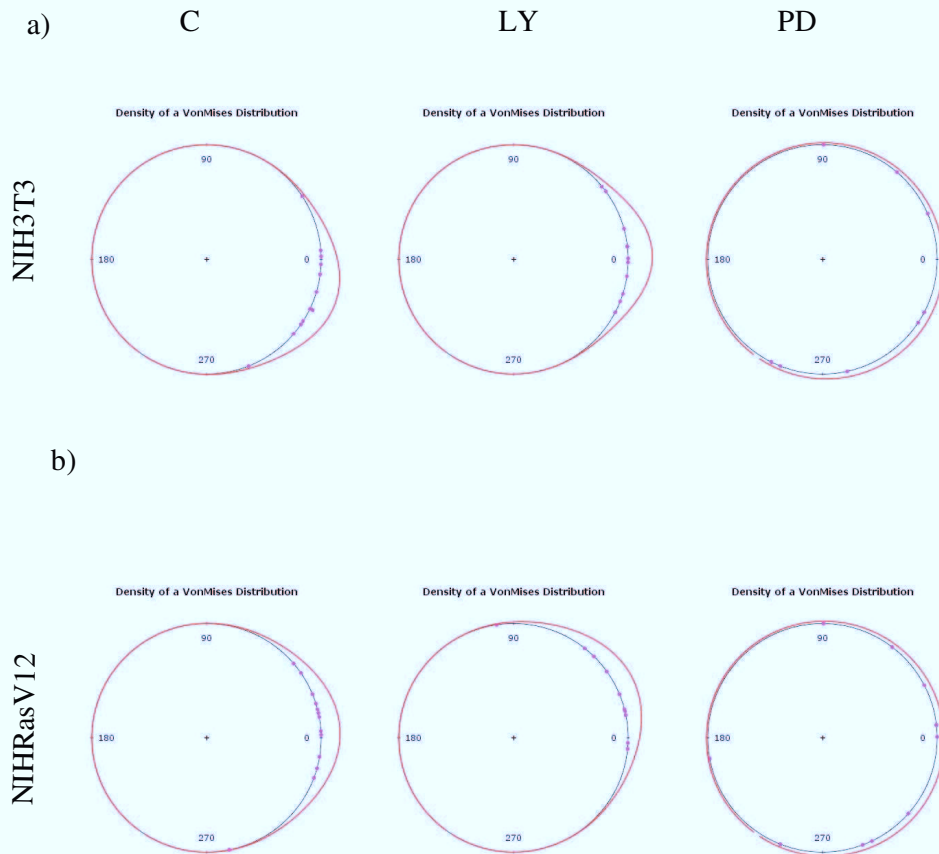


Fig. 16 Fit to Von Mises distribution. Overlays of the theoretical curve (red) with the experimental points obtained for the external sub-populations are reported in **a)** for NIH3T3 and in **b)** for NIHRasV12 cells. The analysis was carried out under control conditions (left), in presence of LY 294002 (center) or PD 98059 (right).

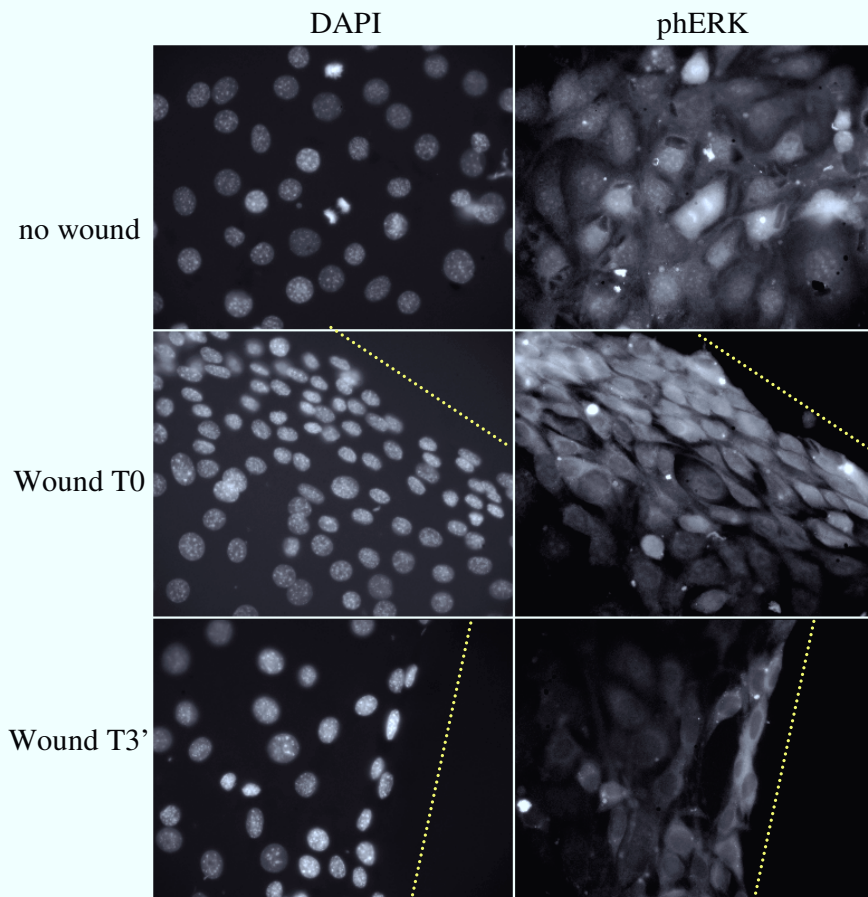


Fig. 17 Phosphorylated ERK quickly appears at the leading edge of migrating cells. Cells were fixed without wounding or after wounding at each time points indicated and stained with DAPI (left) or with anti-phosphoERK1/2 (right). Yellow lines indicate the wound position.

characterized by two peaks of ERK phosphorylation, the first appears immediately after the wound (T0) and reaches its maximum peak at 3'. This first activation is rapid and transient on the time scale of minutes, in fact 10' after the stimulus it is already going down and one hour later reaches values well below the basal level, i.e. that of unwounded cells (NW). After, there is a second onset of ERK activation, with a second phosphorylation peak at 3-5h. This second activation appears less strong but more sustained on the time scale of hours. Under limiting conditions (0,5% serum, fig. 18c) the delayed rise is still present, although the second peak is masked by the slow rise leading to the full recovery at 24h of the pre-wound levels.

ERK activation pattern was also analyzed in situ by immunofluorescence over the whole 24h time (Fig. 19). This experiment again confirms the early ERK activation at the wound edge immediately after injury; after 20' phospho-ERK signal become gradually diffused up to 1h, when it appears decreased. At 3-5h the onset of a new ERK activation is observable. Interestingly, at these times the higher level of ERK activation can be noticed in cells that show higher migratory appearance, which is reflected in elongated cell shape and nucleus retraction. The signal returns to the basal level 24h after the wound.

3.3.3 The two peaks of ERK activation are independent and both depend on neo-phosphorylation

To assess if and how the two peaks of ERK phosphorylation, which occur in the 24h after wounding, are affected by PD 98059, confluent monolayers of NIH3T3 fibroblasts were pretreated for 1h with PD 98059, and then wounded and collected at various times. Fig. 20a displays that PD 98059 (red curve) totally inhibits both ERK activation peaks. The small raise left is not very different from the minor recovery observed after a few hours in PD stability tests, such as the one shown in fig. 20b. In these assays, PD 98059 seems to be a stable and long lasting inhibitor since it maintains its maximum inhibitory activity for about 4h, but it is still active up to 24h, with ERK levels well below the controls.

To study the interdependence of two activation peaks, PD 98059 was added after the first onset of ERK activation, that is 3' after wound (fig. 21). This addition strongly reduces the second event of ERK phosphorylation, which appears therefore to be independent of the first peak. The same is true if the addition of PD 98059 is shifted to 15' before the second rise (fig. 22, green curve): in this way the second peak is completely prevented. Of course, the addition of PD 98059 15' before the

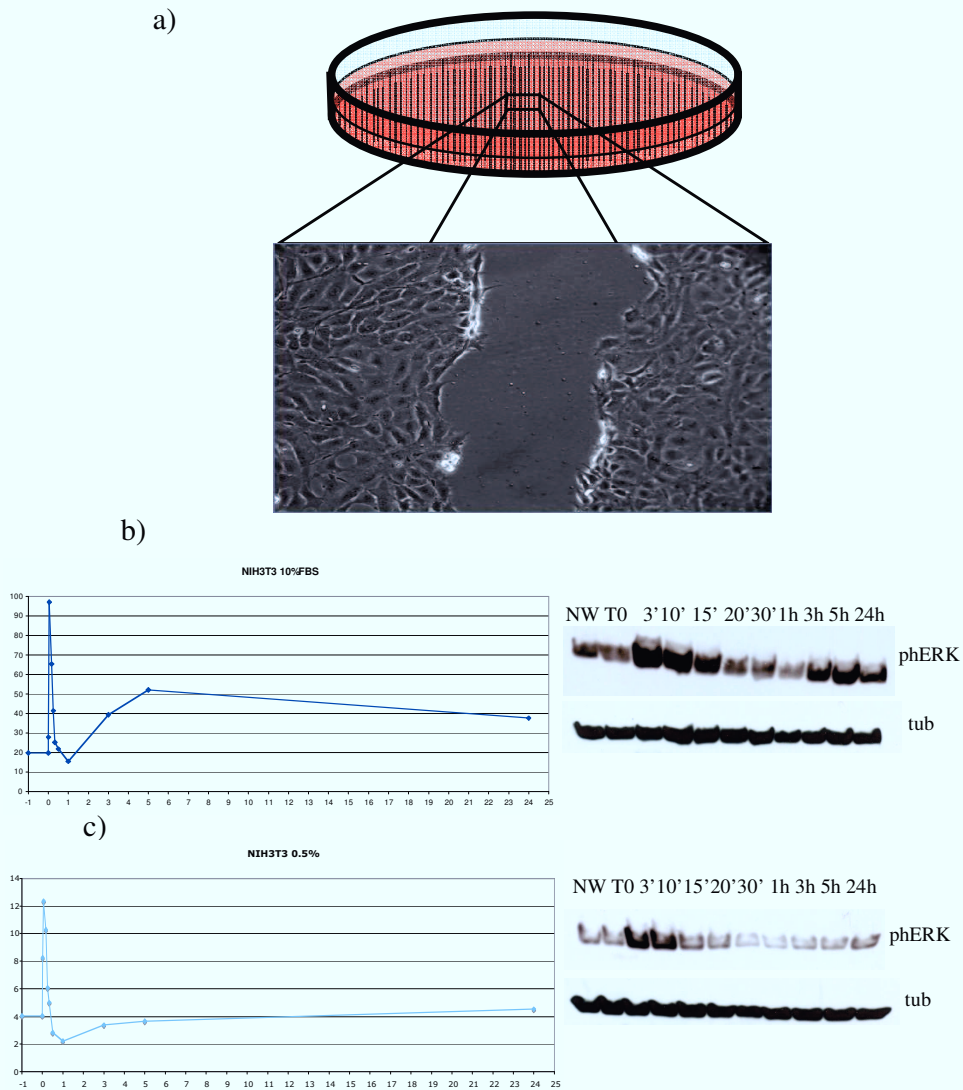


Fig. 18 ERK activation occurs in a prolonged and biphasic way in front cells. In **a)** are visualized small and repeated wounds made, at the distance of about 1mm, on confluent monolayers in order to enrich the cellular populations closer to the wound. Western blots in 10% serum **b)**, and under limiting culture conditions, 0,5% serum, **c)** were quantitatively analyzed and the results are reported on the left side of **b)** and **c)** panels. Each phospho-ERK signal was treated by subtracting the local background, and was normalized to tubulin signal subtracted of its background.

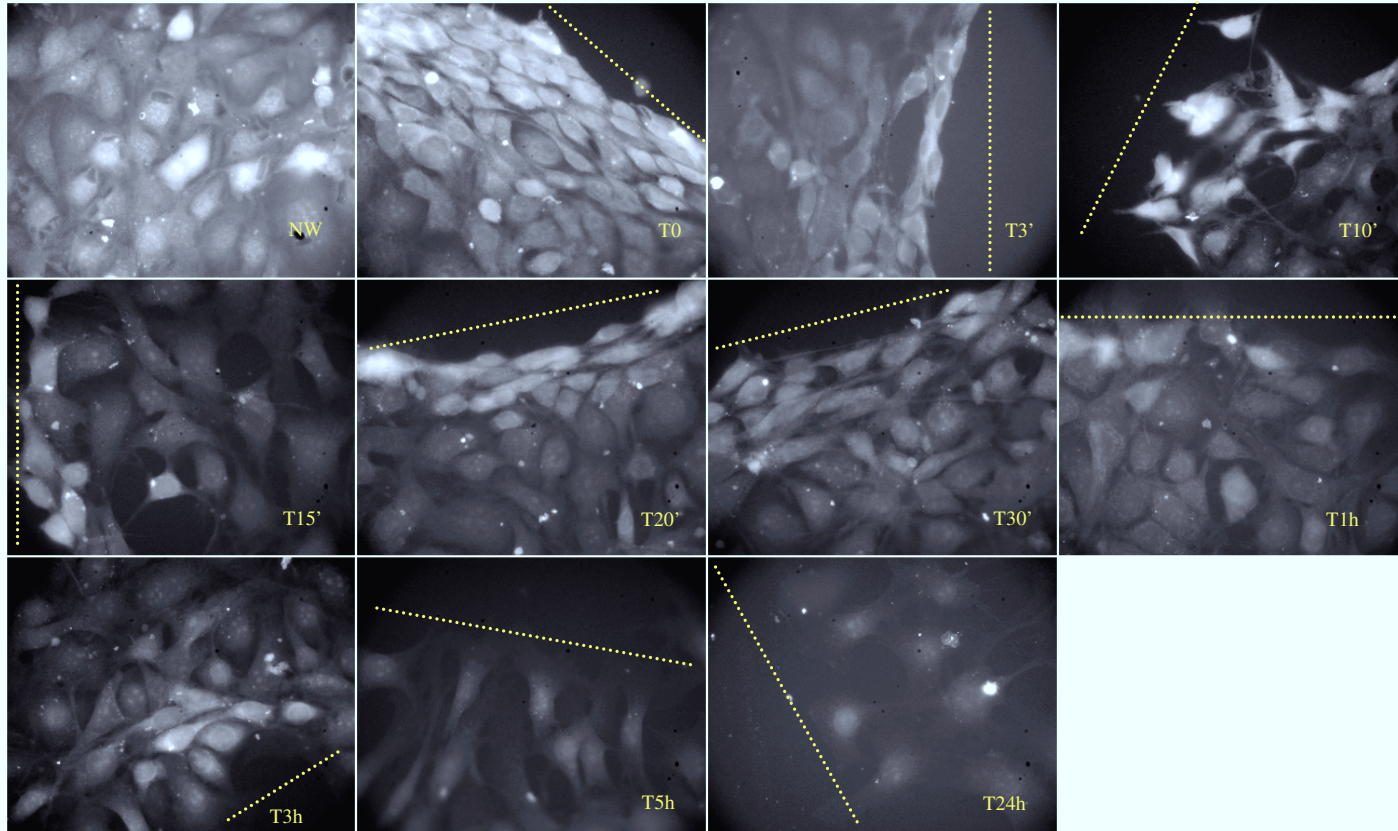


Fig. 19 Spatial and temporal localization of ERK activation following the wound. Cells without wounding (NW) or at indicated time points after wounding, were stained with anti-phosphoERK1 / 2 and revealed with a Fite-conjugated secondary antibody. Yellow lines indicate the wound position.

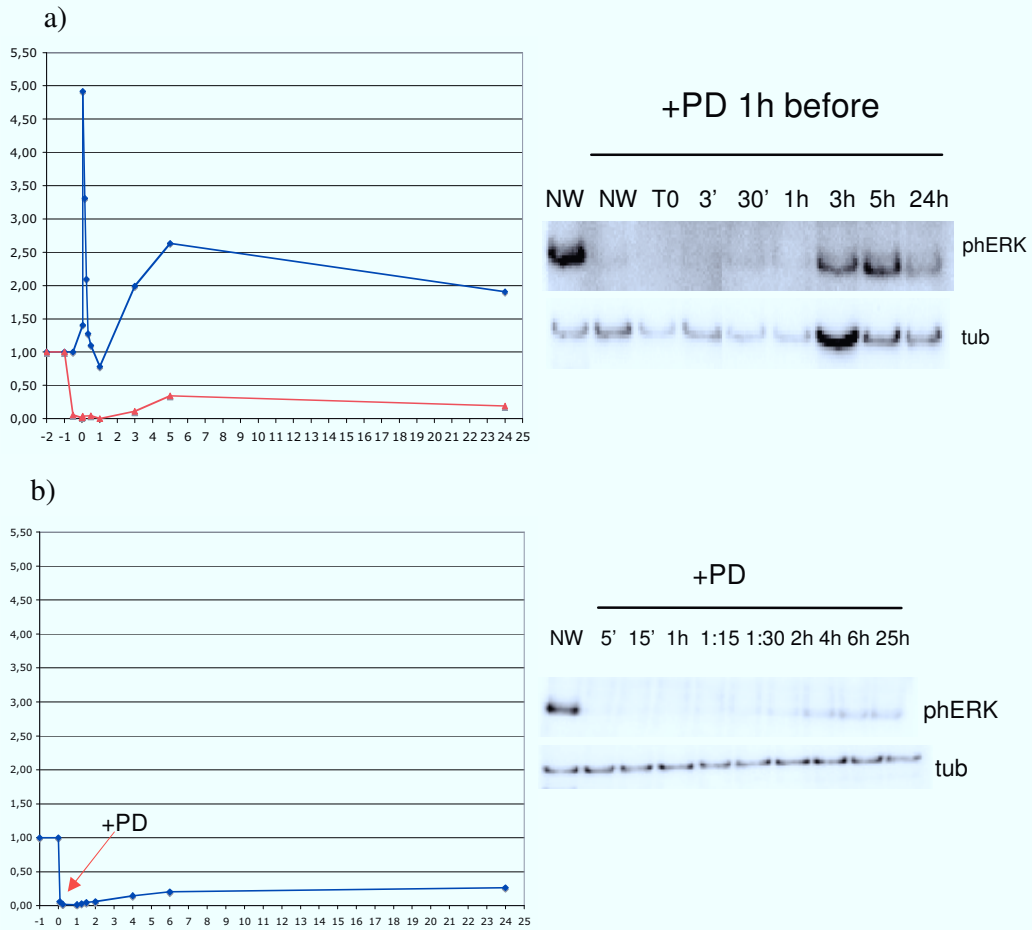


Fig. 20 The biphasic pattern of ERK activation is affected by PD 98059. **a)** Confluent monolayers of NIH3T3 fibroblasts were pretreated for 1h with PD 98059, wounded and collected at various times, then blotted for phospho-ERK1/2. In the chart, the blue curve is obtained in control conditions, the red one in presence of PD 98059. **b)** PD 98059 stability assay: cellular monolayers were treated with PD 98059 for various times, then collected and ERK phosphorylation was assessed by Western Blot analysis. On the left of **a)** and **b)** are shown quantizations of the data from western blots (on the right), obtained as described in fig.18 legend.

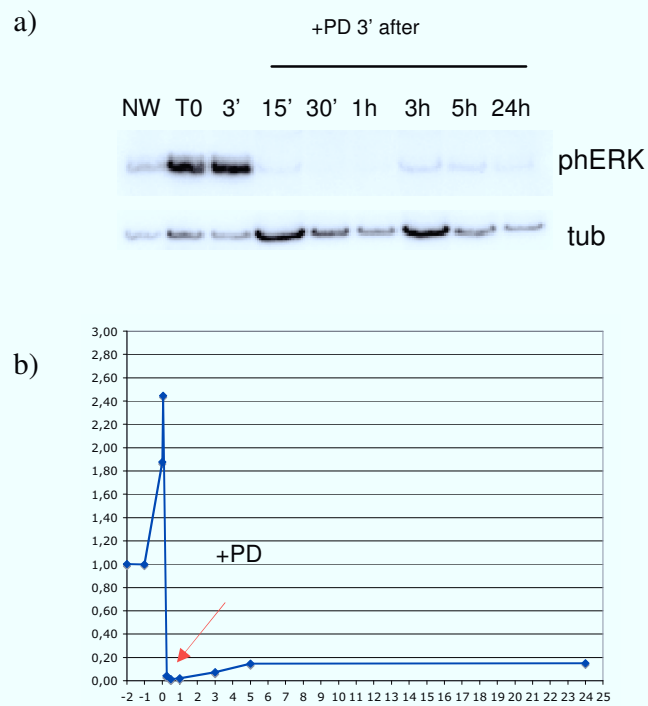


Fig. 21 The two peaks of ERK activation are independent. **a)** Confluent monolayers of NIH3T3 fibroblasts were wounded, after 3' treated with PD 98059, then collected at various indicated times and blotted for phospho-ERK1/2. **b)** Quantization of data from western blot, obtained as described in fig.18 legend.

first peak completely abolishes it (fig. 22, red curve). The loss of the two peaks confirms that they are both due to MEK dependent neophosphorylation of ERK protein.

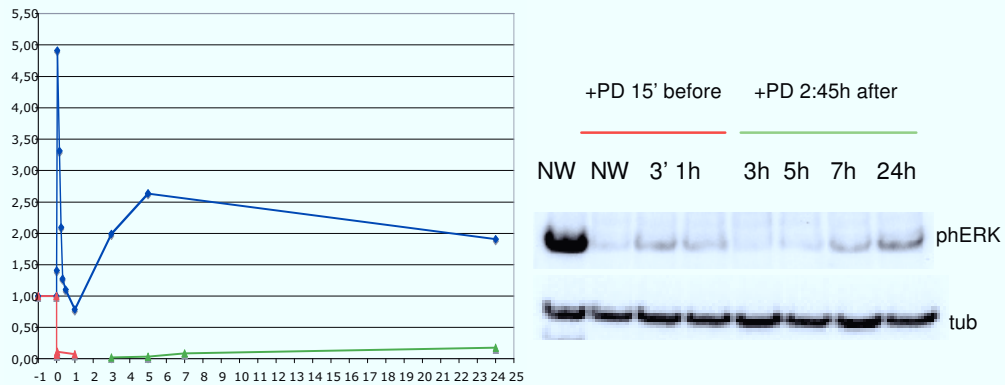
3.4 The actin organization at the leading edge is impaired by MAPK inhibitor PD 98059

To better characterize Ras induced cellular structures related to accelerated wound closure, cytoskeletal organization and formation of focal adhesions was evaluated by means of specific markers: actin cytoskeleton was visualized by using rhodamine-conjugated phalloidin, while focal adhesions were revealed by anti-paxillin antibody.

As reported in fig. 23a, the wound induces changes in actin cytoskeleton organization, in both NIH3T3 and NIHRasV12 cells. In response to the wound injury, both cell lines change shape by extending filopodia and lamellipodia. In NIHRasV12, formation of stress fibers is an early effect and is associated with better actin organization within membrane protrusions than in the parental NIH3T3: 1h after the wound, cytoskeletal structures in lamellipodia appear perfectly oriented towards the direction of migration. This pattern is in contrast with the shape of unstimulated cells, typically characterized by the lack of stress fibers, and may be related with the advantage in directional cell migration determined by Ras. Focal adhesions were visualized by staining NIH3T3 and NIHRasV12 with an anti-paxillin antibody, as shown in fig. 23b. In unstimulated cells paxillin appears to be diffused within the whole cell body, in both cell lines. In both, the wound induces organization of paxillin in spikes at the propulsive extremities. RasV12 fibroblasts again show earlier and better arrangement than NIH3T3, with paxillin spikes mostly oriented in the direction of migration.

To investigate the effective role of the ERK pathway on these cytoskeletal and membrane structures, the experiments were carried on in presence of the MEK inhibitor PD 98059 (fig. 24). NIH3T3 and NIHRasV12 cells were pretreated for 1h, subjected to the wound and fixed immediately after or 1h later. Inhibition of ERK phosphorylation by PD 98059 does not abolish the ability of NIHRasV12 (fig. 24a) and NIH3T3 (fig. 24b) to respond to the injury by acquiring a polarized shape, but their skill to organize actin fibers towards the wound direction appears to be greatly impaired. Again this feature is more evident for NIHRasV12 fibroblasts.

a)



b)

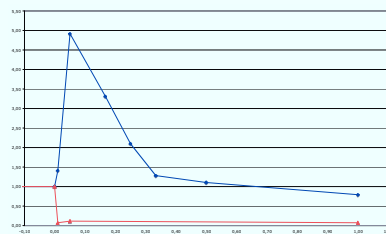


Fig. 22 The two peaks of ERK activation both depend on neo-phosphorylation. **a)** Confluent monolayers of NIH3T3 fibroblasts were pretreated for 15' with PD 98059, then wounded, collected at various times indicated and blotted for phospho-ERK1/2 (red curve in quantization chart); alternatively they were incubated with PD 98059 after 2h and 45' from the wound, collected at various times indicated, and blotted for phospho-ERK1/2 (green curve in quantization chart). **b)** A zoom view of the chart showed in **a)**, which clearly displays the drop of the first peak. The blue curves in **a)**, and **b)** are obtained in control conditions. Quantitative data are obtained as described in fig.18 legend.

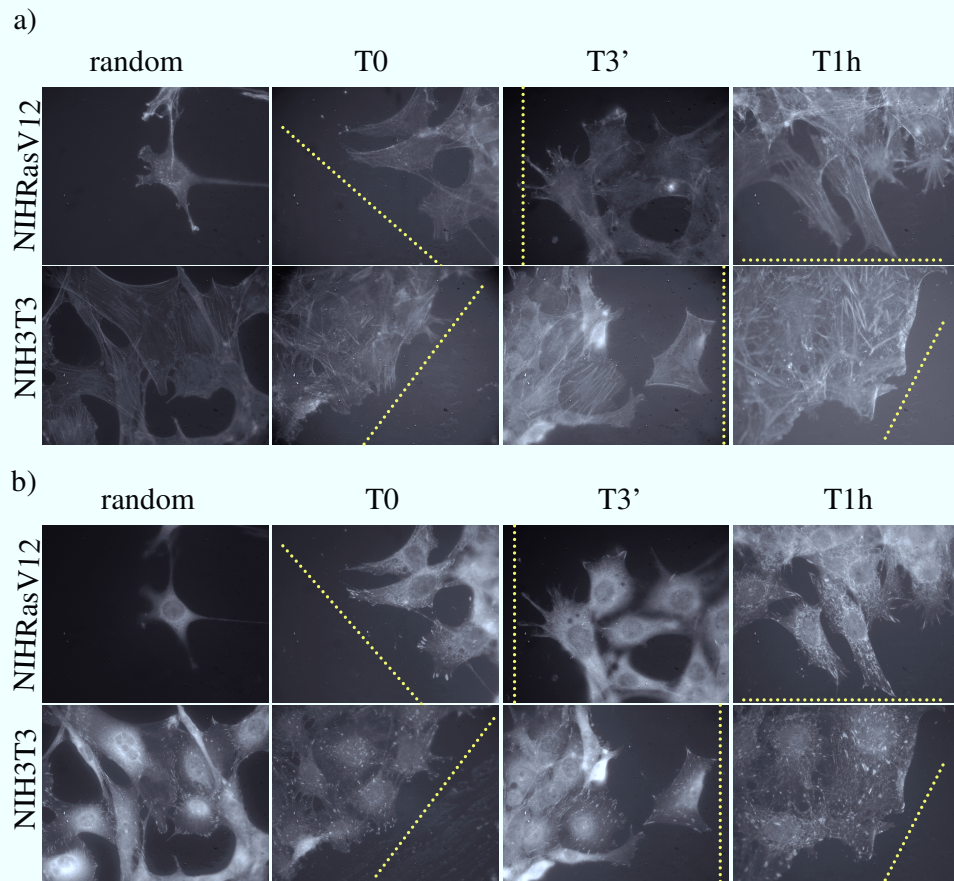


Fig. 23 Actin and paxillin organization at leading edge of migrating cells. Cells were fixed without wounding (random) or fixed after wounding at indicated time points and stained with rhodamine-conjugated phalloidin (panel a) or with anti-paxillin (panel b). Yellow lines indicate the wound position.

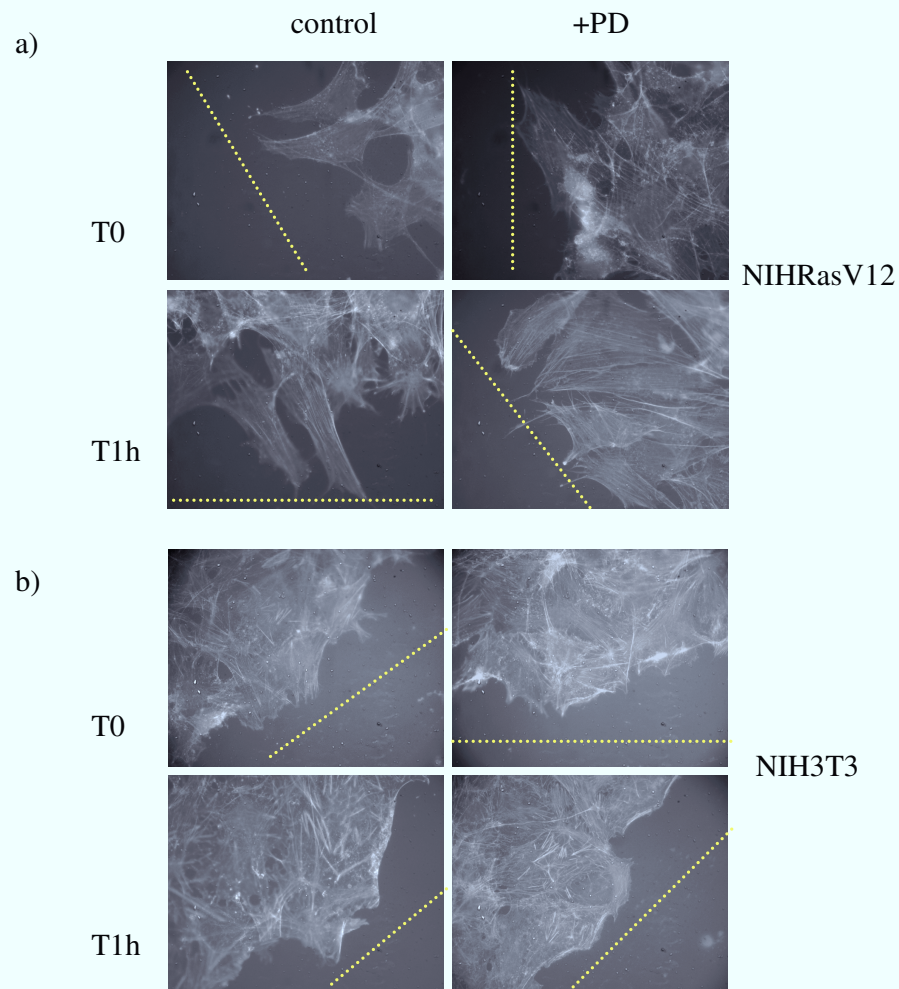


Fig. 24 Actin organization at the leading edge of migrating cells in presence of PD 98059. NIH3T3 cells (a) and parental NIH3T3 (b) were pretreated (+PD) or not (control) with PD 98059 for 1h, then fixed immediately after wounding or at 1h from injury and stained with rhodamine-conjugated phalloidin. Yellow lines indicate the wound position.

DISCUSSION/CONCLUSIONS

Within this work, wound healing assays, performed on fibroblast monolayers, revealed a specific Ras induced migratory behavior: constitutive Ras activation (RasV12) confers to NIH3T3 fibroblasts the ability to close the wound much faster. Moreover, time lapse microscopy of the wound closure process demonstrated that migrating cells move towards the empty space in different ways: RasV12 fibroblasts move more quickly and as isolated cells, unlike NIH3T3, which move together, almost as a sheet-like structure, making little progress at each time step. These results indicate a specific role for Ras activation in determining these phenomena during the wound healing process, and are in line with previous studies on the healing of wounded keratinocyte and other epithelial monolayers, showing that Ras activation is involved in wound healing and leads to accelerated re-epithelization (Tschardt M., 2005; Turchi L., 2002; Tarnawski A.S., 2005). Increased proliferation, alteration of cytoskeleton structures and increased cell migration have all been associated to transformation induced by Ras constitutive activation (Shima Y., 2007, Giehl K., 2005). In NIH3T3 fibroblasts, Ras constitutive activation determines high proliferation rate but this is not directly related to accelerated NIH3T3 wound closure. Morphological and cytoskeletal modifications, induced by Ras overactivation, resulted clearly visible in NIH3T3 and appeared to be associated to the ability to cover longer paths and move with higher speed than parental cell line in random motility assay. In wound healing, the injury by itself stimulates cells to change their shape by extending filopodia and lamellipodia, and the presence of Ras constitutive activation gives advantages in terms of both earlier and better actin cytoskeleton organization, and faster movements. These data suggest that the kinetic advantage, determined by Ras transformation, may be responsible for enhanced wound healing, but the results obtained in limiting conditions (see fig. 7), demonstrate that increased speed alone does not explain enhanced wound healing, and other features, beyond speed, are probably involved.

Studies in other cellular models, such as *Dictyostelium discoideum* and mammalian neutrophils, have implicated Ras in controlling the ability of cells to sense a chemical stimulus and migrate toward it (Sasaki A.T., 2004). This raised the possibility that features related to the directional component of cell migration might be involved. Therefore, wound healing assays were performed not only as an end point assay, but also coupled to time lapse acquisition and quantitative analysis of cell migration to

Discussion

describe parameters characterizing directional migration, such as linearity, persistence and directionality. In random condition, constitutive Ras activation does not alter any of these features: both parental and transformed cells move with comparable linearity and persistence and in a non directional way. The introduction of a wound in NIH3T3 and NIHRasV12 monolayers acts as a directional stimulus, and changes the spatial distribution of cell displacements that begin to converge in the direction of the wound (see fig. 9). The presence of RasV12 gives an advantage to transformed cells by making migration more clearly directed towards the wound and characterized by non tortuous paths. Results obtained in low serum point to a role for Ras in regulating directional response to the wound stimulus, as the enhanced directional component of NIHRasV12 cell migration leads to a consistent and coordinate movement of cells in the right direction to close the wound.

Previous works implicated Ras activation in accelerated wound closure mostly by demonstrating its general effects on migration speed (Tschardt M., 2005; Tètreault M.P., 2008). The above described results further dissect the movement and emphasize a specific role of Ras in regulating directional component of migration in wound healing. When the directional behaviour of a wounded cell population is analyzed, the presence of RasV12 results in extended spatial sensing and directional response, visible even at a distance from the wound. In contrast, NIH3T3 fibroblasts have a stronger dependence on position: only the cells immediately surrounding the wound move in a clearly directional way. These features may reflect the activation status of Ras pathway: higher and constitutive in NIHRasV12, and wound induced in NIH3T3 fibroblasts.

Ras is an upstream component of the “intelligent sensor system”, which detects the stimulus, integrates and analyzes informations and finally induces directional migration. The problem is through which downstream effectors Ras acts. Giving the growing number of Ras effectors, it is not surprising that Ras regulation of cell motility involves many downstream pathways. Within this work, two main pathways downstream from Ras, known to be involved in wound healing process, were analyzed: MAPK and PI3K pathway (Fitsialos, 2007). Inhibition of PI3K pathway, by LY 294002, affected speed, but not directional component of cell migration for both NIH3T3 and NIHRasV12 fibroblasts. These results, together with previous reports, which demonstrated that PI3K activity and localized phosphatidyl-inositol triphosphate (PIP3) gradients are dispensable for chemotaxis under many conditions, suggest that they are

Discussion

mainly involved in controlling cell speed by ensuring rapid movement towards chemoattractants, as well as other stimuli. In *Dictyostelium*, for example, a multiple-knockout strain lacking all five *Dictyostelium* class I *pi3k* genes is still able to undergo chemotaxis in strong chemoattractant gradients, but at reduced speed (Hoeller O., 2007; Wessels D., 2007). In neutrophils, PIP3 accumulates at the leading edge in a PI3K γ -dependent manner. Neutrophils lacking PI3K γ move more slowly than wild-type cells, but do not show defects in directional sensing (Ferguson G.J., 2007).

ERK pathway has previously been involved in cell migration, during wound healing. Inhibition of ERK1/2 activation results in markedly reduced movement of the epithelial sheet in wound healing (Matsubayashi Y., 2004). Also in corneal endothelial cells, ERK was demonstrated to affect migration speed (Teranishi S., 2009; Chen W.L., 2009). However, its role in regulating directional migration is less clear. The results in this work indicate that MAPK and PI3K are both activated by Ras after a wound and both act to determine the observed increase of speed, but only MAPK pathway mediates the directional response. In fact, beyond affecting migration speed, selective block of ERK activation by PD 98059, completely abolishes the directional component of cell migration and renders cells unable to directionally move towards the target.

To quantitatively analyze ERK activation patterns, a simple but effective method was developed where a “wounding device” creates many parallel scratches within a cell culture to enrich the number of cells located in the proximity of a wound, eventually allowing the study of molecular events in response to injury (see fig. 18a). In previous experiments on epithelial monolayers, after damage, two waves of ERK phosphorylation were observed: a fast, transient, first wave followed by a slow, sustained one (Matsubayashi Y., 2004). In this context, ERK activity starts in cells at the wound edge and propagates to cells farther away from it. Close interactions between cells in an epithelial layer have been implicated in the process, as signals have been proposed to be transmitted through cell-cell contacts. Within this work, fibroblasts, which have no tight junctions, also show (fig. 19) rapid ERK activation after the wound in the cell population at the front, which is later reduced; a second ERK activation peak is observable after 3-5h. Quantitative analysis of these enriched front subpopulations, by Western Blot, confirmed the biphasic ERK activation: a strong first peak is followed by a second more sustained one, delayed by 3-5h. The two peaks both depend on neo-phosphorylation by MEK. The

Discussion

results exclude the hypothesis that the second ERK phosphorylation peak is a delayed reappearance of ERK protein phosphorylated in the first one. Dual specificity phosphatases (DUSPs), are known to control ERK activity levels by quickly dephosphorylating both threonine and tyrosine (Caunt C.J., 2008), and may explain the fall after the first peak. The cause of the second peak is a challenging problem, already discussed in literature. Nikolic et al., demonstrated that both waves are necessary for wound healing of epithelial monolayers and proposed a loop where ERK induced migration ultimately results in delayed ERK activation by means of reactive oxygen species (ROS) induced by mechanical stress generated by migrating cells (Nikolic D.L., 2006). Another hypothesis is that the first peak of ERK phosphorylation leads to a second sustained one, by activating an intermediate process, such as de novo RNA and protein synthesis. According to this hypothesis, in vascular smooth muscle cells the first ERK activation leads to the expression of intermediate HB-EGF that further sustains the Ras/Raf/MEK/ERK cascade (Perez Sastre A., 2008).

There is a fervid literature, which associates the duration and magnitude of ERK activation and cell migration (McCawley L.J., 1999; Krueger J.S., 2001; Tian Y., 2007). In fact, it is known that ERK, once activated, regulates cell movement by promoting the activation of proteins, or specific genes transcription, involved in the control of F-actin and focal adhesions formation and turnover (Klemke R.L., 1997; Huang C., 2004; Wu W.S., 2008). Within this work, sustained ERK activation after the wound is associated to the directional migratory response. A link that may explain how ERK effectively regulates directional migration was found by observing the actin cytoskeleton. As described above, RasV12 transformed fibroblasts after wound respond with an earlier and better organization of actin cytoskeleton in membrane protrusions. In contrast, these features are lost in presence of the inhibition of ERK activation, mediated by PD 98059. Therefore ERK, activated by Ras after wound stimulus, is likely to mediate an immediate effect on the actin cytoskeleton, which may start and drive directional migration.

Regarding ERK regulation of focal adhesions, a functional interaction between ERK and paxillin, a key molecule of focal adhesions, is well known, where paxillin acts as a docking site able to bind Raf, together with MEK and ERK. This alignment results in ERK phosphorylation at focal adhesions, where it can then locally exert its role. In addition, paxillin itself is a substrate for phosphorylation by ERK, which results in association of paxillin to FAK and local activation of PI3K. It has been

Discussion

proposed that ERK-paxillin interaction may serve to produce both focal adhesions turnover, by direct FAK activation, and lamellipodia extension, by PI3K mediated Rac activation (Ishibe S., 2004). In corneal epithelial wound healing, an important role is played by the ERK-FAK-paxillin complex induced by MEK as inhibition by PD98059 blocks both complex formation and cell migration during wound healing (Teranishi S., 2009). Paxillin organization within the cell body is induced by the wound (fig. 23b). In both NIH3T3 and NIHRasV12 fibroblasts organization of paxillin in spikes is observed at the propulsive extremity. Ras activation, in NIHRasV12 fibroblasts, confers the ability to earlier and better arrange paxillin in spikes, mostly oriented towards the direction of migration. Taken together the results of this work demonstrate that Ras is greatly involved in regulating and determining directional migration, which drives the processes resulting in wound closure. ERK, activated in a biphasic way after the wound is inflicted, is the key effector that regulates this directional sensing. An effective role of ERK pathway in determining directionality is the regulation of target molecules that are involved in the organization of actin structures that drive the directional movement. Understanding the role of Ras and its effectors helps in better defining the mechanisms of directional cell migration. The process is important in many situations where motion towards a specific direction is involved, such as the repair of tissue discontinuity or tumor progression and metastatic dissemination. Additional work on the subject may lead to the identification of targets, within the ERK pathway, whose block allows specific control of directional migration.

REFERENCES

- Ahmedin J., Siegel R., Xu J., Ward E. (2010) Cancer statistics, 2010. *A Cancer Journal for Clinicians* 60: 1-24.
- Arkowitz R.A., Iglesias P.A. (2008) Basic principles of polarity establishment and maintenance. *EMBO reports* 9(9): 847-852.
- Balan V., Leicht D.T., Zhu J., Balan K., Kaplun A., Singh-Gupta V., et al. (2006) Identification of novel in vivo Raf-1 phosphorylation sites mediating positive feedback Raf-1 regulation by extracellular signal-regulated kinase. *Molecular biology of the cell* 17: 1141–1153.
- Barros J.C. and Marshall J.C. (2005) Activation of either ERK1/2 or ERK5 MAP kinase pathways can lead to disruption of the actin cytoskeleton. *Journal of cell science* 118: 1663-1671.
- Batschelet E. (1981) *Circular statistics in biology*. London, UK: Academic Press.
- Begum R., Nur-E-Kamal M.S.A., Zaman M.A. (2004) The role of Rho GTPase in the regulation of the rearrangement of actin cytoskeleton and cell movement. *Experimental and molecular medicine* 36: 358-366.
- Bentley J. (2006) “Modelling circular data using a mixture of Von Mises and uniform distribution”. Simon Fraser University.
- Bivona T.G., Quatela S.E., Bodeman B.O., et al. (2006) PKC regulates a farnesyl-electrostatic switch on K-Ras that promotes its association with Bcl-XL on mitochondria and induces apoptosis. *Molecular Cell* 21: 481-93.
- Bondy G.P., Wilson S., Chambers A.F.. (1985) Experimental metastatic ability of H-ras-transformed NIH3T3 cells. *Cancer research* 45: 6005-6009.
- Bretscher M.S. (2008) On the shape of migrating cells-a “front-to-back” model. *Journal of cell science* 121: 2625-2628.
- Calvo F., Agudo-Ibanez L., Crespo P. (2010) The Ras-ERK pathway: Understanding site-specific signaling provides hope of new anti-tumor therapies. *Bioessays* 32: 412-421.
- Campbell P.M., Der C.J. (2004) Oncogenic Ras and its role in tumor cell invasion and metastasis. *Seminars in Cancer Biology* 14: 105-114.
- Cantarella C., Sepe L., Fioretti F., Ferrari M.C., Paoletta G. (2009) Analysis and modelling of motility of cell populations which MotoCell. *BCM Bioinformatics Suppl* 12: S12.
- Casar B., Arozarena I., Sanz-Moreno V., et al (2009) Ras subcellular localization

References

defines extracellular signal-regulates kinase 1 and 2 substrate specificity through distinct utilization of scaffold proteins. *Molecular Cell Biology* 29: 1338-53.

Caunt C.J., Armstrong S.P., Rivers C.A., Norman M.R., McArdle C. (2008) Spatiotemporal regulation of ERK2 by Dual specificity phosphatases. *The journal of biological chemistry*. 283(39): 26612-26623.

Chen W.L., Lin C.T., Li J.W., Hu F.R., Chen C.C. (2009) ERK1/2 activation regulates the wound healing process of rabbit corneal endothelial cells. *Current eye research*. 34(2): 103-11.

Chenglu W., Pengbo W. (2007) Tracking motile algal cells with a deformable model. *New Zealand Journal of Agricultural Research*. 50: 1285-1292.

Corbalan-Garcia S., Yang S.S., Degenhardt K.R., Bar-Sagi D. (1996) Identification of the mitogen-activated protein kinase phosphorylation sites on human Sos1 that regulate interaction with Grb2. *Molecular Cell Biology* 16: 862-882.

Costa C., Barberis L., Ambrogio C., Patruocco E., et al. (2007) Negative feedback regulation of Rac in leukocytes from mice expressing a constitutively active phosphatidylinositol 3-kinase gamma. *Proceedings of the National Academy of Sciences of the United States of America* 104: 14354-14359.

Danninger C., Gimona M. (2000) Live dynamics of GFP-calponin: isoform specific modulation of the actin cytoskeleton and autoregulation by C-terminal sequences. *Journal of Cell Science* 113: 3725-3736.

DeNicola G.M., Tuveson D.A. (2009) RAS in cellular transformation and senescence. *European journal of cancer* 45 Suppl 1:211-6.

Der C.J., Krontiris T.G., Cooper G.M. (1982) Transforming genes of human bladder and lung carcinoma cell lines are homologous to the ras genes of Harvey and Kirsten sarcoma virus. *Procl. Natl Acad. Sci. USA* 79: 3637-3640.

Devreotes P., Janetopoulos C. (2003) Eukaryotic chemotaxis: distinctions between directional sensing and polarization. *The journal of biological chemistry* 278(23): 20445-20448.

Dhanasekaran D.N., Kashef K., Lee C.M., et al. (2007) Scaffold proteins of MAP-kinase modules. *Oncogene* 26: 3185-202.

Dmytriyev A., Tkach V., Rudenko O., Bock E., Berezin V. (2006) An Automatic Procedure for Evaluation of Single Cell Motility. *Cytometry. Part A* 69A:979-985.

Drosten M., Dhawahir A., Sum E.Y., Urosevic J., et al. (2010) Genetic analysis of Ras signaling pathways in cell proliferation, migration and survival. *The Embo Journal* 29:1091-1104.

References

- Fehrenbacher N., Bar-Sagi D., Philips M. (2009) Ras/MAPK signaling from endomembranes. *Molecular oncology* 3: 297-307.
- Feig L.A., Cooper G.M. (1988) Inhibition of NIH3T3 cell proliferation by a mutant ras protein with preferential affinity for GDP. *Molecular Cell Biology* 8: 3235–3243.
- Fenteany G., Janmey P.A., Stossel T.P. (2000) Signaling pathways and cell mechanics involved in wound closure by epithelial cell sheets. *Current Biology* 10: 831-838.
- Ferguson G.J., Milne L., Kulkarni S., Sasaki T., Walker S., Andrews S., Crabbe T., Finan P., Jones G., Jackson S., et al. (2007) PI(3)Kgamma has an important context-dependent role in neutrophil chemokinesis. *Nature Cell Biology* 9:86-91.
- Fincham V.J., James M., Frame M.C., Winder S.J. (2000) Active ERK/MAP kinase is targeted to newly forming cell-matrix adhesions by integrin engagement and v-Src. *The EMBO Journal* 19: 2911-2923.
- Fitsialos G., Chassot A. (2007) Transcriptional signatures of epidermal keratinocytes subjected to in vitro scratch wounding reveals selective roles for ERK1/2, p38, and phosphatidylinositol 3-kinase signaling pathways. *The journal of biological chemistry* 282(20): 15090-102.
- Forbes S.A., Tang G., Bindal N., et al (2010) COSMIC (the catalogue of somatic mutations in cancer): a resource to investigate acquired mutations in human cancer. *Nucleic Acid Research* 38: database issue D652-657.
- Formstecher E., Ramos J.W., Fauquet M., Calderwood D.A., Hsieh J.C. et al. (2001) PEA-15 mediates cytoplasmic sequestration of ERK MAP kinase. *Developmental Cell*. 1: 239-250.
- Fujimoto K., Sheng H., Shao J., Beauchamp R.D. (2001) Transforming growth factor-beta1 promotes invasiveness after cellular transformation with activated Ras in intestinal epithelial cells. *Experimental cell research* 266(2): 239-49.
- Fukata M., Nakagawa M., Kaibuchi K. (2003) Roles of Rho-family GTPases in cell polarisation and directional migration. *Current opinion in cell biology* 15: 590-597.
- Geiger B., Spatz J.P., Bershadsky A.D. (2009) Environmental sensing through focal adhesion. *Nature Reviews- Molecular Cell Biology* 10: 21-33.
- Gialeli C., Theocharis A.D., Karamanos N.K. (2010) Roles of matrix metalloproteinases in cancer progression and their pharmacological targeting. *The FEBS journal* (Epub ahead of print).
- Giehl K. (2005) Oncogenic Ras in tumor progression and metastasis. *Biological Chemistry*. 386(3):193-205.

References

- Gildea J.J., Harding M.A., Gulding K.M., Theodorescu D. (2000) Transmembrane motility assay of transiently transfected cells by fluorescent cell counting luciferase measurement. *Biotechniques* 29: 81-86.
- Glading, A., Bodnar, R.J., Reynolds, I.J., Shiraha, H., Satish, L., Potter, D. A., Blair, H.C., Wells A. (2004). Epidermal growth factor activates m-calpain (calpain II), at least in part, by extracellular signal-regulated kinase-mediated phosphorylation. *Molecular Cell Biology*. 24, 2499-2512.
- Greig R.G., Koestler T.P., Trainer D.L. et al. (1985) Tumorigenic and metastatic properties of "normal" and ras-transfected NIH/3T3 cells. *Proceedings of the National Academy of Sciences of the United States of America* 82: 3698-3701.
- Han M.Y., Kosako H., Watanabe T., Hattori S. (2007) Extracellular signal-regulated kinase/mitogen-activated protein kinase regulates actin organization and cell motility by phosphorylating the actin cross-linking protein EPLIN. *Molecular and cellular biology* 27: 8190-8204.
- Hervy M., Hoffman L., Beckerle M.C. (2006) From the membrane to the nucleus and back again: bifunctional focal adhesion proteins. *Current opinion in cell biology* 18: 524-532.
- Hoeller O., Kay R.R. (2007) Chemotaxis in the absence of PIP3 gradients. *Current biology* 17:813–817.
- Horino K., Kindezelskii V.M., Hughes B.A., Petty H.R. (2001) Tumor cell invasion of model 3-dimensional matrices: demonstration of migratory pathways, collagen disruption, and intercellular cooperation. *FASEB journal* 25: 932-939.
- Huang C., Jacobson K., Shaller M.D. (2004) MAP kinases and cell migration. *Journal of cell science* 117(Pt20):4619-28.
- Huttenlocher A., Palecek S.P., Lu Q., Zhang W., Mellgren R.L., Lauffenburger D.A., Ginsberg M.H. and Horwitz A.F. (1997). Regulation of cell migration by the calcium-dependent protease calpain. *Journal of Biological Chemistry*, **272**(52):32719-22.
- Ishibe S., Joly D., Zhu X., Cantley L. G. (2004) Paxillin serves as an ERK-regulated scaffold for coordinating FAK and Rac activation in epithelial morphogenesis. *Molecular Cell* 16: 257-267.
- Jura N., Scotto-Lavino E., Sobczyk A., et al. (2006) Differential modification of Ras proteins by ubiquitination. *Molecular Cell* 21: 679-87.
- Katz M., Amit I., Yarden Y. (2007) Regulation of MAPKs by growth factors and receptor tyrosine kinases. *Biochimica and biophysica acta* 1773: 1161-1176.

References

- Klemke, R.L., Cai, S., Giannini, A.L., Gallagher, P. J., deLanerolle, P. and Cheresch, D.A. (1997). Regulation of cell motility by mitogen-activated protein kinase. *Journal of cell biology* 137, 481-492.
- Kolsch V., Charest P.G., Firtel R.A. (2008) The regulation of cell motility and chemotaxis by phospholipid signalling. *Journal of cell science* 121(Pt5): 551-559.
- Kortholt A., van Haastert P.J. (2008) Highlighting the role of Ras and Rap during Dictyostelium chemotaxis. *Cellular Signalling* 20: 1415-1422.
- Krishnaraj R., Ralf S., Ulf R.R., Stefan A. (2007) Ras oncogenes and their downstream targets. *Biochimica et Biophysica Acta* 1773: 1177-1195.
- Krister W., Kent L.R., Channing J.D. (2005) The Ras superfamily at a glance. *Journal of Cell Science* 118: 843-846.
- Krueger J.S., Venkateshwar G.K., Atanaskova N., Reddy K.B. (2001) Temporal and quantitative regulation of mitogen-activated protein kinase (MAPK) modulates cell motility and invasion. *Oncogene* 20: 4209-4218.
- Liang C.C., Park A.Y., Guan J. (2007) In vitro scratch assay: a convenient and inexpensive method for analysis of cell migration in vitro. *Nature protocols* 2(2): 329-333.
- Machacek M., Hodgson L., Welch C., Elliot H., Pertz O., et al. (2009) Coordination of Rho GTPase activities during cell protrusion. *Nature* 461(7260):99-103.
- Marchetti S., Gimond C., Chambard J.C., Touboul T., Roux D., Pouyssegur J., et al. (2005) Extracellular signal-regulated kinases phosphorylate mitogen-activated protein kinase phosphatase 3/DUSP6 at serines 159 and 197, two sites critical for its proteasomal degradation. *Molecular Cell Biology* 25: 854-864.
- Matallanas D., Sanz-Moreno V., Arozarena I., et al. (2006) Distinct utilization of effectors and biological outcomes resulting from site-specific Ras activation; Ras functions in lipid rafts and Golgi complex are dispensable for proliferation and transformation. *Molecular Cell* 26: 100-116.
- Matsubayashi Y., Ebisuya M., Honjoh S., Nishida E. (2004) ERK activation propagates in epithelial cell sheets and regulates their migration during wound healing. *Current Biology* 14: 731-735.
- McCawley L.J., Li S., Wattenberger E.V., Hudson L.G. (1999) Sustained activation of the mitogen-activated protein kinase pathway. *The Journal of the Biological Chemistry* 271(7): 4347-4353.
- McCubrey J.A., Steelman L.S., Chappell W.H., Abrams S.L., et al. (2007) Roles of the RAF/MEK/ERK pathway in cell growth, malignant transformation and drug resistance *Biochimica et Biophysica Acta* 1773: 1263-1284.

References

- Mitchison T.J., Cramer L.P. (1996) Actin-based cell motility and cell locomotion. *Cell* 84: 371-379.
- Mitra S.K., Hanson D.A., Schlaepfer D.D. (2005) Focal adhesion kinase: in command and control of cell motility. *Nature* 6: 56-68.
- Mor A., Philips M.R. (2006) Compartmentalized Ras/MAPK signalling. *Annual Review of Immunology* 24: 771-800.
- Mulchany L.S., Smith M.R., Stacey D.W. (1985) Requirement for ras proto-oncogene function during serum stimulated growth of NIH3T3 cells. *Nature* 313: 241-423.
- Mushel R.J., Williams J.E., Lowy D.R., Liotta L.A. (1985) Harvey Ras induction of metastatic potential depends upon oncogene activation and type of recipient cell. *The American journal of pathology* 127(1): 1-8.
- Nguyen D.H., Catling A.D., Webb D.J., et al (1999) Myosin light chain kinase functions downstream of Ras/ERK to promote migration of urokinase-type plasminogen activator-stimulated cells in an integrin-selective manner. *Journal of Cell Biology* 146: 149-164.
- Nikolic D.L., Boettiger A.N., Bar-Sagi D., Carbeck J.D., Shvartsman S.Y. (2006) Role of boundary conditions in an experimental model of epithelial wound healing. *American journal of physiology. Cell physiology.* 291: C68-C57.
- Nobes C.D., Hall A. (1999) Rho GTRases control polarity, protrusion, and adhesion during cell movement. *Journal of cell biology.* 144: 1235-1244.
- Parada L.F., Tabin C.J., Shih C., Weinberg R.A. (1982) Human EJ bladder carcinoma oncogene is homologue of Harvey sarcoma virus ras gene. *Nature* 297: 474-478.
- Perez Sastre A., Grossmann S., Reusch H. P., and Schaefer M. (2008) Requirement of an Intermediate Gene Expression for Biphasic ERK1/2 Activation in Thrombin-stimulated Vascular Smooth Muscle Cells. *The Journal of biological chemistry* 283(38): 25871-25878
- Petrie R.J., Doyle A.D., Yamada K.M. (2009) Random versus directionality persistent cell migration. *Nature reviews. Molecular cell biology* 10(8): 538-549.
- Pollard T.D., Borisy G. (2003) Cellular motility driven by assembly and disassembly of actin filaments. *Cell* 112:453-465.
- Pullikuth A.K., Catling A.D. (2007) Scaffold mediated regulation of MAPK signalling and cytoskeletal dynamics: A perspective. *Cell signalling* 19: 1621-1632.

References

- Raftopoulou M., Hall A. (2004) Cell migration: Rho GTPases lead the way. *Developmental Biology* 265: 23-32.
- Ramos J.W. (2008) The regulation of extracellular signal-regulated kinase (ERK) in mammalian cells. *The international journal of biochemistry and cell biology* 40: 2707-2719.
- Raptis L., Yang J., Brownell H., et al. (1997) RasLeu61 blocks differentiation of transformable 3T3 L1 and C3H10T1/2-derived preadipocytes in a dose and time-dependent manner. *Cell Growth and Differentiation* 8: 11-21.
- Riveline D., Zamir E., Balaban N.Q., Schwarz U.S., Ishizaki T., Narumiya S., Kam Z., Geiger B. and Bershadsky A.D. (2001). Focal contacts as mechanosensors: externally applied local mechanical force induces growth of focal contacts by an mDia1-dependent and ROCK-independent mechanism. *Journal of Cell Biology*, **153**(6):1175-86.
- Rodriguez-Viciano P., Waarne P.H., Dhand R., Vanhaesebroeck B., Gout I., Fry M. J., Waterfield M.D., Downwards J. (1994) Phosphatidylinositol-3-OH kinase as a direct target of Ras. *Nature* 370: 527-532.
- Sander E.E., ten Klooster J.P., van Delft S., van der Kammen R.A., Collard J.G. (1999) Rac downregulates Rho activity: reciprocal balance between both GTPases determines cellular morphology and migratory behaviour. *Journal of cell biology* 147: 1009-1022.
- Sasaki A.T., Janetopoulos C., Lee S., Charest P.G., Takeda K., Sundheimer L.W., Meili R., Devreotes P.N., Firtel R.A. (2007) G protein-independent Ras/PI3K/F-actin circuit regulates basic cell motility. *Journal of Cell Biology* 178:185-191.
- Sasaki A.T., Chun C., Takeda K., Firtel R.A. (2004) Localized Ras signalling at the leading edge regulates PIK, cell polarity, and directional cell movement. *The journal of cell biology*. 167(3): 505-518.
- Schaller M.D. (2001) Paxillin: a focal adhesion-associated adaptor protein. *Oncogene* 20: 6459-6472.
- Schubert S., Shannon K., Bollag G. (2007) Hyperactive Ras in developmental disorders and cancer. *Nature Reviews* 7: 295-308.
- Schultz G.S., Wysocki A. (2009) Interactions between extracellular matrix and growth factors in wound healing. *Wound repair and regeneration* 17: 153-162.
- Shima Y., Okamoto T., Aoyama T., et al. (2007) In vitro transformation of mesenchymal stem cells by oncogenic H-Ras V12. *Biochemical and Biophysical Research Communications* 353: 60-66.
- Simpson K.J., Selfors L.M. (2008) Identification of genes that regulate epithelial

References

- cell migration using an siRNA screening approach. *Nature cell biology* 10(9): 1027-38.
- Slack-Davis J.K., Eblen S.T., Zecevic M., Boerner S.A., Tarcsfalvi A., Diaz H.B., et al. (2003) PAK1 phosphorylation of MEK1 regulates fibronectin-stimulated MAPK activation. *Journal of Cell Biology* 162: 281–291.
- Taparowsky E., Shimizu K., Goldfarb M., Wigler M. (1983) Structure and activation of the human N-ras gene. *Cell* 34: 581-586.
- Tarnawski A.S. (2005) Cellular and molecular mechanism of gastrointestinal ulcer healing. *Digestive diseases and sciences* 50 Suppl 1:S24-33.
- Teranishi S., Kinura K., Nishida T. (2009) Role of formation of an ERK-FAK-paxillin complex in migration of human corneal epithelial cells during wound closure in vitro. *Investigative ophthalmology & visual science*. 50(12): 5646-52.
- Tètreault M.P., Chailier P., Beaulieu J.F., Rivard N., Mènard D. (2008) Epidermal growth factor receptor-dependent PI3K-activation promotes restitution of wounded human gastric epithelial monolayers. *Journal of cellular Physiology* 214(2):545-57.
- Tian Y.C., Chen Y.C., Chang C.T., Hung C.C., Wu M.S., Philips A., Yang C.W. (2007) Epidermal growth factor and transforming growth factor- β 1 enhance HK-2 cell migration through a synergistic increase of matrix metalloproteinase and sustained activation of ERK signaling pathway. *Experimental cell research* 313: 2367-2377.
- Torii S., Nakayama K., Yamamoto T., Nishida E. (2004) Regulatory mechanism and function of ERK MAP kinases. *Journal of Biochemistry* 136: 557-561.
- Tscharntke M., Pofahl R., Krieg T., Haase I. (2005) Ras-induced spreading and wound closure in human epidermal keratinocytes. *The FASEB journal* 19(13): 1836-8.
- Turchi L., Chassot A.A., Rezzonico R., Teow K., Loubat A., Ferrua B., Lenegrato G., Ortonne J.P., Ponzio G. (2002) Dynamic characterization of the molecular events during in vitro epidermal wound healing. *The journal of investigative dermatology* 119(1): 56-63.
- Turner C.E. (2000) Paxillin interactions. *Cell Science at a glance* 113 Pt 23:4139-40.
- Ueoka Y., Kato K., Kuriaki Y., Horiuchi S., Terao Y., Nishida J., Ueno H., Wake N. (2000) Hepatocyte growth factor modulates motility and invasiveness of ovarian carcinoma via Ras-mediated pathway. *British Journal of Cancer* 82: 891-899.
- Vial E., Sahai E., Marshall C.J. (2003) ERK-MAPK signalling coordinately regulates activity of Rac1 and RhoA for tumor cell motility. *Cancer cell* 4:67-79.

References

- Watson G.S. (1961) Goodness-of-fit tests on a circle. *Biometrika*. 48:109-114.
- Weiquan L., Tianqing Z., Kun-Liang G. (2004) Transformation potential of Ras isoforms correlates with activation of phosphatidylinositol 3-kinase but not ERK. *The Journal of Biological Chemistry* 279: 37398-37406.
- Wessels D., Lusche D.F., Kuhl S., Heid P., Soll D.R. (2007) PTEN plays a role in the suppression of lateral pseudopod formation during *Dictyostelium* motility and chemotaxis. *Journal of Cell Science* 120:2517–253.
- Wilkins A., Insall R.H. (2001) Small GTPases in *Dictyostelium*: lesson from a social amoeba. *Trends in genetics* 17(1):41-8.
- Wu W.S., Wu J.R., Hu C.T. (2008) Signal cross talks for sustained MAPK activation and cell migration: the potential role of reactive oxygen species. *Cancer metastasis review* 27: 303-314.
- Yan J., Roy S., Apolloni A., Lane A., Hancock J.F. (1998) Ras isoforms vary in their ability to activate Raf-1 and phosphoinositide 3-kinase. *The journal of biological chemistry* 273: 24052-24056.
- Yip S.C., El-Sibai M., Coniglio S.J. et al. (2007) The distinct roles of Ras and Rac in PI3-kinase-dependent protrusion during EGF-stimulated cell migration. *The journal of cell science* 120: 3138-3146.
- Yoon S., Seger R. (2006) The extracellular signal-regulated kinase: multiple substrates regulate diverse cellular functions. *Growth Factors* 24: 21-44.
- Zamir E. and Geiger B. (2001) Molecular complexity and dynamics of cell-matrix adhesions. *Journal of cell Science* 114: 3583-3590.
- Zhang J. and Lodish H.F. (2004) Constitutive activation of the MEK/ERK pathway mediates all effects of oncogenic H-ras expression in primary erythroid progenitors. *Blood* 104: 1679-1687.

Publication

- Cantarella C., Sepe L., Fioretti F., Ferrari M.C., Paoletta G. (2009) Analysis and modelling of motility of cell populations with MotoCell. *BCM Bioinformatics Suppl* 12: S12.

Research

Open Access

Analysis and modelling of motility of cell populations with MotoCell

Concita Cantarella^{†1,2}, Leandra Sepe^{†1}, Francesca Fioretti¹,
Maria Carla Ferrari¹ and Giovanni Paoletta*^{1,3}

Address: ¹DBBM Dipartimento di Biochimica e Biotecnologie Mediche, Università di Napoli FEDERICO II, Via S. Pansini 5, 80131 Napoli, Italy, ²S.E.M.M. – European School of Molecular Medicine – Naples site, Italy and ³CEINGE Biotecnologie Avanzate scrl, Via Comunale Margherita 482, 80145 Napoli, Italy

E-mail: Concita Cantarella - cantarella@ceinge.unina.it; Leandra Sepe - sepe@dbbm.unina.it; Francesca Fioretti - francesca.fioretti@alice.it; Maria Carla Ferrari - ferrari@dbbm.unina.it; Giovanni Paoletta* - paoletta@dbbm.unina.it

*Corresponding author †Equal contributors

from Bioinformatics Methods for Biomedical Complex Systems Applications (NETTAB2008)
Varenna, Italy 19–21 May 2008

Published: 15 October 2009

BMC Bioinformatics 2009, 10(Suppl 12):S12 doi: 10.1186/1471-2105-10-S12-S12

This article is available from: <http://www.biomedcentral.com/1471-2105/10/S12/S12>

© 2009 Cantarella et al; licensee BioMed Central Ltd.

This is an open access article distributed under the terms of the Creative Commons Attribution License (<http://creativecommons.org/licenses/by/2.0>), which permits unrestricted use, distribution, and reproduction in any medium, provided the original work is properly cited.

Abstract

Background: Cell motility plays a central role in development, wound-healing and tumour invasion. Cultures of eucariotic cells are a complex system where most cells move according to 'random' patterns, but may also be induced to a more coordinate migration by means of specific stimuli, such as the presence of chemical attractants or the introduction of a mechanical stimulus. Various tools have been developed that work by keeping track of the paths followed by specific objects and by performing statistical analysis on the recorded path data. The available tools include desktop applications or macros running within a commercial package, which address specific aspects of the process.

Results: An online application, MotoCell, was developed to evaluate the motility of cell populations maintained in various experimental conditions. Statistical analysis of cell behaviour consists of the evaluation of descriptive parameters such as average speed and angle, directional persistence, path vector length, calculated for the whole population as well as for each cell and for each step of the migration; in this way the behaviour of a whole cell population may be assessed as a whole or as a sum of individual entities. The directional movement of objects may be studied by eliminating the modulo effect in circular statistics analysis, able to evaluate linear dispersion coefficient (R) and angular dispersion (S) values together with average angles. A case study is provided where the system is used to characterize motility of RasV12 transformed NIH3T3 fibroblasts.

Conclusion: Here we describe a comprehensive tool which takes care of all steps in cell motility analysis, including interactive cell tracking, path editing and statistical analysis of cell movement, all within a freely available online service. Although based on a standard web interface, the program is very fast and interactive and is immediately available to a large number of users, while exploiting the

web approach in a very effective way. The ability to evaluate the behaviour of single cells allows to draw the attention on specific correlations, such as linearity of movement and deviation from the expected direction. In addition to population statistics, the analysis of single cells allows to group the cells into subpopulations, or even to evaluate the behaviour of each cell with respect to a variable reference, such as the direction of a wound or the position of the closest cell.

Background

Cell migration is involved, at various extents, in fundamental processes as embryo development and organogenesis, organism growth and survival and response to pathological situations. In the developing embryo, coordinated cell migration involves movement of cells of different origin throughout the embryo, over short and long distance paths; defects of migration at all stages of development lead to severe embryonic malformations and result in drastic overall consequences [1]. In adult organisms, cell movement is essential in wound-healing, where epidermal repair, initiated by the progressive extension of a tongue of epidermal cells, results in complete closure of the wound. Cell migration is also involved in inflammation and atherosclerosis and is responsible for primary invasion of cancer cells and metastatization [2].

Cell cultures are often studied as model systems for movement, as a population of cells growing *in vitro* moves on the culture surface using the same complex membrane machinery used by cells *in vivo*. A large amount of experimental work, carried out in many laboratories, has provided a good understanding of the processes and interactions which control cell motility. Integrin receptors, focal adhesion structures, cytoskeletal elements and signalling molecules are important players both *in vivo* and *in vitro* [3-5]. Mathematical and computational methods have also been developed to model specific aspects of movement, such as formation of membrane protrusions and actin dynamics, [6,7]. In addition, cell movement has been studied with approaches which take into account the whole cell, where mechanical events such as protrusion, contraction and relaxation all contribute to produce cell displacement [8-10].

The behaviour of the cell population has also been analyzed. In absence of particular conditions, cells move on the culture plate over smaller or larger distances, depending on the cell type and culture conditions, and in all possible directions; the culture can also be exposed to specific stimuli which can affect both speed and direction. Video time-lapse microscopy is used to dynamically study the phenomenon. By acquiring multiple images of the same field over time, a stack of images

is produced which together describe migration in two, or even three, dimensions. Cell motion is evaluated by tracking subsequent cell positions either manually, by marking, with the assistance of a computer, the positions assumed by individual cells in stacks of recorded images, or automatically. Cell tracking algorithms may not be as accurate as manual recording, but require less time and may be used for the analysis of a large number of cells. They use simple methods which calculate the position assumed by a labelled cell or the nucleus, after segmenting the image on the basis of intensity [11], or with more sophisticated methods, where subsequent deformations of an initial contour model are used to identify cell boundaries in the next frames [12]. Paths are typically described by list of coordinates corresponding to the trail followed by moving cells, and are subsequently analyzed in order to extract descriptive parameters.

Different tools have been developed in recent years. Support for cell tracking has been integrated into commercial applications, such as softWoRx Suite (Applied Precision) and MetaMorph (Molecular Devices), but freely available research tools have also been described such as Particle Tracker <http://weeman.inf.ethz.ch/particletracker/> and MtrackJ <http://www.image-science.org/meijering/software/mtrackj/>, two plugins that work within ImageJ <http://rsb.info.nih.gov/ij/index.html> [13]. Specific tools have been described to process the paths followed by cells: examples are a trajectory segmentation algorithm, based on supervised support vector classification, or the evaluation of a path according to a brownian model [14,15]. Other methods have been used to describe the population behaviour, often borrowing from techniques used in other fields [16].

Here we present the application of methods for quantitative analysis of the movement of cell populations, which evaluate descriptive statistical parameters and use circular statistics and curve fitting to model directional movement. The methods have been implemented in a software package, which uses an online approach to create an environment where cell tracking, parameter evaluation and statistical analysis is all integrated. This is seen as a web application, MotoCell, which may be conveniently used from the operator desktop, without installation at <http://motocell.ceinge>.

unina.it. The system has been used to study and model the motility of cell populations as well as the behaviour of single individual cells.

Results and discussion

MotoCell

MotoCell is a web application, designed to track and evaluate the paths followed by cultured cells moving on a surface. Its main goal is to merge a cell tracking module with the ability to statistically evaluate motility of cells or particles. It can directly load both acquisition obtained and stored locally, within the Images database, or external files, organized as a series of frames collected within a folder. Various file formats are accepted (see methods).

The user interface is organized in two main areas, a control panel and an area for visualizing cells and paths and to input cell coordinates (Fig. 1). The control panel includes sections containing commands for uploading external acquisitions and change image magnification, to take advantage of the available screen size and better recognize cell compartments or other small structures. The status bar, located immediately below the upload section, is used to select and visualize the 'Insert', 'View', 'Select' and 'Modify' modes. 'View' mode is used to go through the movie, frame by frame or at fixed intervals, whereas the 'Insert' mode is used for input of cell coordinates by clicking on subsequent frames of a movie. Cell coordinates (Fig. 1a) for each time steps are stored in text files and used to perform calculations through the web interface. Tables and plots reporting the results of statistical analysis may be downloaded as text or pdf files.

Cell tracking is performed by clicking at the various positions occupied by a moving cell in subsequent frames (Fig. 1b); x-y coordinates are recorded and written to a table. The destiny of each cell following its path is also recorded: paths may last for the whole observation time, but may also prematurely end with the death of a moving cell, with a cell split in two as a consequence of a mitotic event, or with the loss of a cell, which moves beyond the limits of the observation field. The coordinates of a path may be modified during or after the tracking phase, in order to correct errors without relicking the entire data set. 'Select' mode is used to identify the path which needs editing, while the 'Modify' mode is used to assign new coordinates or to change the end of the path. Sometimes researchers are interested in studying subsets of the whole population: the system permits the association of cells to different subsets, which may be separately evaluated (Fig. 1b).

The results of cell tracking, typically stored as a list of cell coordinates in a text file, are evaluated by MotoCell

which calculates statistical parameters for each cell path, or the whole population. Sample output windows are reported in Fig. 2, where linear and circular statistics parameters are presented as tables (a) or plots (b), designed to quantitatively describe typical experimental situations, as detailed in the following section.

MotoCell in the study of cell motility

MotoCell is organized around distinct objects. A Movie object takes care of storing and analyzing the behaviour of the whole population. It contains many path objects, which in turn include step objects, corresponding to each elementary movement of a single cell between two contiguous frames. Point and vector objects are used to represent the corresponding physical entities.

Within MotoCell, the path length is defined as the sum of all subsequent smaller steps made by a cell, the speed as the average length of all the steps (Fig. 3a) performed by a cell within the time interval, and linearity as the ratio of net displacement (i.e. the distance between the starting and end point) to path length. (Fig. 3b). For a population, speed is the average of all the steps performed by all the cells, linearity is the harmonic average of linearity independently calculated for each cell.

The average direction of a population is the direction of the resulting vector obtained by composing the displacement vectors for each cell path, while coherency is defined as the ratio between length of the same resulting vector and sum of the single net displacement vector lengths (Fig. 3c). Circular statistics analysis is used to evaluate descriptive parameters R and S, by treating the displacements during each step as circularly varying quantities, corresponding to the angle of each displacement vector, and without taking into account its module [16,17]. The average angle describing a path (ϕ) is obtained from the arithmetic means of cosine and sine values for each angle (Fig. 3d):

$$\phi = \arctan \frac{\bar{y}}{\bar{x}}$$

where

$$\bar{x} = \frac{\sum_{i=1}^n \cos \alpha_i}{n}$$

and

$$\bar{y} = \frac{\sum_{i=1}^n \sin \alpha_i}{n}$$

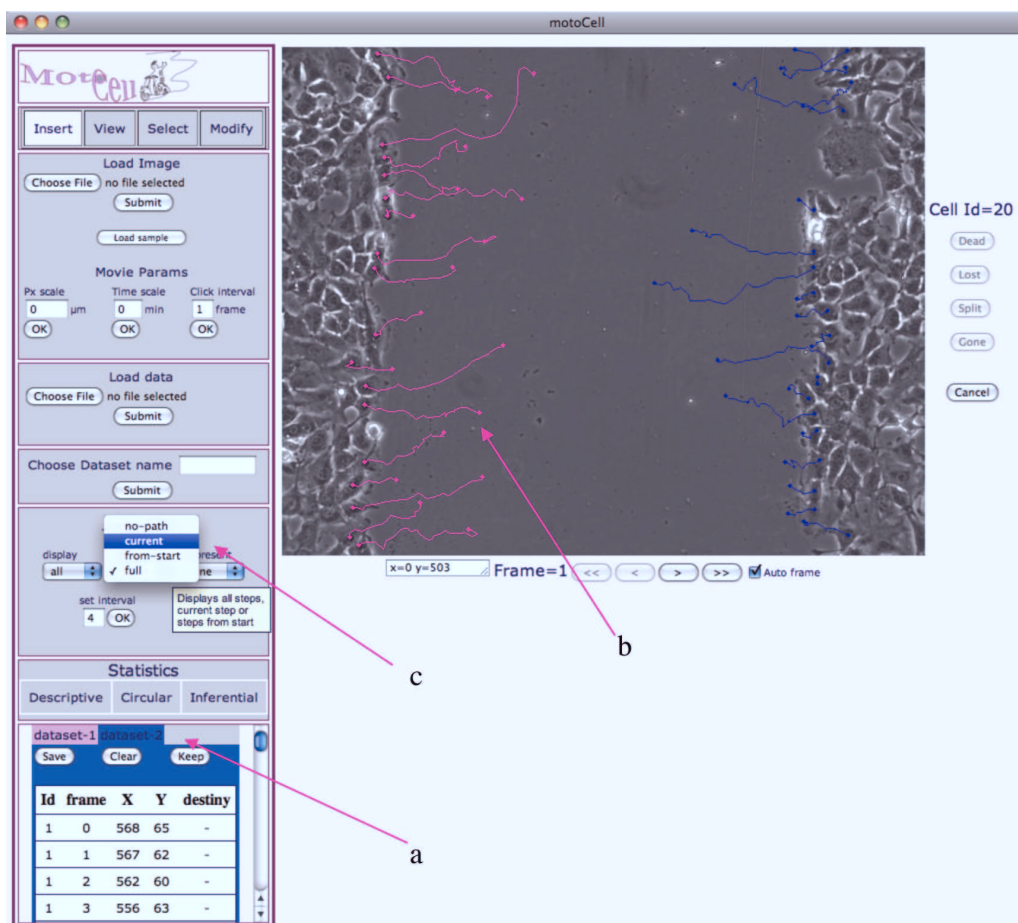


Figure 1
MotoCell web interface. The main Motocell interface is used for all operations, including tracking, data handling and evaluation of statistical parameters. in MotoCell assists in cell tracking by recording the users clicks at the various positions in subsequent frames. For each step, coordinates are recorded within the table (a) located at the bottom of the Control area and displayed on the image as paths (b). When more datasets are used at the same time, they are alternatively visualized according to the chosen data tab; tab colors are used to match the tables with the corresponding paths on the image. A popup menu (c) allows to choose alternative path visualizations: incrementally from the beginning, only at the current time point or as a point sliding along the full path.

The angle of the obtained average vector has its origin in the center of a circle with unit radius and direction φ . The module of this vector is named linear dispersion coefficient (R) and may be easily calculated as

$$R = \sqrt{\bar{x}^2 + \bar{y}^2}$$

R is not dependent on the length of each step, and is descriptive of the distribution of the angles of the step vectors. Its value ranges from 0 to 1, being close to 0 when the angles have a uniform distribution with no directional trend, but gets larger for an asymmetric distribution of angles clustered around a specific

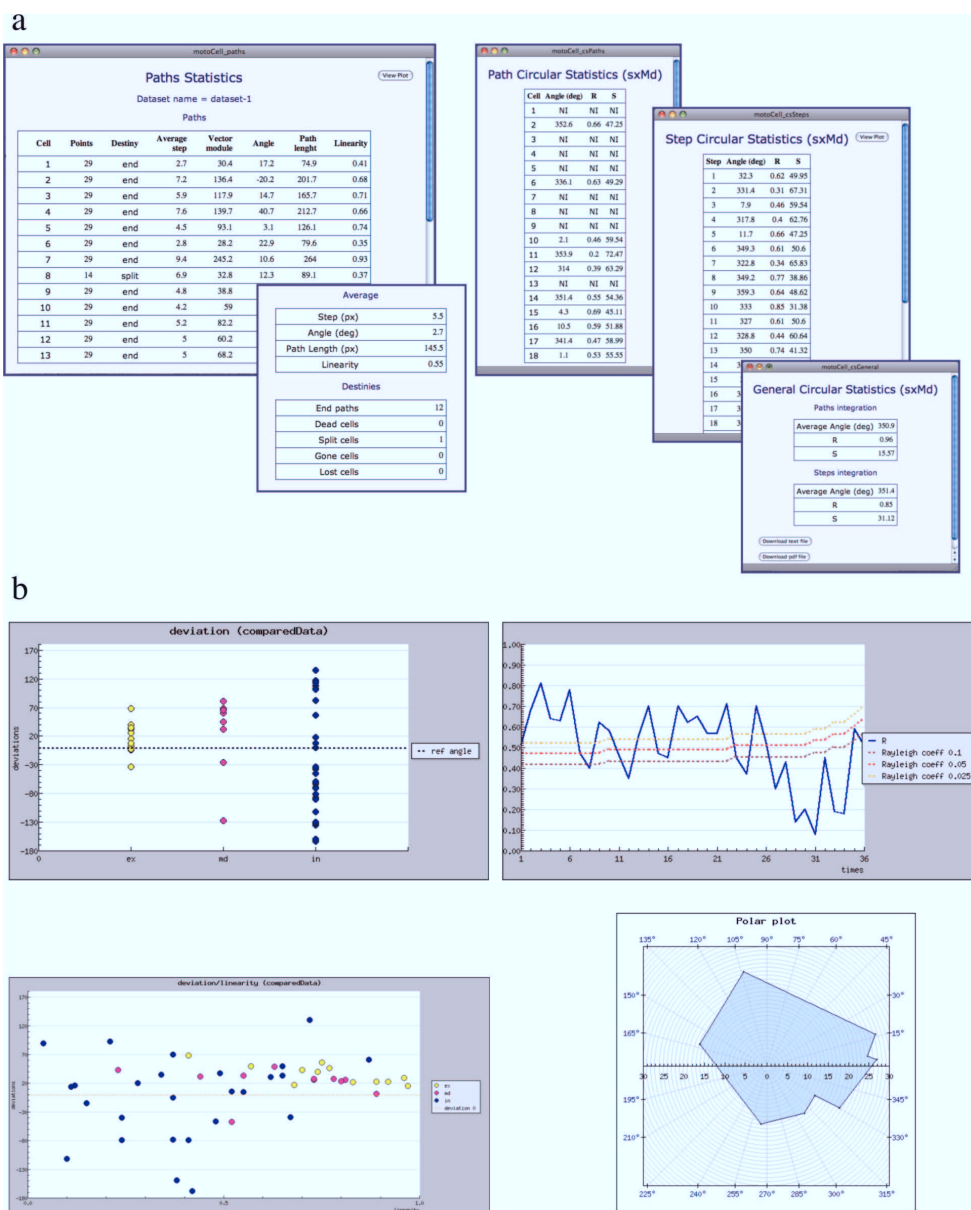


Figure 2
Output of statistical analysis. Examples of MotoCell results visualization: a) descriptive and circular statistics parameters, reported for each cell and as average values for the whole population; b) scatter plots, graphs and polar plots, used to show trends in time, path parameters, spatial distribution of directions.

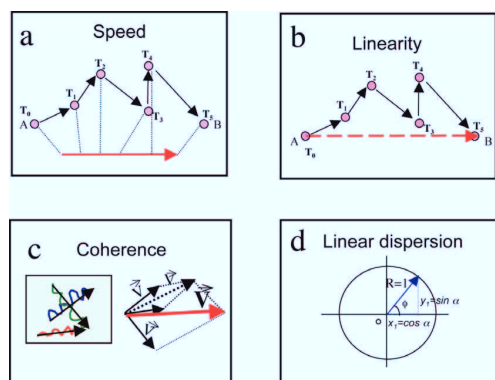


Figure 3
Statistical parameter evaluation. a) Speed was calculated as the average of all step lengths; b) linearity as the ratio of net displacement, i.e. the distance between start and end point of a path, to path length; c) coherence of a population is defined as the ratio between length of the resulting vector, obtained by composing the displacement vectors for each cell path, and sum of the single net displacement vector lengths; d) linear dispersion coefficient R is defined as the module of a vector having its origin in the center of a circle with unit radius and direction the average angle φ .

direction, reaching 1 for the special case when all the angles are identical (Fig. 3d). Angular dispersion (S) is calculated starting from R :

$$S = \sqrt{2(1 - R)}$$

and represents the dispersion of the angles around the average direction.

Random motility of NIH3T3 fibroblasts

In the absence of specific stimuli the movement of cells growing on a culture surface is expected to be randomly oriented in all possible directions and not dependent on time, thus producing a purely random distribution of displacements. Figure 4 shows, on the left, the paths covered by three mouse cell populations maintained in culture plates: NIH3T3 fibroblasts under standard (a) and limiting (b) growth conditions and transformed (NIHRas) by overexpression of Ras oncogene (c) are followed during 10 hours in culture. In order to provide a global representation of the behaviour of each individual cell within a population, polar plots have been generated with MotoCell to graphically represent the distribution of observed net cell displacements. On the right side of figure 4, the directions of the same paths

have been represented as a polar graph to graphically visualize their spatial distribution: the randomness of directions can be easily recognized in all cell populations by observing the circular shape of the three areas in the charts. Furthermore, the size of the areas delimited by the polar plots highlights the different ability of the three populations to move away from the starting point. NIH3T3 move much more in 10% serum (d) than under low serum conditions (e); NIHRas (f) show the longest paths.

In order to quantitatively describe movement in better detail, synthetic parameters were calculated within MotoCell for speed, persistence and coherency of movement, by averaging their values at each time point. Although cells obviously change during the period they are kept in culture, time is expected not to be influential as long as a number of conditions are verified: 1) the observation period is kept relatively short, 2) sufficient distance is maintained from critical events, such as culture splitting, cell cycle synchronization, addition of reagents etc., 3) availability of space or nutrients does not become limiting, as for example in cells reaching confluence. These assumptions were verified by observing the behaviour of a NIHRas population, plated at sub-confluent density, starting the observation 12 hours after seeding and prolonging it for 10 hours; the speed values recorded at each time point, tend to remain stable around the average values during the whole observation period as shown in Fig. 5a for NIHRas; similar results are obtained for the other lines (not shown). The average speed values, evaluated for NIHRas and NIH3T3 fibroblasts, are reported in figure 5b: NIHRas cells move faster than NIH3T3 under standard culture conditions; speed is further reduced under low serum conditions, as shown for NIH3T3 in the same plot. For all experimental conditions, linearity values are not very high, ranging between 0.2 e 0.6 (c) while coherence is generally low (d), as expected for random movement, where there is no specific reason for preferring one direction rather than another.

Directional migration of NIHRas fibroblasts

The marked ability of NIHRas cells to migrate on culture surfaces has been studied under different experimental conditions, some of them known to affect the migration of cell populations. For example, when a wound is open within a cell layer, by scratching the surface with a sharp object, the removal of cells from the wounded area acts as a stimulus for the remaining cells to invade and fill the space left empty by the wound. In this type of movement the directional component may be clearly detected as increased coherence and, often, also linearity, as cells moving in a defined direction also tend to maintain the same direction in time (Table 1).

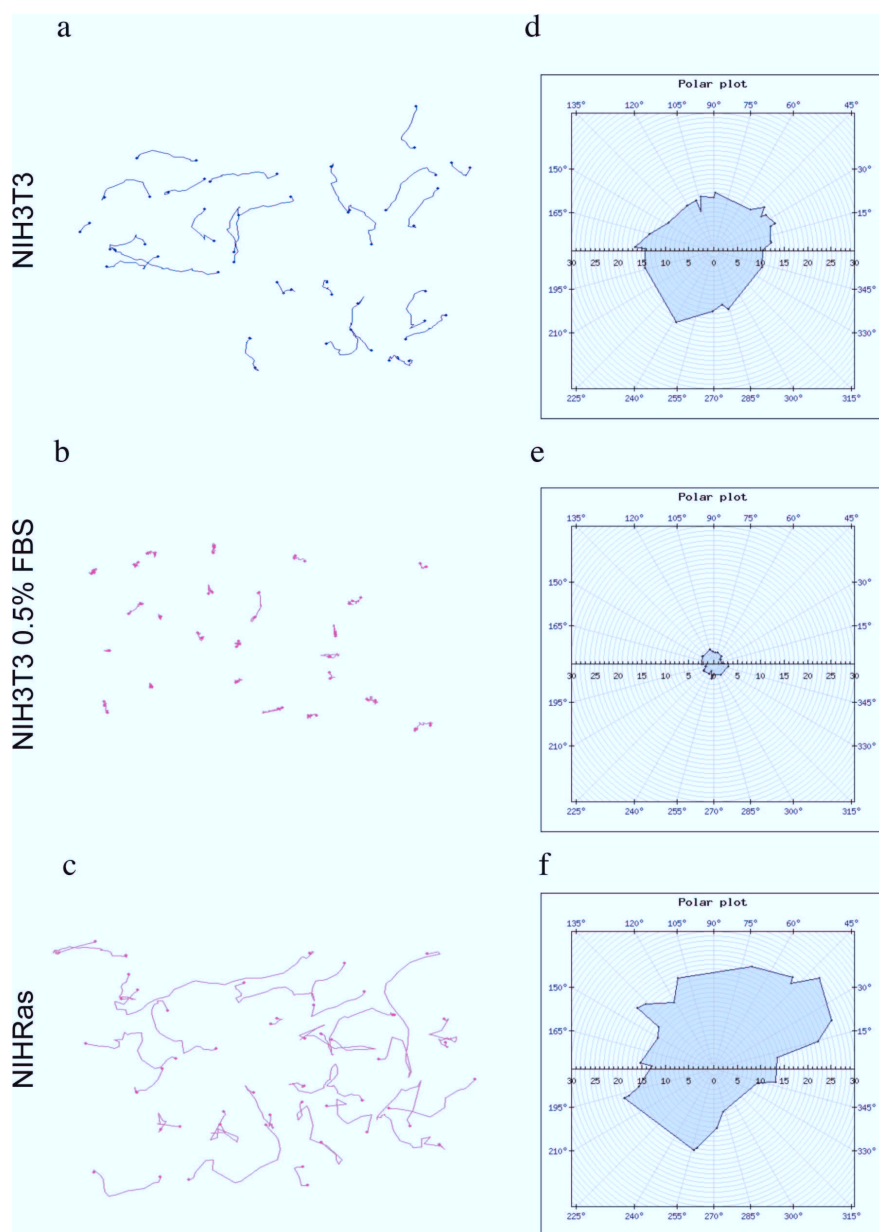


Figure 4
Random motility analysis. Paths covered by NIH3T3 (a) and NIH3T3 in 10% (b) and 0.5% serum (c) moving on the culture surface. (d, e, f) Representation of the paths by using polar coordinates, for the three populations.

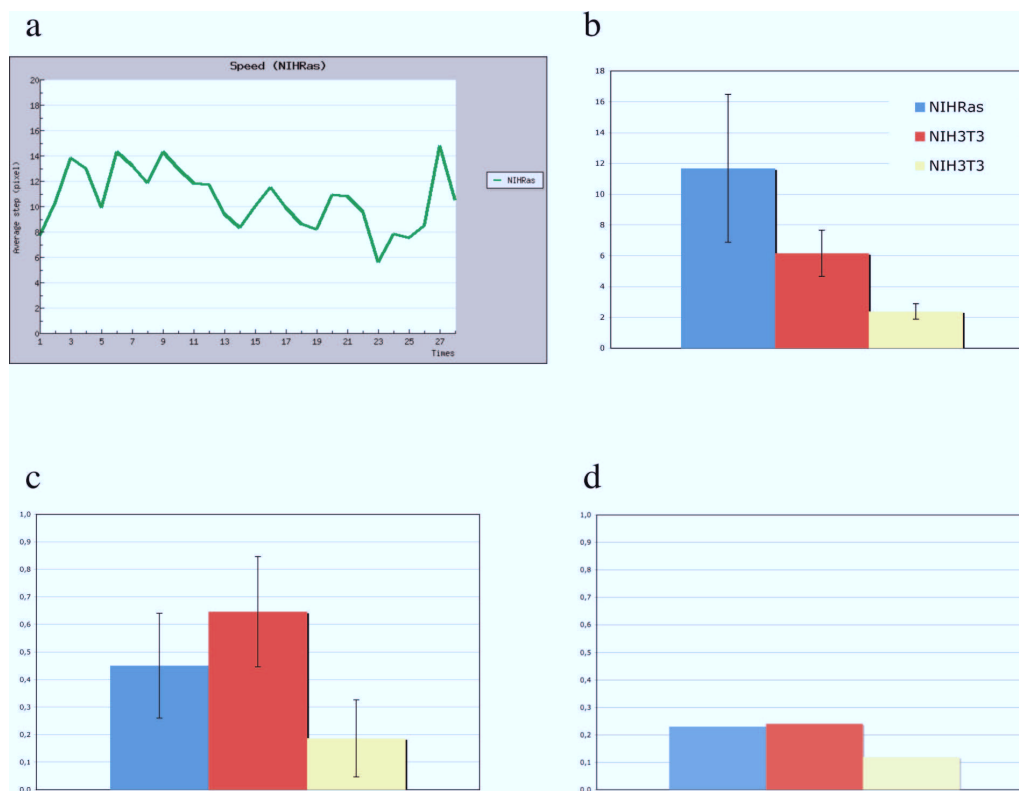


Figure 5
Evaluation of kinetic parameters. a) Average step length during the observation time. Plots showing average values for speed (b), expressed as $\mu\text{m}/40'$ step, linearity (c) and coherency (d). NIH3T3 cells are in blue, NIH3T3 in 10% (red) and 0.5% (yellow) populations.

Table 1: Linearity and coherence of NIH3T3 and NIH3T3 cell motility

| | NIH3T3 | | NIHRas | |
|-----------|--------|-------|--------|-------|
| | Random | Wound | Random | Wound |
| Linearity | 0.44 | 0.54 | 0.45 | 0.62 |
| Coherency | 0.24 | 0.71 | 0.23 | 0.8 |

Values are reported for random motility and wound-healing assays. See details under 'Results'

The circular statistics functions within MotoCell have also been used to analyse the directional movement of different cell populations in wound-healing experiments, as reported in Fig. 6a. Linear dispersion values show much better directionality for NIH3T3 (0.365) than

NIH3T3 (<0.1) cells; NIH3T3 score even better under 0.5% serum (0.65), although speed is reduced from 11.5 to 5.2 $\mu\text{m}/\text{step}$ (data not shown). The significance of parameters evaluated by circular statistics were assessed by using the Rayleigh test [18], which compares the parameters with threshold levels corresponding to values expected for random datasets following the von Mises distribution. Under the used conditions, confidence values better than 0.01 or 0.05, were obtained even for datasets consisting only of a small number of cells. In Fig. 6a, the significance levels for $P < 0.01$ are reported as transparent boxes overlaid onto the histogram.

NIHRas fibroblast subpopulations in wound healing assays

In order to test the response of the cell layer to a wound, linear dispersion R is plotted in MotoCell as a function

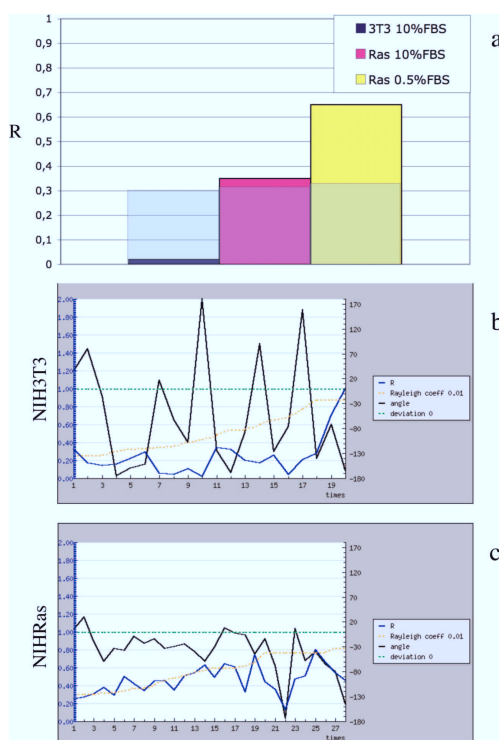


Figure 6
Evaluation of linear dispersion coefficient (R). R coefficients calculated for three cell populations in wound-healing assay (a). Deviation from the expected, i.e. towards the center of the wound, direction and R values are reported for each time point for NIH3T3 (b) and NIH3T3 (c) populations.

of time, together with the average angle, reported as deviation from the expected direction of wound closure. The results obtained for the NIH3T3 population are reported in Fig. 6b and show the average direction to be very variable in time, with angles widely ranging between + and -180° of the expected value. Under such condition, R values consistently remain well below the chosen significance threshold, during the whole observation time. The scenery is changed when we consider the behaviour of NIH3T3 populations (Fig. 6c): the deviation angles become close to the expected direction, and R is either above or immediately below the threshold values except at the end of the observation time, when angles start to drift away from the reference, and linear dispersion values go below the threshold,

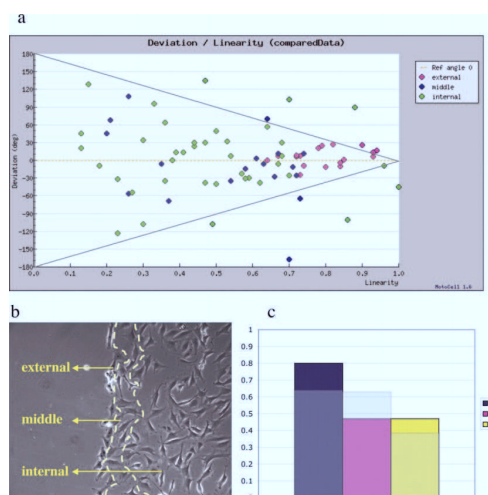


Figure 7
Relationship between deviation angle and linearity. a) Deviation from the expected direction, plotted as a function of linearity, in a population subjected to the wound stimulus. b) External, middle and internal sub-populations, identified according to their distance from the wound edge. c) R coefficient for the three sub-populations, compared to the threshold level for P = 0.01.

probably reflecting loss of directional movement when the wound is almost closed.

Linearity of movement in time, usually low or moderate in randomly moving cells, might become higher when cells are stimulated to move towards an attractant or other stimuli. The relation between directionality and linearity was evaluated in the previously described wound-healing assay. The results are shown in Fig. 7a where deviation from the reference angle is plotted as a function of linearity. Cells following non linear paths cluster around the left side of the plot and do not show any preferred angle, while those showing high linearity, move according to angles that cluster around the expected direction, i.e. towards the middle of the wound. If different colors are used to distinguish cells located at varying distance from the wound, it is clear that cells showing better linearity and directionality mostly belong to a subpopulation placed at the edge of the wound. Cell with lower linearity are either located in an intermediate position, or far away from the wound. This analysis therefore induces to distinguish different sub-populations, defined as external, middle and internal according to their distance from the wound (Fig. 7b).

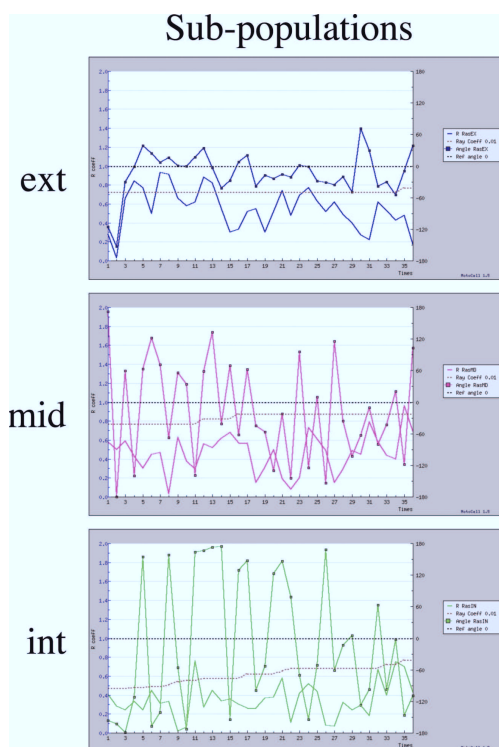


Figure 8
Time plots for the three subpopulations described in figure 7. Deviation angle and R coefficient, for the external, middle and internal cell subpopulation. In all plots, expected angle (black) and threshold level for P = 0.01 (red) are reported as a reference.

If these sub-population are separately analyzed, the predominant effect of the wound edge on the front population is clearly indicated by the very high R value, well above the threshold for P < 0.01 obtained in circular statistics analysis (Fig. 7c).

Time analysis of directional movement of the three separated sub-populations allows to observe that deviations from the expected direction are always small and R values are generally high for the subpopulation close the wound (ext). For the middle subpopulation and much more for the internal one, more scattered values can be observed (Fig. 8). This is believed to be a strong indication that the distance from the wound stimulus can modulate cellular movement by acting on

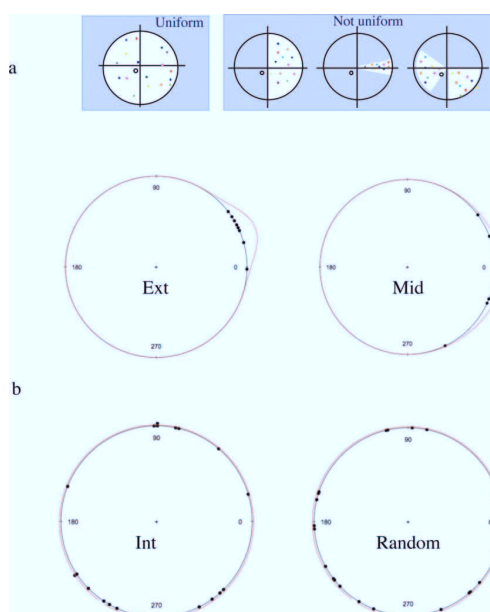


Figure 9
Circular plot of path directions. a) Examples of uniform and non-uniform distributions. b) Curves describing the best fitting von Mises distributions, overlaid onto the experimental points for external, middle, internal, and random populations.

directional component of cell migration in a distance dependent fashion.

Modelling directional movement with von Mises distribution

Circular statistics detects the not uniform distribution of a given dataset, but is not able to discriminate between different non-uniform distribution models, as shown in Fig. 9a. The von Mises distribution is commonly used as a model for many circular data problems. It fits well to points tightly concentrated around a mean direction. It is defined by:

$$f(\vartheta; \mu, \kappa) = \frac{1}{2\pi I_0(\kappa)} e^{\kappa \cos(\vartheta - \mu)}$$

where $0 \leq \vartheta < 2\pi$, $\kappa \geq 0$, $0 \leq \mu < 2\pi$ and $I_0(\kappa) = \frac{1}{2\pi} \int_0^{2\pi} e^{\kappa \cos(\vartheta)} d\vartheta$ is the zeroth Bessel function, μ indicates the mean direction and κ the concentration parameter, in some way recalling the gaussian distribution [19].

In order to attempt to model the behaviour of a cell population according to a von Mises distribution, the net displacements of each cell following a path have been used to compute the maximum likelihood estimates for the parameters of a von Mises distribution. Overlays of the theoretical curve with the experimental data are reported in Fig. 9b, while the calculated parameters are in Table 2.

In order to evaluate the fit of the calculated model to the experimental data, the Watson test was used to test for both a von Mises and a uniform distribution [20]. The results are reported in Table 2, where for all tested datasets the hypothesis of von Mises distribution may be accepted while the uniform hypothesis should be rejected for the external and middle population. In all cases a significance level of 0.01 was chosen. It should be noted that fitting to a von Mises is compatible, but not indicative of unidirectional movement, because a very wide and flat distribution is still acceptable as a von Mises. Of course such a distribution is easily recognized, as it would also fit a circular model and produce lower linear dispersion values in the circular statistics test. With this approach, a bimodal distribution, is also easily recognized as it may result acceptable as a circular, but not as a von Mises distribution model (not shown).

Conclusion

Cell migration is involved in important processes in embryo development and adult life and is mediated by a very complex machinery, which includes a large number of membrane bound, soluble and nuclear factors. The web application presented here, MotoCell, may be used to describe the behaviour of both single cells and whole cell populations by separately analyzing and quantitatively evaluating parameters, descriptive of speed and directionality of cell movement. MotoCell integrates all the relevant tasks within a unique environment, where cell tracking, plot generation and statistical evaluation may be quickly and easily performed. The software, originally developed as a collection of scripts for single user PCs, in its present web form, offers important advantages, such as tight integration with a shared image database, and no need for data transfer between hosts

before analysis. Although based on a standard web interface, by exploiting the web approach in a very effective way, the program results very fast and interactive and is immediately available to a large number of users.

The described case study allowed to analyze the directional movement of NIH3T3 transformed cells as a function of time and in relation to stimuli. Statistical parameters describing consistency of directional movement in time (linearity) and across the cell population (coherency) were evaluated for this cell line, together with circular statistics parameters as linear dispersion coefficient (R) of the cell paths and angular dispersion (S) values around the average angles. The results clearly show the Ras transformation increases both speed and directionality of cell movement.

The ability to evaluate the behaviour of single cells allows to draw the attention on specific correlations, such as persistence of movement and deviation from the expected direction as shown in figures 6, 7, 8. By using the Rayleigh test to assess the significance of circular statistics parameters, it was possible to recognize that confidence limits better than 0.01 may be achieved in tests involving even a limited number of cells. Fitting the observed data to the von Mises model, as well as to the circular model, allowed to decide whether an observed non-uniform directional movement, determined by circular statistics and directed towards a given direction, is correctly assigned to a unidirectional model.

The application of these methods to the study of fibroblast movement supports a relationship between cell path linearity and population coherency in many experimental situations and allowed to detect the existence of defined subpopulations, located at increasing distance from the wound edge and characterized by different motility features.

Methods

Most analysis are performed within a web application, MotoCell, which is used to track moving cells by interactively clicking at the various positions occupied

Table 2: Fit to von Mises distribution

| | μ (degree) | κ | K | Cr. value vM | Test Circ. | Cr. value Circ. |
|----------|------------------|------------------|--------------|--------------|--------------|-----------------|
| external | 21.62 +/- 4.385 | 19.48 +/- 9.056 | 0.073 | 0.164 | 0.625 | 0.267 |
| middle | -6.49 +/- 10.12 | 4.542 +/- 2.084 | 0.037 | 0.158 | 0.395 | 0.267 |
| internal | -99.43 +/- 43.23 | 0.4133 +/- 0.319 | 0.060 | 0.09 | 0.113 | 0.267 |
| random | -122.4 +/- 56.13 | 0.2963 +/- 0.293 | 0.036 | 0.09 | 0.058 | 0.267 |

First and second columns report mean direction μ and concentration κ for best fitting von Mises distributions, respectively for external, middle, internal and random populations. In columns 3 to 6, results for von Mises (3) and uniform (5) tests are reported, next to their critical values (4 and 6) for the populations described in fig. 9

by them in subsequent frames; x-y coordinates are recorded and written to a table. The destiny of each cell following its path is also recorded: paths may end with the death of the moving cell, with a mitotic event, where the cell is split in two or by loss of the cell, which goes out of the observation field. The paths are shown superimposed upon the image and grow while the movie progresses towards the final frame. The coordinates of the recorded paths are saved to a text file, which may be stored for further analysis. Editing of the coordinates is possible both during and after the tracking phase; to correct errors without relicking the entire set of data.

MotoCell calculates descriptive parameters such as average speed and linearity, along with circular statistics analysis of linear and angular dispersion. Statistical analysis is performed by using the saved coordinates list, either just acquired or stored in previous sessions. MotoCell is accessible online at the address <http://motocell.ceinge.unina.it>; users datasets may be uploaded from the remote client PC. Statistical analysis is performed by using the saved coordinate lists.

Analysis of cell behaviour consists of the evaluation of the parameters of descriptive statistics such as average speed, linearity, mean angle, vector length, calculated for the whole population examined as well as for each cell and for each step of the migration; in this way the behaviour of whole cell population may be assessed as a whole or as a sum of individual entities. In addition to population statistics, the analysis of single cells allows to group the cells into subpopulation, or even to evaluate the behaviour of each cell with respect to a variable reference, such as the direction of a wound or the position of the closest cell.

Circular statistics analysis is used to study the directional movement of objects and produces linear dispersion coefficient (R) and angular dispersion (S) values, together with average angles. The data are examined in relation to the Rayleigh coefficient for evaluating the significance of data derived from small cell populations.

Competing interests

The authors declare that they have no competing interests.

Authors' contributions

CC, LS and GP thought and designed the MotoCell application and its interface and gave major contribution to the writing; CC and FF developed most of the code; LS and MCF carried out the wet-lab experiments, while GP provided oversight of the work.

Acknowledgements

This work has been supported by Ministero dell'Istruzione dell'Universita' e della Ricerca (MIUR) under the PON2004 (SCoPE), FIRB (LITBIO) Projects. CC was the recipient of a SEMM phd fellowship.

This article has been published as part of *BMC Bioinformatics* Volume 10 Supplement 12, 2009: Bioinformatics Methods for Biomedical Complex System Applications. The full contents of the supplement are available online at <http://www.biomedcentral.com/1471-2105/10?issue=S12>.

References

1. Kurosaka S and Kashina A: **Cell biology of embryonic migration.** *Birth Defects Res C Embryo Today* 2008, **84(2)**:102-122.
2. Sahai E: **Illuminating the metastatic process.** *Nat Rev Cancer* 2007, **7(10)**:737-149.
3. Ridley AJ, Schwartz MA, Burridge K, Firtel RA, Ginsberg MH, Borisy G, Parsons JT and Horwitz AR: **Cell migration: integrating signals from front to back.** *Science* 2003, **302(5651)**:1704-1709.
4. Pollard TD and Borisy GG: **Cellular motility driven by assembly and disassembly of actin filaments.** *Cell* 2003, **112(4)**:453-465.
5. Stupack DG: **The biology of integrins.** *Oncology (Williston Park)* 2007, **21(9 Suppl 3)**:6-12.
6. Martens L, Monsieur G, Ampe C, Gevaert K and Vandekerckhove J: **Cell motility: a cross-platform, open source application for the study of cell motion paths.** *BMC Bioinformatics* 2006, **7(1)**:289.
7. Flaherty B, McGarry JP and McHugh PE: **Mathematical Models of Cell Motility.** *Cell Biochem Biophys* 2007, **49**:14-28.
8. Horwitz AR and Parsons JT: **Cell biology: Cell migration-movin' on.** *Science* 1999, **286(5442)**:1102-1103.
9. Mogilner A and Oster G: **Polymer motors: Pushing out the front and pulling up the back.** *Current Biology* 2003, **13(18)**:R721-R733.
10. Fletcher DA and Theriot JA: **An introduction to cell motility for the physical scientist.** *Physical Biology* 2004, **1(1-2)**:T1-T10.Y.
11. Dmytryiev A, Tkach V, Rudenko O, Bock E and Berezin V: **An Automatic Procedure for Evaluation of Single Cell Motility.** *Cytometry A* 2006, **69**:979-985.
12. Chenglu W and Pengbo W: **Tracking motile algal cells with a deformable model.** *New Zealand J of Agricultural Research* 2007, **50**:1285-1292.
13. Abramoff MD, Magalhaes PJ and Ram SJ: **Image Processing with ImageJ.** *Biophotonics International* 2004, **11**:36-42.
14. Helmuth JA, Burckhardt CJ, Koumoutsakos P, Greber UF and Sbalzarini IF: **A novel supervised trajectory segmentation algorithm identifies distinct types of human adenovirus motion in host cells.** *Journal of Structural Biology* 2007, **159**:347-358.
15. Codling EA, Plank MJ and Benhamou S: **Random walk models in biology.** *J R Soc Interface* 2008, **5(25)**:813-34.
16. Batschelet E: **Circular statistics in biology.** London, UK: Academic Press; 1981.
17. Mardia KV and Jupp PE: **Directional Statistics.** John Wiley & Sons: Chichester; 2000.
18. Wilkie D: **Rayleigh Test for Randomness of Circular Data.** *Applied Statistics* 1983, **32(3)**:311-312.
19. Lockhart RA and Stephens MA: **Tests of fit for the von Mises distribution.** *Biometrika* 1985, **72**:647-652.
20. Watson GS: **Goodness-of-fit tests on a circle.** *Biometrika* 1961, **48**:109-114.